A NOVEL APPROACH TO TARGETED THERAPY FOR PROSTATE CANCER: COMBINATION OF BCL-2 AND AKT INHIBITORS

by
Ezgi Avşar Apdik

Submitted to Graduate School of Natural and Applied Sciences
in Partial Fulfillment of the Requirements
for the Degree of Doctor of Philosophy in
Biotechnology

Yeditepe University
2017

A NOVEL APPROACH TO TARGETED THERAPY FOR PROSTATE CANCER: COMBINATION OF BCL-2 AND AKT INHIBITORS

APPROVED BY:

Prof. Dr. Sabire Ferda Kaleağasıoğlu (Thesis Supervisor) .....

Prof. Dr. Ahmet Arman .....

Prof. Dr. Ertuğrul Kılıç .....

Prof. Dr. Fikrettin Şahin .....

Assist. Prof. Dr. Ayşegül Kuşkucu .....

DATE OF APPROVAL: ..../..../2017

ACKNOWLEDGEMENTS

First and foremost, I would like to express my deepest appreciation to my supervisor, Prof. Ferda KALEAĞASIOĞLU for her guidance, and continuous support during the experimental, and writing stages of my Ph.D. thesis. I would like to thank Prof. Martin BERGER for providing the investigational drug, erufosine. I also would like to thank to my jury members; Prof. Fikrettin ŞAHİN, Prof. Ertuğrul KILIÇ, and Assist. Prof. Dr. Ayşegül KUŞKUCU for their professional guidance during the thesis process. I would like to specially thank to my lovely husband Mr. Hüseyin APDİK for being in my life, supporting my career at any situation and his cooperation during this study. It would not be a possible reality to complete this challenging Ph.D. journey without him. I am also thankful to gene and cell therapy group (molecular diagnostic lab.) members and my undergraduate intern student Duygu TURAN. I would like to thank to Başak KANDEMİR, Görkem CEMALİ, Anıl ÖZDEMİRLİ, Seçil DEMİR and Dr. Merve SEVEN. It is hard to express the meaning of always being there.

I am deeply indebted to TUBITAK (The Scientific and Technological Research Council of Turkey) for the fund of my PhD education (2211-A National PhD Scholarship Programme) and partial financial support of my thesis (TUBITAK project number: 315S039).

Finally, I would like to express my deepest gratitude to my mum Saadet AVŞAR and dad Ziya AVŞAR for their endless love, unconditional support and understanding throughout my life.

ABSTRACT

A NOVEL APPROACH TO TARGETED THERAPY FOR PROSTATE CANCER: COMBINATION OF BCL-2 AND AKT INHIBITORS

Prostate cancer still remains the second rank in cancer-related deaths. The development of novel molecules with low toxicity on healthy tissues and evaluating their synergistic effects will provide considerable guidance to the preparation of effective and safe treatment protocols.

In the current study, anticancer activity of ABT-737 and erufosine (ErPC3) alone and in combination, on hormone-independent prostate cancer (PC-3, DU-145) and healthy (PNT-1A) cell lines were evaluated under in vitro conditions. The combination of ABT-737 and ErPC3 displayed a synergistic effect in PC-3 cell lines. DU-145 cell lines exhibited resistance against the combination and no increase in cytotoxicity was observed as compared to ErPC3 alone. ABT-737 and ErPC3 alone and in combination slightly decreased the survival of PNT-1A cells only at the highest concentrations. The results obtained from wound healing, Annexin V apoptotic cell analysis, Western Blot and RT-PCR experiments also seemed to support these findings. According to these results, DU-145 cell line is less sensitive to ABT-737 due to the highly expressed anti-apoptotic Mcl-1 protein. Therefore, ABT-737 and ErPC3 combination can be considered less effective in the prostate cancer cell lines in which Mcl-1 protein is highly expressed.

This is the first study in the literature which evaluates *in vitro* anti-cancer activity of ABT-737 and ErPC3 combination in hormone independent prostate cancer. In line with these *in vitro* findings, designing and conducting *in vivo* studies are expected to significantly contribute to the results of the current study and also to provide the basis of clinical trials.

ÖZET

PROSTAT KANSERİ İÇİN HEDEFLEME TEDAVİSİNDE YENİ BİR YAKLAŞIM OLARAK: BCL-2 VE AKT İNHİBİTÖRLERİNİN KOMBİNASYONU

Prostat kanseri günümüzde halen kansere bağlı ölümlerde ikinci sırada yer almaktadır. Sağlıklı dokular üzerinde toksik etkileri düşük olan yeni moleküllerin geliştirilmesi ve sinerjistik etkilerinin değerlendirilmesi etkili ve güvenli tedavi protokollerinin hazırlanmasında önemli ölçüde yol gösterici olacaktır.

Bu çalışmada, hormona bağımlı olmayan prostat kanseri (PC-3, DU-145) ve sağlıklı (PNT-1A) hücre hatları üzerinde, ABT-737 ve erufosinin (ErPC3) hem tek başına hem de birlikte kullanımının *in vitro* koşullardaki antikanser etkisi değerlendirilmiştir. ABT-737 ve ErPC3 kombinasyonu PC-3 hücre hattında sinerjistik etki göstermiştir. DU-145 hücre hattı ise kombinasyon uygulamasına karşı direnç sergilemiş ve tek başına ErPC3 uygulamasına oranla sitotoksik etkide bir artış gözlenmemiştir. ABT-737 ve ErPC3'ün tek başına ve birlikte kullanımı PNT-1A hücrelerinde sağkalımı ancak en yüksek dozlarda ve düşük oranda etkilemiştir. Yara iyileşmesi, Annexin V apoptotik hücre analizi, Western Blot ve RT-PCR deneylerinden elde edilen sonuçların da bu bulguları desteklediği görülmektedir. Elde edilen sonuçlara göre, DU-145 hücre hattının ABT-737'ye daha az duyarlı olması anti-apoptotik Mcl-1 proteininin yüksek oranda eksprese olmasından kaynaklanmaktadır. Dolayısıyla, Mcl-1 proteininin ekspresyonu yüksek olan prostat kanseri hücre hatlarında ABT-737 ve ErPC3'ün birlikte kullanımının daha az etkili olacağı düşünülmektedir.

Bu çalışma, ABT-737 ve ErPC3 kombinasyonunun hormona bağımlı olmayan prostat kanseri üzerindeki *in vitro* antikanser aktivitesini değerlendiren literatürdeki ilk çalışmadır. Söz konusu *in vitro* bulgular doğrultusunda, *in vivo* çalışmaların tasarlanıp yürütülmesinin elde edilen sonuçlara anlamlı katkı sağlaması ve aynı zamanda klinik çalışmalar için de bir temel oluşturması beklenmektedir.

TABLE OF CONTENTS

LIST OF FIGURES

LIST OF TABLES

LIST OF SYMBOLS/ABBREVIATIONS

4E-BP1	4E-binding protein 1
ABL	Abelson murine leukemia viral oncogene homolog
ADT	Androgen deprivation therapy
Akt	Protein kinase B
ALL	Acute lymphoblastic leukemia
AMCAR	α-methylacyl-CoA racemase
APAF-1	Apoptotic protease activating factor-1
APCs	Alkylphosphocholines
AR	Androgen receptor
ATGs	Autophagy-related genes
BAX	Bcl-2-associated X protein
BER	Base excision repair
CML	Chronic myeloid leukemia
CRC	Colorectal cancer
CRPC	Castration resistant prostate cancer
DISC	Death-inducing signaling complex
DMSO	Dimethyl sulfoxide
EBRT	External beam radiation therapy
EBV	Epstein-barr virus
EGFR	Epidermal growth factor receptor
ErPC3	Erufosine
FADD	Fas-associated death domain
FasL	Fas ligand
FBS	Fetal bovine serum
FKHR	Foxo family of forkhead transcription factors
GBM	Glioblastoma
GIST	Gastrointestinal stromal tumor
GnRH	Gonadotropin-releasing hormone
GnRHA	Gonadotropin releasing hormone agonist

HBV	Hepatitis B virus
HCQ	Hydroxychloroquine
HCV	Hepatitis C virus
HDR	Homology directed repair
HER2	Human epidermal growth factor receptor 2
HNSCC	Head and neck squamous cell carcinoma
HPC	Hereditary prostate cancer
HPV	Human papilloma virus
HR	Duble-strand breaks by homologous recombination
HTLV	Human T-lymphotropic virus
IAP	Inhibitor of apoptosis
IGF-1R	Type I IGF receptor
IKK I	Kappa B kinase
KIT	Proto-oncogene receptor tyrosine kinase
KSHV	Kaposi’s sarcoma-associated herpes-virus
MCV	Merkel cell polyomavirus
MMR	Mismatch repair
MOMP	Mitochondrial outer membrane permeabilization
mTOR	Mammalian target of rapamycin
MTT	(3-[4,5-dimethylthiazol-2-yl]-2,5-diphenyltetrazolium bromide)
NER	Nucleotide excision repair
NF-kB	Nuclear factor kappa B
NHEJ	Non-homologous end joining
NSCLC	Non-small cell lung cancer
PDGFR	Platelet-derived growth factor receptor
PDK-1	Phosphoinositide-dependent kinase-1
PI	Propidium iodide
PI3K	Phosphoinositide 3-kinase
PIP2	Phosphatidylinositol-3,4-bisphosphate
PIP3	Phosphatidylinositol-3,4,5-triphosphate
PS	Phosphatidylserine
PSA	Penicillin/Streptomycin/Amphotericin

PSA	Prostate specific antigen
PTEN	Tumor suppressor phosphatase and Tensin homolog deleted on chromosome 10
RAF	Rapidly Accelerated Fibrosarcoma
RB	Retinoblastoma
RCC	Renal cell carcinoma
RET	Rearranged during Transfection
Rheb	Ras homolog enriched in brain
ROS	Reactive oxygen species
RPMI-1640	Roswell park memorial institute medium
RTKs	Receptor tyrosine kinases
S6 K	S6 kinase protein
SAPK/JNK	Stress activated protein kinase/c jun N-terminal kinase
Smac	Second mitochondria-derived activator of caspases
TNF	Tumor necrosis factor
TNFR	Tumor necrosis factor receptor
TRADD	TNF receptor domain-associated death domain
TRAIL	Tumor necrosis factor related apoptosis inducing ligand
TSC2	Tuberous sclerosis complex 2
VEGF	Vascular endothelial growth factor

1. INTRODUCTION

1.1. CANCER

Cancer is a multifactorial disease arising from both genetic and environmental factors and characterized by uncontrolled cell division and invasion, acquired ability to spread to other sites of the body. Most of the cancers are characterized by some hallmarks although each cancer type has specific features [1]. The six hallmarks delineated by Hanahan and Weinberg in 2000 are self-sufficiency in growth signals, evasion of apoptosis, insensitivity to growth-inhibitory signals, sustained angiogenesis, unlimited replicative potential tissue, metastasis and invasion. In 2011, two significant hallmarks have also been added, which are called reprogramming energy metabolism and avoiding immune destruction [2].

The integrity and the stability of DNA is essential for the maintenance of health. DNA damage, if irreparable, will induce cell death but efficient repair of DNA damage, can protect against cancer development. There are many types of DNA repair systems; some of them are evolutionarily conserved from bacteria to humans. Five major types of repair systems were identified in mammalian cells namely, DNA mismatch repair, MMR; excision repair mechanisms; nucleotide and base excision, NER and BER; double-strand breaks by homologous recombination, HR and non-homologous end joining pathway, NHEJ [3]. Excision repairs are major kind of mechanisms in higher organisms [4]. BER is responsible for repairing DNA bases that have been damaged by oxidative stress, deamination hydrolysis and ionizing radiation. BER process does not disrupt the structure of the DNA helix. NER is a versatile repair process which prevents the effects of mutagenic-lethal functions of UV radiation, environmental mutagens and chemical carcinogens, to recognize and remove bulky DNA lesions that generally disrupt replication and transcription. The mechanistic features of BER and NER are similar although NER pathway is more complicated, requiring thirty different proteins for cut and patch like process [5]. MMR recognizes and removes mismatched bases generated during replication and homologous recombination. On the other hand, mismatch repair proteins restore insertion and deletion loops which are occurred by polymerase slippage. Two repair mechanisms are used if both DNA strands are damaged. In the first mechanism, homology directed DNA repair, HDR can be used homologous

chromosome and undamaged sister chromatid as a template [6]. HDR mechanism is error-free whereas the second mechanism, non-homologous endjoining (NHEJ), is normally error-prone. NHEJ involves the modification and ligation of broken DNA ends [7].

In case of inefficient DNA repair, inheritable mutations can trigger the carcinogenic process. The complex pathogenesis of cancer has been associated with various causes including chemical carcinogens, UV radiation, and viruses. The most well known cause is chemical carcinogenesis. Chemical carcinogens may be converted to ultimate forms which bind to the target molecules and initiate the carcinogenic process, by forming DNA adducts, or causing mutations at tumor suppressor genes and proto-oncogenes. Following this initiation step, accumulation of genetic mutations activates proto-oncogenes and inactivates tumor suppressor genes contributes to progression of cancer [8]. Chemical carcinogens also induce epigenetic changes such as acetylation and methylation during carcinogenesis. Hypermethylation within the promoter related to tumor suppressor genes is one of the most common features of carcinogenesis. UV radiation induces carcinogenesis by the same mechanisms. Other potent carcinogens are viruses and reactive oxygen species (ROS) which is generated as a result of metabolic reactions and aging, can cause damage of the DNA, proteins and membranes inducing carcinogenesis. Viruses directly affect the genome and indirectly activate the cellular mechanisms such as proliferation. There are several viruses known to act as a role in cancer development such as hepatitis B and C virus, HBV and HCV, Human papilloma virus, HPV, Merkel cell polyomavirus, MCV, Kaposi's sarcoma-associated herpes-virus, KSHV, Human T-lymphotropic virus, HTLV and Epstein-Barr virus, EBV [9].

Healthy tissues tightly regulate the production and the release of growth signaling molecules that modulate cell growth and division in order to ensure homeostasis. If these growth signals are deregulated, uncontrolled cell division occurs. Cancer cells are able to produce growth signals in an autocrine manner or trigger healthy cells for generation and release of several growth factors. Up-regulation of growth factor receptors [2] or dysregulation of downstream proliferation pathways contribute to uncontrolled cell division in cancer cells. Cancer cells also inhibit anti-growth signals via different mechanisms. For example, tumor suppressor genes control cell growth and proliferation but dysregulation of these tumor suppressor gene pathways can bypass apoptotic signals. Apoptosis, programmed cell death, is disrupted in

cancer cells which activate and inactivate several mechanisms to trigger carcinogenesis and to evade apoptosis [2, 10]. Cancer initiation, promotion and progression are related to downstream and upstream regulators of apoptotic pathway [11]. Inactivation of tumor suppressor genes (for example p53) cause blockage of apoptosis and promotion of tumor development. Similarly, the anti-apoptotic BCL-2 gene inhibits apoptosis and contributes to tumor development [8].

Alterations of cell signaling pathways are essential but not enough for carcinogenesis. Each cell has telomerase activity, also called as intrinsic mechanism for regulating cell life span [12]. Cancer cells escape telomere shortening. Telomere maintenance is needed for the conservation of tumor cells, replication potential and neoplastic state [2, 10].

1.1.1. Oncogenes and Tumor Suppressor Genes

Carcinogenesis develops from gene mutations associated with growth, differentiation, or death. Two main types of genes that lead to carcinogenesis were discovered such as oncogenes and anti-oncogenes called as tumor suppressor genes [9]. Oncogenes and tumor suppressor genes, activated and inactivated by mutations, respectively, are the key genes for cancer initiation and promotion.

Oncogenes stimulate signaling pathways associated with proliferation while other group of genes which are anti-oncogenes encode several proteins that regulate apoptosis and cell cycle arrest [13]. Oncogenes are activated by chromosomal translocations, gene amplification, mutation and retroviral insertion [14]. More than 100 oncogenes and around 30 tumor suppressor genes have been discovered [15].The first oncogenes found in naturally-occurring cancers are RAS alleles. Mutated forms of Ras protein is observed to be frequent in many solid tumors [13]. Normally growth factors bind to receptors and activate Ras protein which leads to signaling cascades activation. However, mutated Ras signaling results in uncontrolled cell proliferation and carcinogenesis [16].

Tumor suppressor genes are called anti-oncogenes which are included inhibition of proliferation and tumor progression. In many tumors, these genes are lost or inactivated, thus promoting tumor development. Genetic alterations such as point mutations and deletion of both alleles of genes inactivated tumor suppressor genes [17]. The most famous tumor

suppressor genes are TP53 and RB (retinoblastoma). The first tumor suppressor gene, RB, was identified in a childhood eye tumor. Both copies of RB genes are called recessive cancer genes must be inactivated for tumor development. Mutated RB gene does not only contribute to the retinoblastoma development process but is also related to the development of many human cancer types [18]. The protein encoded by RB gene modulates cell cycle, apoptotic cell death and cell differentiation. The RB is an important tumor suppressor gene which regulates cell cycle, cell survival and differentiation for tumor development [15]. The other important anti-oncogene, p53 is generally inactivated in many human cancer types and acts as an important role in several cellular processes including repair mechanisms, apoptotic cell death, cell cycle arrest and senescence [19]. The p53 gene is inactivated through point mutations and small deletions/insertions [20]. Mutations in p53 is observed early or late stages of carcinogenic process [21].

1.1.2. Cancer Initiation, Promotion and Progression

Carcinogenesis which is a multistage process, is separated into three main stages, including initiation and promotion which are triggered by agents have initiator and promotor activities, and finally progression. In the initiation phase, cellular damage is occurred. Then, cellular damage becomes constantly, proliferated cells enter into the progression phase. Genetic instability is characteristic feature of progression phase of carcinogenesis and leads to the mutations and chromosomal translocations. The initiation phase requires a short period of exposure time to carcinogenic agents [4]. It is irreversible and must be heritable because the initiated cell transfers the genetic alterations to the daughter cells. Initiation phase is stimulated directly by DNA mutations or indirectly by epigenetic changes. However, promotion phase requires longer exposure time to carcinogenic agents. Promotion phase constitutes the long latent period of carcinogenesis and is partially reversible. Cell proliferation occurs at the promotion phase and the “altered” clonal cells enter into the progression phase [22]. Initiation and progression phases of carcinogenesis include genetic alterations which, however, are not required for promotion phase. Progression phase covers a long period of time and includes some pronounced cellular changes such as differentiation, invasion and metastasis which are also thought to be irreversible [4]. In this phase,

proliferating cells also gain cellular adaptations to the challenges such as hypoxia and acidic environment and to invade to the other tissues [23] (Figure 1.1).

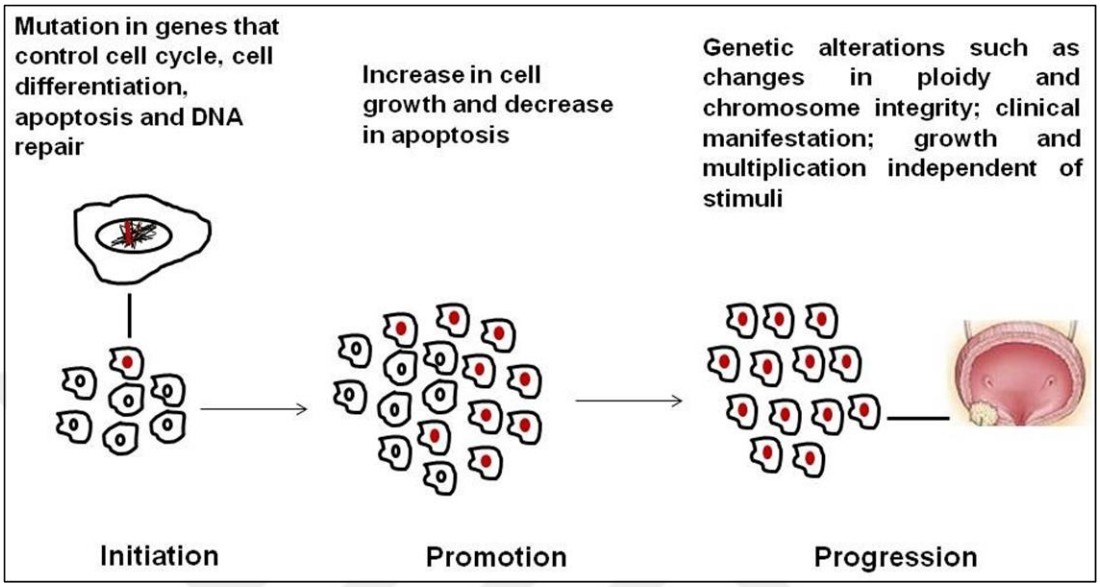

Figure 1.1. Multistep process of carcinogenesis [24]

1.2. CELL DEATH MECHANISMS IN CANCER

Cell death act as a role in cell survival, proliferation, regulation of tissue homoeostasis, development and stress response. Up to date, in mammalian cells, cell death categorizes three main groups which are apoptotic, autophagic and necrotic, according to morphological changes observed during death process. Apoptosis is identified by nuclear fragmentation, condensation of nuclear chromatin, blebbing of plasma membrane, shrinkage of cells and formation of apoptotic bodies called as membrane bound-vesicles which contain cytoplasmic or nuclear material. Autophagic cell death which is identified by the formation of double or multiple membrane cytoplasmic vacuoles known as autophagosomes. Necrosis lacks the characteristics of autophagy and apoptosis. It is accompanied by plasma membrane rupture, cell swelling, dilatation of mitochondria and cell lysis [25]. Cancer is a result of complex interaction between signaling pathways including apoptosis, autophagy and necrosis.

1.2.1. Autophagy

Autophagy ("self-eating") is very conservative catabolic activity which occurs in all eukaryotic cells. Several stress conditions including ER stress, starvation, hypoxia, and oxidative stress cause autophagic cell death. Under stress conditions, including nutrient deficiency, cells undergo autophagic cell death. In addition, autophagy removes dysfunctional and defective organelles, long-lived proteins, foreign particles (involving microorganisms) and homeostasis [26].

During autophagy, the fusion of the membrane with autophagosome or autophagic vacuoles involves the formation of double or multiple membrane bond structures. The external membrane of autophagosome formation interact with the vacuoles in plants and yeast and lysosomes in mammalian cells to form autolysosomes that contain digested materials. Degradation of cellular components generates free fatty and amino acids that are recycled for new proteins synthesis and ATP production [27].

A set of highly conserved genes known as autophagy-related genes (ATGs) are responsible for autophagy regulation. ATG genes were first discovered in yeast and some of them have orthologs in higher eukaryotes. Beclin 1 (yeast ortholog Atg6) plays an important role in autophagic formation. Beclin 1 is expressed in several human and murine tissues. B-cell lymphoma 2 (Bcl-2) protein is a negative modulator of Beclin 1. Bcl-2 acts as a role in both autophagy and apoptosis regulation. Bcl-2 and Bcl-xL anti-apoptotic proteins interact with Beclin-1 autophagy protein via BH3 homology domain resulting in inhibition of autophagy. Beclin 1 cannot reduce the anti-apoptotic functions of Bcl-2 and Bcl-xL but they neutralize the pro-autophagic activity of Beclin 1 (Figure 1.2a) [28]. Caspases cleave Beclin 1. Beclin 1C, produced by C-terminal cleavage of Beclin 1, inhibits autophagic cell death, also triggers mitochondria-mediated apoptotic cell death, where it directly releases cytochrome c [29]. In addition, Beclin 1 prevents activation of BH3 only protein Bid and hence inhibits apoptosis. Another Atg family member, Atg5, has a regulatory role like Beclin 1. The cleavage of Atg5 by calpains at N-terminal generates 24K Atg5 which induces cytochrome c released in mitochondria and initiates apoptotic cell death [30]. Caspase 3 cleaves another family member Atg4D and produces ΔN63 Atg4D that stimulates apoptosis (Figure 1.2b) [28].

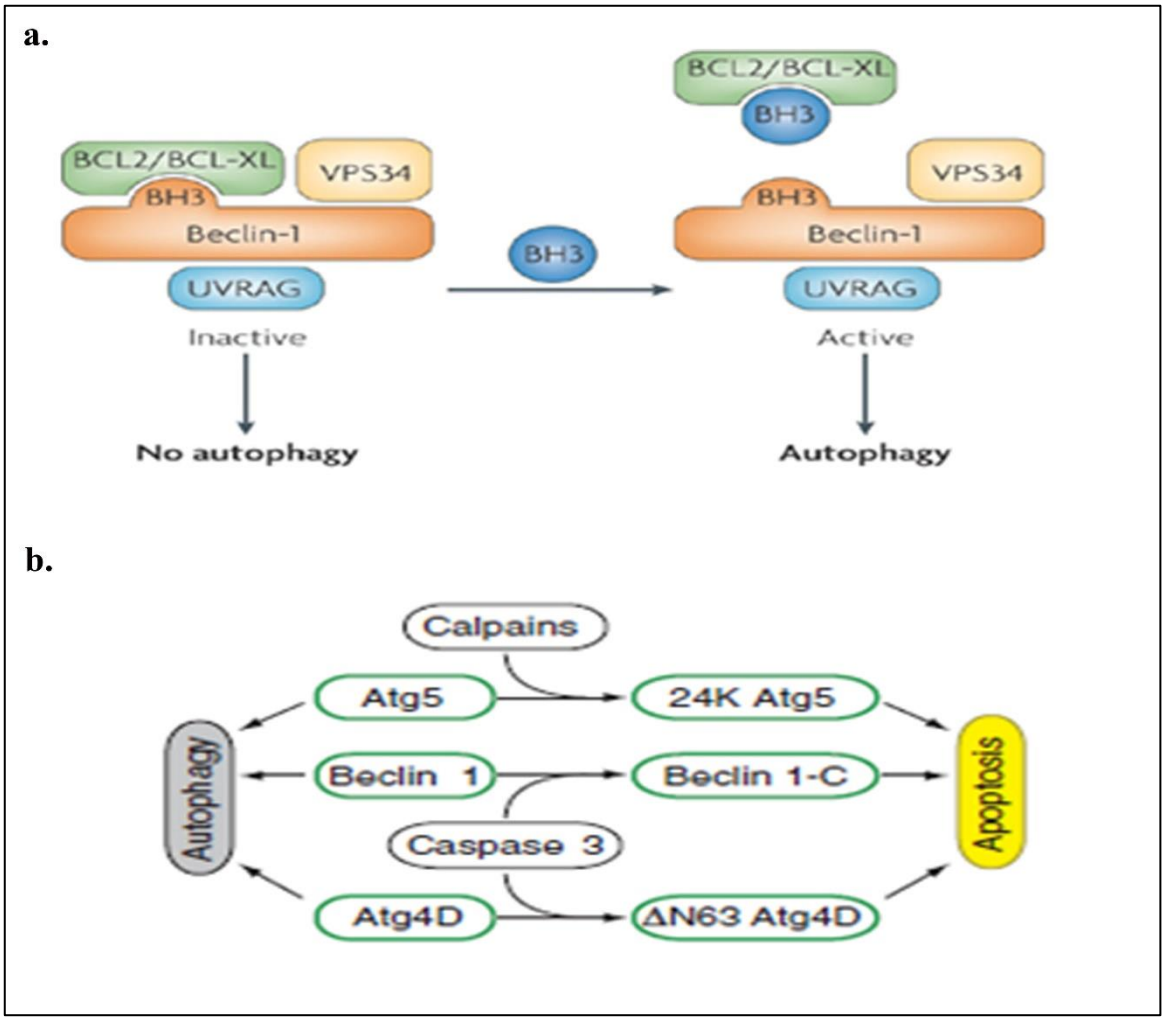

Figure 1.2. Regulation of autophagic and apoptotic cell death by Beclin 1 and Atg proteins in mammalian cells. Bcl-2/Bcl-xL interacts with Beclin 1 and blocks autophagy (a) [31]. Autophagy proteins Atg5, Beclin 1 and Atg4D induce autophagy but their cleavage products induce apoptosis (b) [32]

1.2.2. Necrosis

Necrosis is an uncontrolled and non-programmed type of cell death. Necrotic cell death usually occurs as a result of accidental (physical and chemical) injury or cell damage (acute pathological situations). Necrosis is usually detrimental and can be fatal. Morphologically, necrosis is different from other types of cell death mechanisms. Necrosis is identified by swelling of organelles, plasma membrane permeabilization. However, the nucleus does not

demonstrate chromosomal condensation, fragmentation during necrosis. Unlike apoptosis, necrosis does not include activation of caspases. Recently, it has been highlighted that programmed form of necrosis is necroptosis which is a type of non-apoptotic cell death mechanism stimulated by receptors responsible for death such as TRAIL, FasL and TNF. When caspase activation is inhibited, necroptosis can be a substitute form of death which can replace apoptosis [33].

1.2.3. Apoptosis

Apoptosis, a synonym of programmed cell death mechanism, which acts homeostasis and development [30]. Kerr and colleagues were described apoptosis in 1972 [34]. Apoptotic process eliminates mutant, damaged, aged, and unattached cells. Failure of the apoptotic pathway causes numerous diseases involving cancer, autoimmune and degenerative diseases. Caspases act a pivotal role in apoptotic cell death and belong to the large family of intracellular cysteine proteases. The inactive forms of caspases called procaspases present in the cytosol which are activated via the cleavage of the peptide bond on aspartic acid residues following apoptotic signal [35]. Initiator caspases (2, 8, 9 and 10) initiate apoptosis. The caspase 8 is essential for extrinsic apoptotic pathway, while caspase 9 is necessary for mitochondria mediated apoptosis. Both pathways activate caspase-3, thus trigger the caspase cascade. Effector caspases 3,6 and 7 execute apoptosis [26]. There are two types of pathways for apoptotic cell death, namely the extrinsic and intrinsic pathways (Figure 1.3).

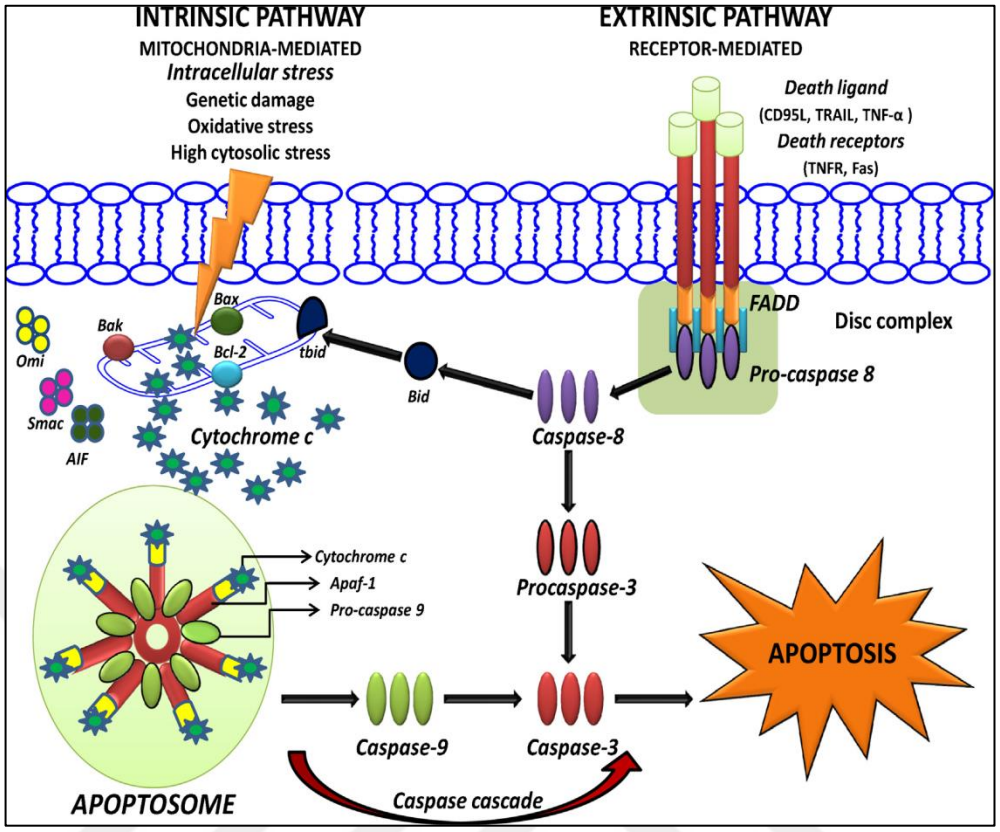

Figure 1.3. A comparison of the extrinsic and mitochondria-mediated apoptotic pathways [36].

1.2.3.1. The Extrinsic Pathway

The receptor-mediated pathway, extrinsic pathway, is initiated by receptors which belong to tumor necrosis factor receptor (TNFR) gene family, involving Fas/CD95, TNFR-1 and tumor necrosis factor related apoptosis inducing ligand (TRAIL) receptors. Binding of ligands to their death receptors and stimulates TNFR-associated death domain (TRADD) or Fas-associated death domain (FADD) adapter protein and consequently, activates procaspase 8. Thereby, death inducing signaling complex, DISC, is formed that allows activation of the initiator caspase8, hence transduction of the signaling pathway. Active caspase 8 triggers caspase cascade activation. Downstream effector caspases, caspase 3, 6 and 7, are activated by caspase 8 and leading to apoptosis (Figure 1.3). Additionally, caspase 8 indirectly activates mitochondria-mediated pathway by cleavage of pro-apoptotic Bid protein. Then, cytochrome c released from the mitochondria [37].

1.2.3.2. The Intrinsic Pathway

The mitochondria-mediated or intrinsic pathway is triggered by apoptosis stimuli such as pro-apoptotic proteins, hypoxia, anticancer drugs, DNA damage, metabolic stress, and a defective cell cycle. These signals trigger the release of second mitochondria-derived activator of caspases (Smac) and cytochrome c mitochondrial inter-membrane space proteins from mitochondria to the cytosol. In addition, apoptosome complex is formed by cytochrome c, procaspase 9 and apoptotic protease activating factor-1 (APAF-1). Then, the activated caspase 9 which is the backbone of the mitochondria mediated pathway stimulates downstream effector caspases 3, 6, 7 and triggers apoptotic cell death. Smac inhibits Inhibitor of Apoptosis (IAP) proteins that block the function of caspases (Figure 1.3) [35].

1.2.3.3. Bcl-2 Family Proteins

Bcl-2 family members act as a significant role in mitochondria-mediated apoptotic pathway. The BCL-2 gene has been identified as a reciprocal translocation in the chromosomes 14 and 18 in follicular lymphomas. These proteins control mitochondrial outer membrane permeabilization (MOMP). More than 25 members of anti- and pro-apoptotic proteins which are presented in endoplasmic reticulum, mitochondria and cytosol have been identified. They are classified into three main groups according to their structure and function. The anti-apoptotic proteins such as Bcl-2, Bcl-W, Bcl-xL, Bcl-B, Mcl-1 and BclAl have all four BH (1-4) homology domains. Bax, Bok and Bak pro-apoptotic proteins have three BH (1-3) domains. Noxa, Puma, Bad, Bim, Bmf, Bid, Hrk and Bik pro-apoptotic proteins known as ‘BH3-only proteins’ contain only one BH3 domain. Bid builds a bridge between two apoptotic pathways. The imbalance between anti-and pro-apoptotic proteins, rather than highly expressed of anti-apoptotic proteins, is suggested to be the cause of carcinogenesis [38]. BH3-only proteins are classified into two subgroups as the sensitizers (Bad, Bik and Noxa) and the activators (Bim, tBid). Two patterns have been offered for Bax and Bak activity multi-domain proteins. In the direct activation model, Bim and tBid activator proteins interact with directly Bax and Bak to initiate their activations, whereas Bad, Bik and Noxa sensitizer proteins cannot directly stimulate Bax and Bak, however they bind to and block anti-apoptotic Bcl-2, Bcl-xL, Bcl-W, BclAl and Mcl-1 proteins [39]. In the

indirect activation model, all activator and sensitizer proteins interact and inhibit anti-apoptotic proteins. Consequently, Bax and Bak are activated to start the apoptotic process (Figure 1.4) [40].

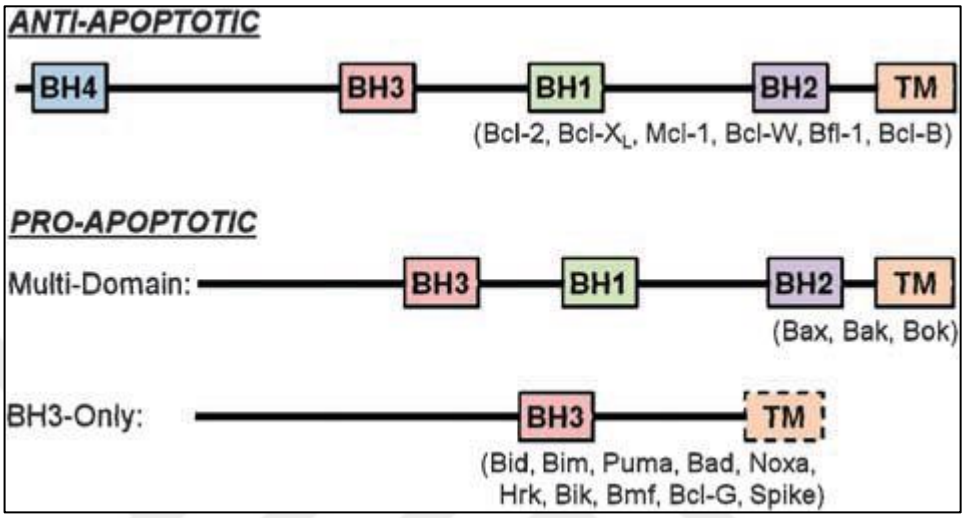

Figure 1.4. Comparisons of domain structures of Bcl-2-family proteins [41].

1.3. PI3K/AKT/mTOR PATHWAY

Phosphatidylinositol 3-kinase (PI3K) / Akt / mammalian target of rapamycin (mTOR) pathway stimulates cell survival, proliferation, motility, metabolism and angiogenesis. This pathway act as a crucial role in carcinogenesis and response to cancer treatment. Many of the new agents have been developed to act on PI3K/Akt/mTOR-related targets.

Growth factor receptor tyrosine kinases (RTKs) activates PI3K signaling. PI3K phosphorylates phosphatidylinositol-3,4-bisphosphate (PIP2) and then PIP2 convert to phosphatidylinositol-3,4,5-triphosphate (PIP3). PI3K signaling is inhibited through the dephosphorylation of PIP3 by the tumor suppressor phosphatase and Tensin homolog deleted on chromosome 10 (PTEN).

PIP3 binds to phosphoinositide-dependent kinase-1 (PDK-1) and protein kinase B via N-terminal pleckstrin homology [42] domain [43]. Akt is a critical signaling molecule in PI3K signaling. For this reason, Akt is regarded as an attractive therapeutic target in cancer

chemotherapy. PDK-1 phosphorylates and stimulates activation of Akt at threonine 308. As a result of interaction of Akt PH domain with PIP3, Akt translocates to the plasma membrane [44]. Distinct cell survival mechanisms are triggered by Akt activation. Akt directly regulates apoptotic cell death. Bad and caspase-9 are phosphorylated and inactivated by Akt. And also, Akt inhibits Foxo family of forkhead transcription factors (FKHR) which stimulate proapoptotic factor Fas ligand expression. In addition, Akt phosphorylates and activates I kappa B kinase (IKK) which is a positively regulates nuclear factor kappa B (NF-κB). NF-κB stimulates anti-apoptotic genes expression. Akt phosphorylates and activates Mdm2 which inhibits p53-mediated apoptosis (Figure 1.5) [45].

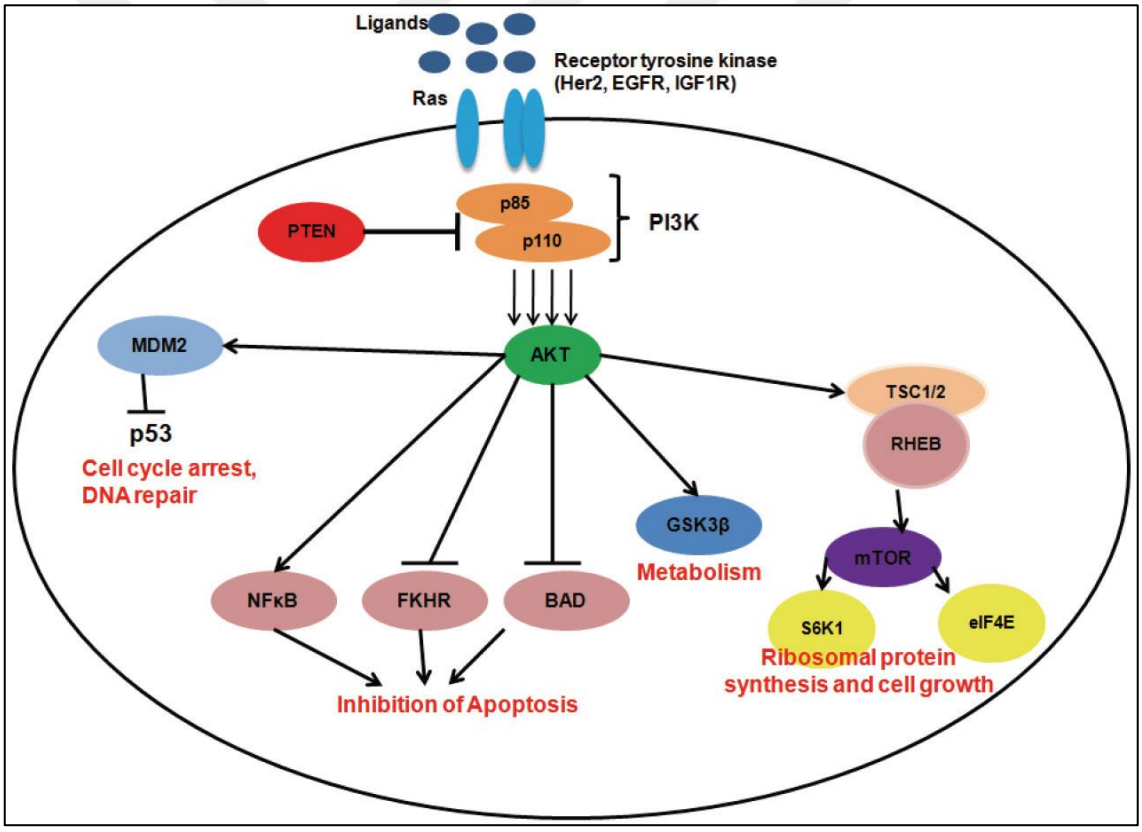

Figure 1.5. The PI3K/Akt/mTOR signaling pathway [46]

In addition, Akt directly phosphorylates and activates mTOR. A serine/threonine kinase mTOR is an evolutionary conserved and a member of PI3K-related kinase family. mTOR regulates protein synthesis, cell proliferation and metabolism. Many types of cancer possess

abnormal activation of the mTOR pathway, so targeting of mTOR is an important approach in treatment of cancer. mTOR is divided into two complex, mTORC1 and mTORC2. mTORC1 is a sensor of energy and nutrient at both systemic and cellular levels. mTORC1 is highly sensitive but mTORC2 is not sensitive to rapamycin [47]. The TSC1/2 complex is a significant mTORC1 regulator. The TSC1/2inhibits small G-protein Ras homolog enriched in brain (Rheb) by switching GTP-bound form to GDP-bound form. Tuberous sclerosis complex 2 (TSC2) is phosphorylated and inactivated by Akt and thereby TSC1/2 dimer inhibits the Rheb GTPase activity. Activated Rheb induces the mTORC1 [43]. mTORC1 transmits the signals following Akt activation and phosphorylates two main downstream molecules, the translational regulator eukaryotic initiation factor 4E-binding protein 1 (4E-BP1) and S6 kinase protein (S6K) which are important for the activation of protein synthesis. After the phosphorylation, S6K inactivates mTORC2 and thereby contributes to inhibition of PI3K signal transduction pathway. mTORC2 phosphorylates Akt on serine 473, thereby contributes to activation of Akt and supports to PI3K signal transduction pathway (Figure 1.5) [44].

1.4. TARGETED THERAPIES IN CANCER

Targeted cancer therapies (also called molecularly targeted therapies, molecularly targeted drugs and precision medicines) are agents that inhibit the growth, progression, and spread of cancer cells by targeting specific molecules. In contrast to targeted therapies, standard chemotherapies usually target all rapidly proliferating healthy and cancer cells. In addition, targeted therapies are often cytostatic because they halt cancer cell proliferation, whereas standard chemotherapies are cytotoxic because they kill the cells [48].

Today, many targets have been identified, which are associated with cell survival pathways [49]. Among the currently available targeted therapeutic drugs are hormone therapies, signal transduction inhibitors, gene expression modulators, apoptosis inducers, angiogenesis inhibitors, immunotherapies, and toxin delivery molecules. In the light of these findings, targeted therapies are currently used for the treatment of various tumors including hematologic malignancies, colorectal, pancreatic, non-small cell lung, breast, prostate, and renal cancers [48].

There are two main types of targeted therapeutics, monoclonal antibodies, and small molecules. Monoclonal antibodies such astrastuzumab, bevacizumab, and cetuximabare large compounds which cannot enter the cells, hence they inhibit specific targets on the cell surface or surrounding cells. In addition, small molecules such as everolimus, imatinib, sorafenib, sunitinib and temsirolimus can easily enter the cells and inhibit specific intracellular targets (Table 1.1) [50].

Table 1.1. US FDA Approved Targeted Therapies and Indications

Agent	**Target(s)**	**FDA-approved Indication(s)**
Monoclonalantibodies		
Trastuzumab	HER2	Breast cancer (HER2+), Gastric Cancer (HER2+)
Bevacizumab	VEGF	CRC, GBM, NCLC, RCC
Cetuximab	EGFR	CRC, HNSCC
Small Molecule Inhibitors		
Erlotinib	EGFR	NSCLC, pancreatic cancer
Enzalutamide	AR	Metastatic castration-resistant prostate cancer.
Everolimus	mTOR	RCC, breast cancer, pancreatic neuroendocrine tumor
Imatinib	KIT, PDGFR, ABL	GIST, ALL, CML, dermatofibrosarcoma protuberans
Sorafenib	KIT, VEGFR, PDGFR, RAF	Hepatocellular carcinoma, RCC

Sunitinib	VEGFR, PDGFR, RET, KIT	GIST, RCC, Pancreatic neuroendocrine tumor
Temsirolimus	mTOR	RCC

1.5. PROSTATE CANCER

Cancer is classified in more than 100 types, each type displaying different characteristics based on its tissue of origin. Approximately 85% of cancer originates from epithelial cells, called carcinomas. Among carcinomas in men, prostate cancer is the second most common type of malignant tumor and the fifth leading cause of cancer-related deaths worldwide. Prostate cancer (PCa) is a significant healthcare challenge and mortality rate is 3 to 30 per 100. 000 men worldwide [51].

Such differences are due to certain risk factors including age, race/ethnicity, diet, and family history. The incidence of prostate cancer is higher over the age of 50 years but also varies according to the population and the geographic regions. In more developing countries including, North America, Australia, Western and Northern Europe, prostate cancer incidence is the highest because screening and early detection techniques are frequently used for cancer diagnosis. However, mortality rate of prostate cancer is the highest in Africa [52]. High amounts of fat, dairy product or meat intake are the established factors known to increase the risk of prostate cancer development. Also, androgens, especially testosterone is related to a higher risk of prostate cancer incidence [53].

Hereditary prostate cancer (HPC) is a more specific type of familial prostate cancer, inherited by a susceptibility gene via Mendelian rules [54]. Epidemiological studies have shown that having first-degree relatives with a diagnosis of PCa increases the incidence of PCa approximately by two or three fold [55]. HPC is observed in nearly 43% of prostate cancer cases that develop before the age 55 [56]. Family-based linkage studies identified a series of genes associated with HPC including, HPC1, PCAP, HPCX, CAPB, HPC20 and HOXB.

In addition to the genomic factors, somatic alterations play crucial roles in PCa etiology. The biomarkers identified to date can act as a significant role in screening, prognosis, and determination of treatment options. These biomarkers can be alternative or supplement to prostate specific antigen (PSA) testing. Studies have reported differences in biomarkers between ethnic groups, including AMCAR, ERG, SPINK1, NXK3.1, GOLM1, AR, Ki67 and SRD5A2 [52].

1.5.1. Treatment of prostate cancer

PCa is divided into four distinct stages by U.S. National Cancer Institute classification. In stage I, the cancer cells are located only in prostate tissue. In stage II, the tumor cells are bigger than first stage however still presented in the prostate gland. In stage III, the cancer cells diffuse outside the tissue and reach the seminal vesicles. Finally, in stage IV, the cancer cells diffuse to distant part of the body, such as lymph nodes, rectum and bladder [57]. Metastasis to distant organs refers to advanced prostate cancer [58].

Standard therapies for prostate cancer involve surgery, hormonal therapy, and radiotherapy which are selected according to the stage of the cancer. Stage I therapy covers removal of the prostate gland (prostatectomy), interstitial implantation of radioisotopes and external beam radiation therapy (EBRT). Hormone therapy (androgen deprivation therapy, ADT) may be added to EBRT at the stages II-IV.

Prostate is an androgen dependent tissue. For this reason, androgen deprivation is important for the inhibition of tumor progression. ADT has clear benefits and prolongs overall survival when added to radiotherapy, before starting brachytherapy, for minimizing the cancer-related complications in patients with advanced metastatic disease [59]. There are different types of hormone therapy such as estrogens, gonadotropin releasing hormone (GnRH) agonists, GnRH antagonists, and anti-androgens [60]. Estrogens decrease serum testosterone level but they are seldom used today due to their serious side effects including venous thromboembolism, myocardial infarction, breast, and endometrial cancer [59, 61]. Gonadotropin releasing hormone agonists (GnRHAs) are mostly used for ADT. GnRHAs (e.g. leuprolide, goserelin, and buserelin) and GnRH antagonists (degarelix) eventually reduce testosterone levels, hence inhibit prostate tumor growth [62]. Androgen receptor

antagonists (e.g. flutamide, nilutamide, and bicalutamide) compete with the natural hormone for binding to AR & prevent its translocation into the nucleus. The first AR signaling inhibitor, Enzalutamide, interferes with the androgen receptor (AR) signaling pathway in three steps. Enzalutamide blocks androgen binding to ARs, nuclear translocation of hormone/androgen receptor complex, and binding of hormone/androgen receptor complex to DNA. Thus, enzalutamide promotes tumor cell death and reduces tumor volume with proven benefit in CRPC Phase 3 trials [63]. The androgen biosynthesis inhibitor, abiraterone acetate, inhibits CYP17-dependent synthesis of dehydroepiandrosterone, hence reduces serum testosterone and other androgens in prostate cancer patients [64]. In spite of substantial clinical benefits, ADT has been associated with an undesired side effect profile, covering osteoporosis, obesity, sarcopenia, resistance of insulin, diabetes, metabolic disorder and cardiovascular mortality [59].

PCa can ultimately become resistant to hormone therapy. Castration-resistant PCa (CRPC) is defined by disease progression although ADT is continued. CRPC covers either a continuous elevate in serum prostate-specific antigen (PSA) levels, development of pre-existing disease, and appearance of new metastases [65]. Therefore, appearance of CRPC necessitates other approaches [66]. Estramustine, a linked molecule of estradiol plus nornitrogen mustard, can be combined with both taxanes and vinca alkaloids for the treatment of CRPC [67]. Taxanes (docetaxel, paclitaxel, cabazitaxel), and radium 223 dichloride have been approved by FDA [68]. Taxanes interact with the β subunit of the tubulin and promote the stabilization of microtubules, thus inhibit cell division [69, 70]. Vinca alkaloids (vinblastine and vincristine) are destabilizing agents which bind to tubulin and inhibit polymerization. Radium 223 dichloride, a targeted alpha-emitting radiopharmaceutical and a T cell immune response stimulator (sipuleucel-T) are also indicated for the treatment of CRPC [71]. Mitoxantrone is an anthracycline antibiotic which inhibits topoisomerase II, is another FDA-approved therapeutic option as a palliative treatment for hormone-refractory PCa.

A better understanding of the molecular basis of the prostate cancer has been helpful for developing new drugs or drug combinations. Novel molecules against various targets (AR, heat shock proteins, PI3K/Akt/mTOR, IGFIR, cluterin, src, Hedgehog, PARP) are under development for prostate cancer [72]. Although prostate cancer has an intrinsic molecular

heterogeneity, the PI3K /NF-κB/Bcl-2 survival mechanism is being considered as a dominant pathway at especially in the pathogenesis of androgen-independent PCa [73, 74]. The PI3K/Akt/mTOR is a crucial oncogenic pathway that has been related to both carcinogenesis and resistance to chemotherapy and radiotherapy in prostate cancer and other tumor types. The hyperactivity of PI3K signaling pathway is adequate for prostate cancer initiation [75]. Aberrant PI3K signaling pathway activation has been shown to act as a role in prostate cancer progression [76]. Several studies indicate that PI3K/Akt/mTOR pathway is upregulated and PTEN activation is downregulated in prostate cancer [77]. The upregulation of anti-apoptotic protein Bcl-2 through the PI3K /NF-κB pathway emerges as an important mechanism in prostate cancer progression [74, 78]. Therefore, novel drugs targeting PI3K/Akt/mTOR or Bcl-2 pathways, alone or in combination, currently seem to be quite promising agents against prostate cancer [79].

1.6. ABT-737

Overexpression of anti-apoptotic Bcl-2 family proteins may be a reason for the resistance of prostate cancers against apoptosis when exposed to various chemotherapeutic drugs. Several studies indicate that castration-resistant and metastatic prostate cancers are positively related to overexpression of Bcl-2.

The Bcl-2 inhibitor, ABT-737, was the first BH3 mimetic compound based on structure design and screening through rational NMR spectroscopy (Figure 1.6). ABT-737 interacts with high affinity to Bcl-2, Bcl-xL, Bcl-W and inhibits their anti-apoptotic activity [42, 80]. On the other hand, ABT-737 interacts with low affinity to the anti-apoptotic proteins, Bcl-B, Mcl-1, and Bfl-1/A1 and stimulates mitochondrial apoptotic pathway through disrupting Bcl-2/Bax complex and activating pro-apoptotic protein Bax [81].

ABT-737 is a small molecule that has shown anticancer activity as a single agent or combination with other chemotherapeutics against many cancer cells, including hematopoietic cell lines (lymphoma, multiple myeloma and leukemia) and solid tumor cell lines (urinary, renal and prostate cancer) [82]. ABT-737 interact with low affinity to Mcl-1, so overexpression of this protein may provide drug resistance in several cancer types. On the other hand, ABT-737 induces Akt and Bad phosphorylation which is responsible for

development of resistance against therapeutic agents. Mcl-1 is overexpressed in PCa cell lines which may reduce the activity of ABT-737. BH3 mimetics have a proven adjuvant role when combined with conventional therapy. Studies have shown that ABT-737 has little pro-apoptotic activity in PCa. However, the combined use of ABT-737 with other chemotherapeutic agents and radiation has been shown to synergistically improve apoptosis [83].

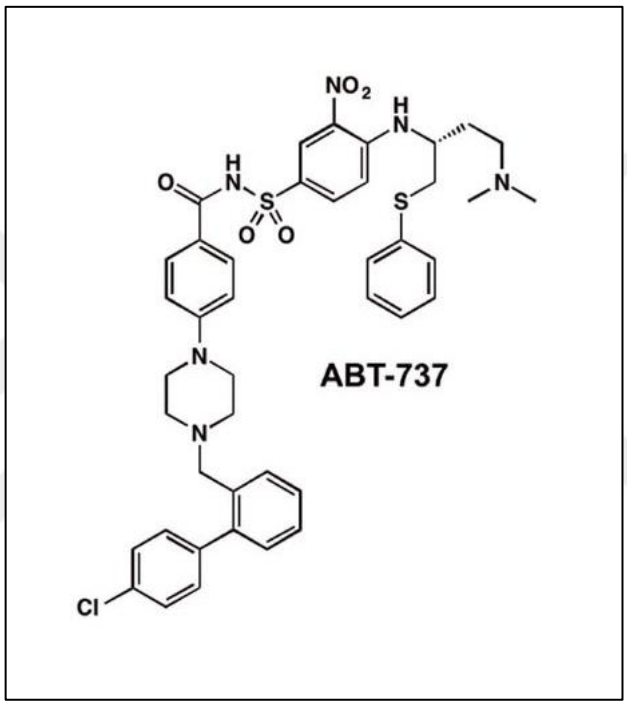

Figure 1.6. Chemical structure of ABT-737 [84]

1.7. ERUFOSINE

Alkylphosphocholines (APCs) are antineoplastic drugs which display pro-apoptotic and cytotoxic activities. APCs are structurally similar to and derived from lysophosphatidylcholine. In contrast to traditional chemotherapeutics, APCs interact with the cell membrane rather than DNA, therefore they are called membrane-targeted agents. APCs interfere with the plasma and membrane phospholipid turnover resulting in disruption of lipid-based signaling pathways. APCs modulate pro-apoptotic and anti-apoptotic signaling, such as PI3K/Akt/mTOR, Ras-Raf-MAPK/ERK, and SAPK/JNK (stress activated

protein kinase/c jun N-terminal kinase) pathways. An important anti-apoptotic signal transduction pathway is the Ras-Raf-MAPK/ERK pathway which can stimulate cell survival and proliferation. Under appropriate circumstances, Raf translocates to the mitochondria and inhibits the pro-apoptotic protein Bad. APCs interact with Raf and inhibit Ras-Raf interaction, thereby block downstream survival and proliferative signals. The pro-apoptotic signal transduction pathway is the SAPK/JNK pathway which triggers apoptosis via intrinsic or extrinsic pathways. APCs activate SAPK/JNK pathway and induce apoptosis [85]. APCs also deregulate cholesterol homeostasis, thus perturb lipid rafts which perturb cell-signaling processes. APCs were recently shown to disturb the maturation of the cell adhesion complexes resulting in inhibition of tumor cell adhesion and migration [86, 87].

Erufosine (erucylphospho-N,N,N-trimethylpropylammonium, ErPC3) is a recent experimental chemotherapeutic agent that belongs to alkylphosphocholine group (Figure 1.7). ErPC3 is the first intravenously applicable APC. ErPC3 is capable of passing the blood-brain barrier. For this reason, ErPC3 seems to have a great potential as a chemotherapeutic for brain tumors [86]. ErPC3 dephosphorylates Akt at Ser473 residue and inhibits its translocation to the plasma membrane [88]. ErPC3 inhibits both apoptotic pathways. Several experiments indicate that ErPC3 induces apoptosis in AML (acute myeloid leukemia) [89, 90], CLL (chronic lymphocytic leukemia) [91], ALL (acute lymphocytic leukemia) [92], oral squamous carcinoma [93], human glioblastoma [94, 95] and prostate cell lines from originate human.

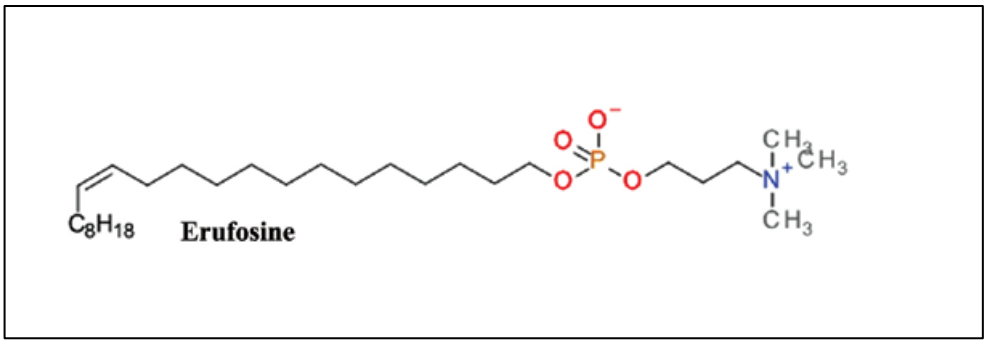

Figure 1.7. Chemical structure of Erufosine (ErPC3) [96]

1.8. AIM OF THE STUDY

The impact of the two pathways, PI3K/Akt/mTOR and the PI3K/NF-κB/Bcl-2, in the development and progression of PCa has been clearly demonstrated. Therefore, targeting these two pathways with the relevant inhibitors, alone and in combination may provide a valuable alternative for PCa therapy.

Anti-apoptotic Bcl-2 family proteins and PI3K/Akt/mTOR signaling pathway have been shown to be aberrant in PCa cells. Overexpression of Bcl-2 proteins is related to CRPC development and has been shown to affect the response to treatment [97]. In addition, PI3K/Akt/mTOR signaling pathway is also deregulated in prostate cancer development. Especially, Akt overexpression in prostate epithelial cells, which causes hyperactivation of PI3K pathway, may induce prostate cancer initiation [98].

An Akt inhibitor, ErPC3, and a Bcl-2 inhibitor, ABT-737, can trigger apoptosis via interfering with the above-mentioned pathways. Although ABT-737 blocks Bcl-2 and Bcl-xL proteins, it also induces the increase of Akt/Bad phosphorylation, thereby apoptotic signals are diminished (Figure 1.8). Therefore, ABT-737 / ErPC3 combination may overcome ABT-737-induced pro-survival signals, hence enhance apoptosis. Therefore, combining ErPC3 with ABT-737 may be a promising approach in prostate cancer chemotherapy.

The aim of this project is to determine the effect of ErPC3/ABT-737 combination on cell viability and apoptotic signaling pathways in hormone-independent PCa cell lines and to investigate the probable synergistic potential of this combination. This novel therapeutic strategy is expected to improve the response to targeted therapy and to select targeted anticancer agents or their combinations according to the expression of specific biomarkers in CRPC.

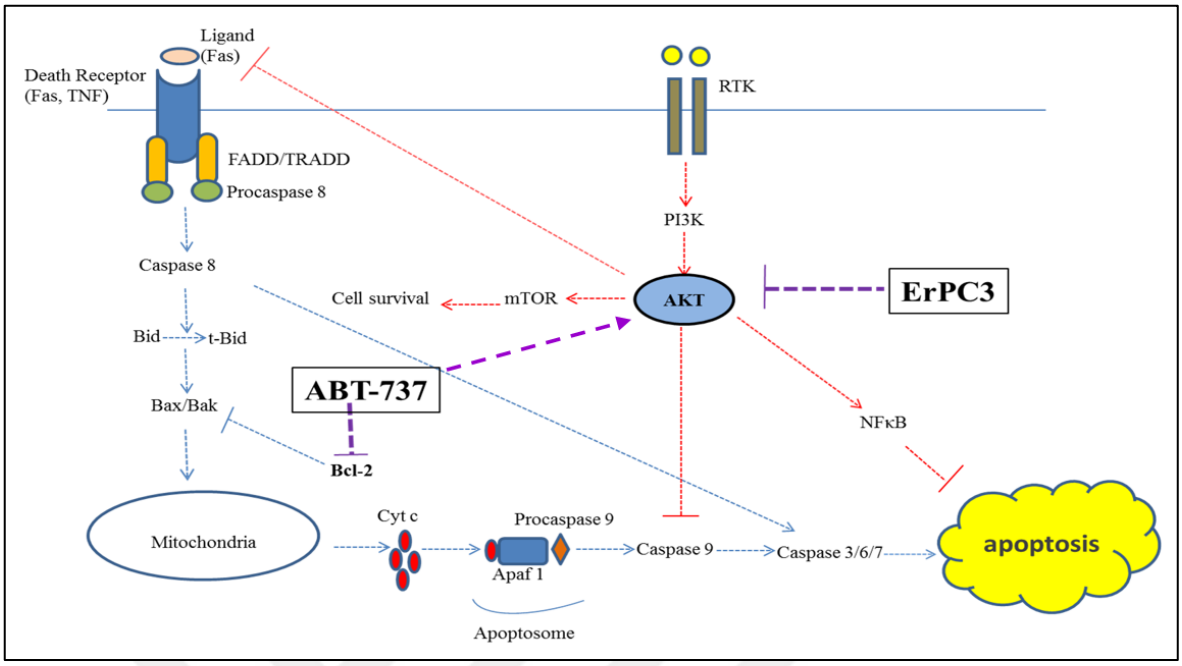

Figure 1.8. Schematic representation of signaling pathways affected by ABT-737 and ErPC3

2. MATERIALS AND METHODS

2.1. CELL LINES AND REAGENTS

DU-145 (HTB 81, human prostate cancer cells), PC-3 (CRL-1435, human prostate cancer cells) and PNT-1A (normal prostate epithelium cells) were supplied by Biotechnology Department of Yeditepe University. All cells were cultured in Roswell Park Memorial Institute medium (RPMI-1640, #21875-034, Invitrogen, Gibco, UK) supplemented with 1% Penicillin/Streptomycin/Amphotericin (PSA, Invitrogen, Gibco, UK) and 10% fetal bovine serum (FBS,#10500-064, Invitrogen, Gibco, UK) in an incubator at 37ºC and 95% O_2 / 5% CO_2. Cells were trypsinized in 0.25% trypsin/EDTA (#25200-056, Invitrogen, Gibco, UK). Cells were passaged as they reach enough confluence (~80%). ErPC3 was provided by H. Eibl (Max Planck-Institute of Biophysical Chemistry) and Prof. M.R. Berger (German Cancer Research Center) at a stock concentration of 20 M. ErPC3 was kept at +4ºC until use. ABT-737 was purchased from Abbott Laboratories (Abbott Park, IL, USA) and dissolved in dimethyl sulfoxide (DMSO, #D4540, Sigma-Aldrich, USA) to prepare a stock solution of 50 M. ABT-737 was kept at -20ºC in until use. Main stock solutions were diluted to 1% in complete RPMI-1640 medium for *in vitro* studies.

2.2. CELL VIABILITY ASSAY

To detect the cytotoxic effects of drugs alone and in combination under the current laboratory conditions, growth curves were drawn for PC-3, DU-145 and PNT-1A at the end of the 24, 48, 72, and 96h, and their doubling times were determined. All cell lines were seeded at varying densities (2000, 3000, 4000, 5000 and 6000 cells/well) in a 96-well plate with 10 wells tested for each cell density.

In *in vitro* studies, Doubling time [14] is identified as the time required for a cell population to double its number of cells. Growth Rate is the cell division amount per unit of time.

Cell viability assay was utilized for determining the cytotoxic effects capacity of drugs used either alone or in combination on all cell lines. Cell viability rates was evaluated by MTT

(3-[4,5-dimethylthiazol-2-yl]-2,5-diphenyltetrazolium bromide) dye reduction assay (#M2128, Sigma-Aldrich, St. Louis, MO, USA)described by Mossman [99]. All cells were exposed to 3.13, 6.25, 12.5, 25, 50, 100µM of ErPC3 and 1, 2.5, 5, 10, 20µM of ABT-737 prepared in complete medium. Combinations of 6.25, 12.5 and 25 µM ErPC3 with 5, 10, 20 µM ABT-737 were used for PC-3, DU-145 and PNT-1A.

Briefly, 5000 cells were seeded in each well of 96-well plates (#CLS6509, Corning Plasticware, Corning, NY) by incubating in an incubator at 37ºC and 95% O_2 / 5% CO_2 overnight. After 24h, cells were exposed to determined concentrations of drugs and their combinations for a 3-day incubation period (24, 48, and 72h). After incubation periods, 10 µl/well MTT reagent (10 mg/ml in PBS) was added to the 96-well plates and incubated at 37 ºC for 3h in a humidified incubator. At the ends of incubation periods, medium was aspired from each wells and 100 µl solvent was added (0.04 N HCl in 2-propanol) for dissolving formazan crystals. The absorbance of solvent was evaluated at 540 nm (reference 690 nm) by using an ELISA plate reader (Biotek, Winooski, VT).

2.3. WOUND HEALING ASSAY

Wound healing assay (scratch assay) was carried out in prostate cancer and healthy cell lines to probe collective cell migration in two dimensions following exposure to drugs used either alone or in combination [100]. The concentrations of 12.5, 25, 50 µM for ErPC3, 5, 10, 20 µM for ABT-737 for 24h incubation were selected for scratch assays. After completing single agent testing, the following drug combinations were chosen: PC-3 and PNT-1A / 6.25 µM for ErPC3 and 5 µM for ABT-737; DU-145 / 12.5 µM for ErPC3 and 5 µM for ABT-737.

$1x10^5$ cells were seeded in each well of 24-well plates (#92024, TPP, Switzerland) and incubated for 24h in an incubator at 37ºC and 5% CO_2. After 24 hours, a scratch model was created with a sterile 200µl pipette tip and then wells were washed with 1X PBS to avoid re-attachment of scratched cells. Determined concentrations of ABT-737, ErPC3 and their combinations were applied in the cell culture medium. Scratch zones were photographed at 0 and 24 hours by using Zeiss PrimoVert light microscope with an AxioCam ERc5s camera

(Carl Zeiss Microscopy, LLC, Thornwood, NY, USA). Wound closure area was calculated by three randomly selected regions using Zen 2011 software.

2.4. APOPTOSIS ANALYSIS

Apoptosis process starts with the translocation of phosphatidylserine [64] from the inner membrane to outer membrane and then its binding to Annexin V. In late apoptotic and necrotic events, propidium iodide (PI) penetrates the damaged membrane and binds to nucleic acid. In late apoptotic events, PI is conjugated with Annexin V. At the end of the Annexin V - fluorescein isothiocyanate (FITC) and propidium iodide [20] staining; Annexin V-FITC+ labels early apoptotic or late apoptotic cells. PI- labels early apoptotic or viable cells but PI+ labels late apoptotic or necrotic cells.

Annexin V-FITC and PI [20] staining was performed for the detection of apoptosis level in prostate cancer and healthy cell lines which were exposed to drugs used either alone or in combination [101]. The following concentrations were selected for Annexin V assay for 24h incubation: PC-3 and PNT-1A / 6.25 μM for ErPC3 and 5 μM for ABT-737; DU-145 / 50 μM for ErPC3 and 5 μM for ABT-737. $2x10^5$ cells were seeded in each well of 6-well plates and incubated for 24h. After 24h, determined concentrations of ABT-737, ErPC3 and their combinations were applied in the cell culture medium. Following the incubation period, cells were harvested and washed with cold 1X PBS twice and resuspended in 400 μl binding buffer (10 mM Hepes pH: 7.4, 140 mM NaCl ve 2.5 mM $CaCl_2$). Then, 100 μl cell suspension was transferred to each tube. 5 μl Annexin V-FITC (# 556547, BD Biosciences Pharmingen, San Diego, CA, USA) and then 5 μL PI staining solution were added according to the manufacturer's protocol. Each tube was incubated at room temperature for 20 min in the dark, and was analyzed using BD FACS Calibur Cell Sorting System (BD Biosciences Pharmingen; San Diego, CA, USA).

2.5. CELL CYCLE ANALYSIS

Cell cycle analysis was used to determine how cells are distributed in cell cycle phases in prostate cancer and healthy cell lines following exposure to test drugs used either alone or

in combination. The following concentrations were selected for cell cycle assay for 24h incubation: PC-3 and PNT-1A / 6.25 μM for ErPC3 and 5 μM for ABT-737; DU-145 / 50 μM for ErPC3 and 5 μM for ABT-737.

Briefly, $2x10^5$ cells were seeded in each well of 6-well plates (#92006, TPP, Switzerland), and incubated for 24h. Following the incubation period, determined concentrations of ABT-737, ErPC3 and their combinations were applied in the cell culture medium. After 24h, cells were harvested, washed in 1ml cold 1X PBS twice, and centrifuged. 700 μl ethanol was added to each tube for fixing the cells which were then incubated at -20°C for 2h. After the incubation, cells were again centrifuged, re-suspended in 1X PBS and incubated 10μg/ml RNase A and 0.1% Nonidet for 30 min at 37°C. 5 μL PI staining solution was added to each tube which remained for 5 min in the dark. Analysis for cell phase distribution was made by the sub-G1 peak in the DNA histogram using BD FACS Caliber system.

2.6. REAL TIME PCR (RT-PCR) ANALYSIS

RT-PCR detects gene expression at the molecular level [102]. Primers for Bcl-2, Akt, NF-κB and GAPDH (Table 2.1.) were designed by Primer-BLAST software from the National Center for Biotechnology (Bethesda, MD, USA) and were synthesized by and ordered from Macrogen (Seoul, Korea). RT-PCR reagents and conditions are given in Tables 2.2. and 2.3., respectively. The following concentrations were selected for qRT-PCR for 24h incubation: PC-3 and PNT-1A / 6.25 μM for ErPC3 and 5 μM for ABT-737; DU-145 / 50 μM for ErPC3 and 5 μM for ABT-737.

Briefly, total RNAs were isolated from treated prostate cancer and healthy cell lines by using RNAeasy plus mini kit (#74136, Qiagen, Hilden, Germany) according to the manufacturer's instructions. High Fidelity cDNA synthesis kit (#05081955001, Roche, USA) is used for cDNA synthesis. To detect mRNA levels of the target genes, reverse transcription polymerase chain reaction (RT-PCR) with SYBR Green was performed. A mixture with a final volume of 20 μl, which is consist of cDNAs, primers, SYBR-mix (#K0221, Fermentas, USA) and PCR grade distilled water (#SH30538.02, Hyclone, Utah, USA) for RT-PCR. Data was normalized regarding by GAPDH. CFX96 RT-PCR system was used for performing RT-PCR experiments (Bio-Rad, Hercules, CA).

Table 2. 1. Primers used in RT-PCR assays

Gene	**Species**	**Sequence**	**Product length**
AKT	Human	F 5’ GAAGCTGCTGGGCAAGGGGCA 3’ R 5’ GTGGGCCACCTCGTCCTTGG 3’	124bp
BCL-2	Human	F 5’ AACGGAGGCTGGGATGCCTTTGTG 3’ R 5’ ACCAGGGCCAAACTGAGCAGAGT 3’	104bp
NF-κB	Human	F 5’ GCCACCCGGCTTCAGAATGGC 3’ R 5’ TATGGGCCATCTGCTGTTGGCAGT 3	147bp
GAPDH	Human	F 5’ TGGTATCGTGGAAGGACTCA 3’ R 5’ GCAGGGATGATGTTCTGGA 3’	205bp

Table 2. 2. RT-PCR reagents

Reagents	**Volume**
Maxima™ SYBR Green qPCR Master Mix	5 µl
Primer Forward (10 pmol)	0.5 µl
Primer Reverse (10 pmol)	0.5 µl
Distilled water	1.5 µl
Template (100 ng/ml)	2.5 µl

Table 2. 3. RT-PCR conditions

Cycle	**Repeats**	**Step**	**Dwell time**	**Set point**
Initial Denaturation	1	1	3min	95 °C
Denaturation	36	1	30sec	95 °C

Annealing		2	40sec	60 °C
Elongation		3	45 sec	72° C
Final extension	1	1	10min	72 °C
Melt curve	110	1	12sec	-0.5 °C/cycle

2.7. WESTERN BLOT ANALYSIS

Western blot was performed for the evaluating of expression levels of specific proteins that are significant for prostate cancer progression in prostate cancer cell lines and normal prostate epithelium cell line. All chemicals used in western blot analysis were purchased from Biorad Laboratories (Richmond, CA). Solutions were utilized for western blot analysis is given in Table 2.4. Primary antibodies for Bcl-2 (#2872), Bcl-xL (#2762), Mcl-1 (#4572), Bak (#3814), Akt (#9272), p-Akt (#9271), cleaved caspase 3 (c-caspase 3) (#9662), cleaved caspase 9 (#9502) (c-caspase 9), cleaved PARP (c-parp) (#9532), p-65 NF-κB (#8242) and GAPDH (#8884) were purchased from Cell Signaling Technology (Beverly, MA, USA). All antibodies were used to detect marker proteins in prostate cancer and healthy cells which were applied drugs alone and their combinations, determined according to MTT test results. PC-3 and PNT-1A cells were exposed to 6.25 μM ErPC3, 5 μM ABT-737 and 6.25 μM ErPC3 plus 5 μM ABT-737 and DU-145 cells were treated with 50 μM ErPC3, 5 μM of ABT-737 and 50 μM ErPC3 plus 5 μM ABT-737 for western blot analysis.

Briefly, total protein was isolated from cells were treated with the drugs alone and combinations by RIPA Buffer (#sc-24948, Santa Cruz, USA). Protein concentrations were determined by BCA assay (#23227, Pierce, Rockford, USA). Sufficient amount of protein samples were prepared and denatured for 5 min at 95 ºC. Any kD™ Mini-PROTEAN® TGX™ precast gels (#456-9033, Biorad, USA) are used in electrophoresis of proteins. Proteins are loaded 20μg per well and electrophoresed by applying 90V for 10 min and 120V

for 60 min. Then, proteins were transferred from gel to nitrocellulose membranes (#162-0115, Biorad, Germany) with the 0.45 μm pore size using semi-dry transfer technique at 250 mA for 60 min. Following the transfer step, membranes were blocked by incubating for 1h at room temperature in a blocking solution containing 5% non-fat dry milk powder (#170-6404, Biorad, USA) prepared in tris-buffered saline and Tween-20 solution (TBS-T). Membranes were incubated with primary antibodies (dilution 1:3000) in blocking solution at 4 °C overnight. After the incubation, the membranes were washed in TBS-T three times for 10 min and then incubated with anti-rabbit (#7074, dilution 1:5000) or anti-mouse (#7076, dilution 1:5000) IgG secondary antibody prepared in TBS-T for 1h at room temperature. Then, the membranes were washed again with TBS-T three times for 10 min. The membranes were then incubated with Clarity™ ECL Western Blotting Substrate (# 1705060, BioRad, USA) at room temperature for 1 min and images were taken by using a ChemiDoc MP imaging system (BioRad, USA).

Bands were normalized by using certain GAPDH band intensities and intensities were calculated by using Image Lab software program. Results were evaluated as fold change of control groups.

Table 2. 4. Western blotting solutions

10X Running Buffer	25 mM Tris base 190 mM Glycine 0.1% SDS, pH 8.3
10X Transfer Buffer	25 mM Tris base 190 mM Glycine 20% Methanol
TBS-T	20 mM Tris-HCl 150 mM NaCl 0.1% Tween 20, pH 7.6

Blocking Buffer	5% Non-fat dry milk prepared in TBS-T

2.8. STATISTICAL ANALYSIS

One-way analysis of variance and Tukey post hoc tests were applied to all experimental datas to assess statistically. The values of $^{*}P<0.05$ were agreed as significant.

3. RESULTS

3.1. CELL VIABILITY ANALYSIS

The doubling times (Td) and growth rates of PC-3, DU-145 and PNT-1A calculated for 24–96h were 24.12, 29.36, 59.68 hours and $0.0287h^{-1}$, $0.0236h^{-1}$, $0.0116h^{-1}$, respectively. According to the analysis of the growth curves, the cell number which enabled exponential growth during 96 hours was determined for each cell line. For PC-3, DU-145, PNT-1A 5000 cells/well were chosen for drug testing.

Cell viability analysis was conducted in order to check the cytotoxic effects of various concentrations of ABT-737 (1-20 μM) and ErPC3 (1-100 μM) alone and in combination in PC-3, DU-145 and PNT-1A cell lines.

In PC-3 cells, ABT-737 and ErPC3 alone and in combination exhibited time and dose dependent cytotoxicity over 72-hours of incubation period. The difference between the control group (0.1% DMSO; negative control) and low concentrations of ABT-737 (1 and 2.5 μM) were not significant for 24, 48 and 72h of incubation (Figure 3.1a). Similarly, for the same incubation periods, the difference between ErPC3 at a concentration of 3.13 μM and control group (growth medium only) also were not significant. After 72h of incubation, ABT-737 and ErPC3 when applied at concentrations over 2.5 μM and 3.13 μM, respectively, significantly decreased cell viability of PC-3 cells. IC_{50} values (μM; 72 hours) for ABT-737 and ErPC3 alone, were determined as 14 μM and 12.5 μM, respectively (Figure 3.1b).

Following 24, 48 and 72h exposure to ABT-737 (5 μM), cell viability decreased to 98±11%, 96±10% and 86±12% of the control group, respectively. Following 24, 48, and 72h treatment with ErPC3 (6.25 μM) cell viability decreased to 97±15%, 81±9% and 69±12% of the control group, respectively. After 72h, a ceiling effect was observed with ABT-737 and ErPC3 combination at concentrations equal to and greater than 5 μM and 6.25 μM, respectively. The combination of ABT-737 (5 μM) plus ErPC3 (6.25 μM) reduced the cell viability to 84±10%, 48±5%, and 30±4%, for 24, 48 and 72 hours of incubation (Figure 3.4a). These results indicate that ABT-737 plus ErPC3 combination displays a synergistic cytotoxic effect in PC-3 cells.

DU-145 cells exhibited a relatively more resistant phenotype compared to PC-3 cells. In DU-145 cells, when compared to the control group, a significant dose-dependent cytotoxicity was not observed with ABT-737 alone, at the tested concentrations, but a time dependent cytotoxic effect was observed at 20 μM. The difference between the control group (0.1% DMSO; negative control) and all concentrations of ABT-737 treatment after 24h were not significant. Following 48 and 72h of incubation, only the highest concentration of ABT-737 (20 μM) reduced cell survival to 89±7%, and 70±8% (C %), respectively (Figure 3.2a). In DU-145 cells, ErPC3 showed a dose- and time-dependent cytotoxic effect only at high doses (50 and 100 μM) following all the incubation periods (Figure 3.2b). IC_{50} values (μM; 72hours) for ABT-737 and ErPC3alone were determined as 30 μM and 45.4 μM, respectively.

Anti-cancer activity of ABT-737 in DU-145 cells significantly increased when specified concentrations were combined with ErPC3. The combination of 50 μM ErPC3 plus 5 μM ABT-737 was more effective than other combination treatments and a ceiling effect was reached. Following treatment with 5 μM ABT-737 for 24, 48, and 72h, survival rates (C %) were 108±9%, 108±14%, and 108±9%, respectively. Following treatment with 50 μM ErPC3 for 24, 48, and 72h, survival rates (C %) were 86±4%, 51±5%, and 40±3%, respectively. Following treatment with 5 μM ABT-737 plus 50 μM ErPC3 combination for 24, 48, and 72h, survival rates (C %) were 92±5%, 52±5%, and 41±2%, respectively (Figure 3.4b). These results indicate that combining 5 μM ABT-737 with 50 μM ErPC3 provides no added value for all the incubation periods.

Proliferation of PNT-1A cells was also inhibited by ABT-737 and ErPC3 alone at high concentrations. All concentrations of ABT-737 (Figure 3.3a) and ErPC3 (Figure 3.3b) did not significantly reduce cell viability after 24h. ABT-737 (5, 10 and 20 μM), following 48 and 72h, and ErPC3 (25, 50 and 100 μM) following 72h, exerted cytotoxic effects. Following 72 hours of exposure, cell survival rates (C %) were 79±8%, 70±6%, and 67±5% for ABT-737 (5, 10, and 20 μM, respectively) and 82±6%, 82±5%, and 83±5% for ErPC3 (25, 50, and 100 μM, respectively). IC_{50} values (μM; 72hours) for ABT-737 and ErPC3 alone, were 40 μM and 430.3 μM, respectively. However, combination treatments, even at the highest concentration (20 μM ABT-737 plus 50 μM ErPC3), did not demonstrate significantly

higher cytotoxicity (76±5%) when compared to both agents used alone following 72 hours of incubation (Figure 3.4c).

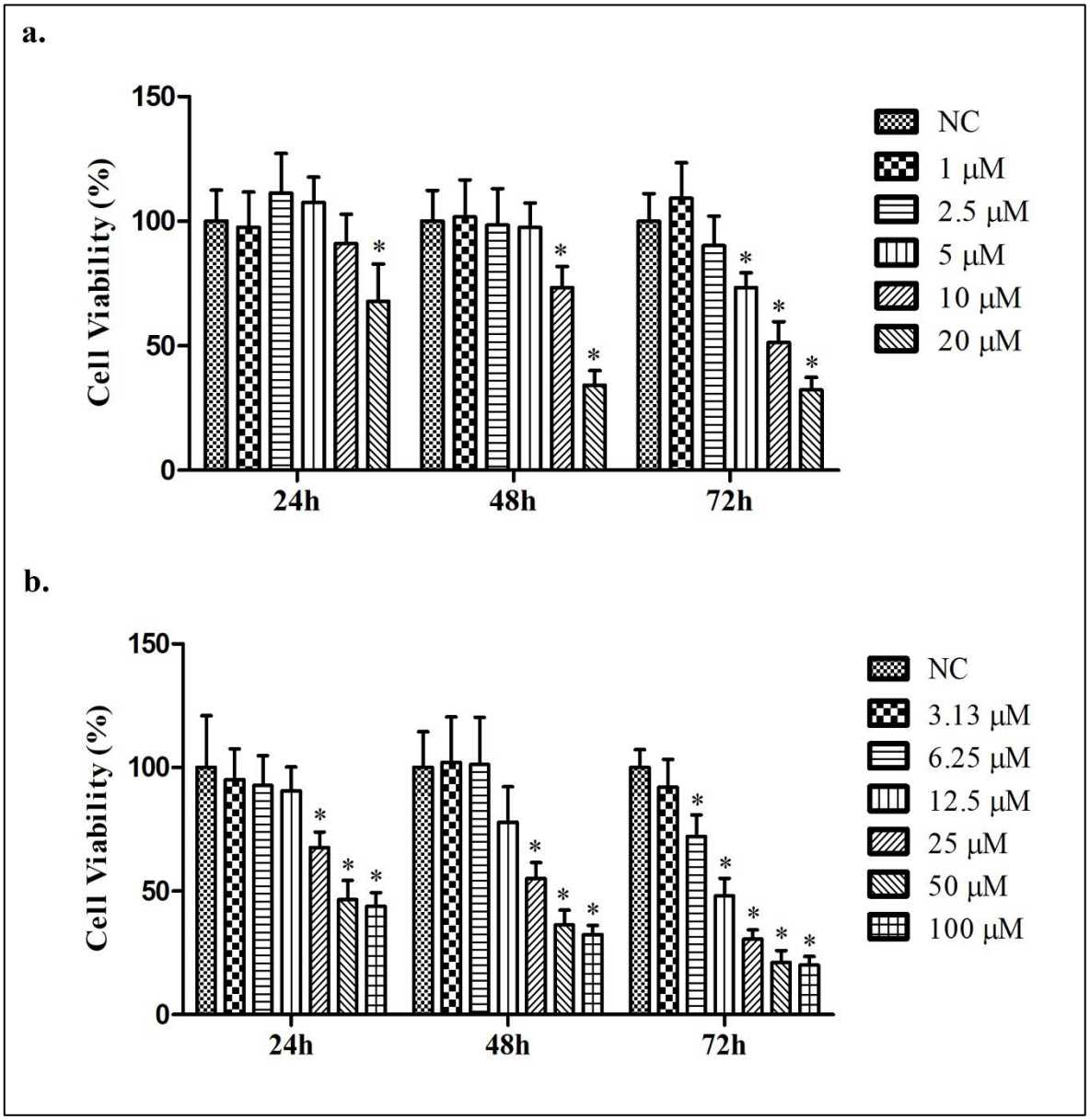

Figure 3.1. Effects of various concentrations of ABT-737 (a) and ErPC3 (b) on PC-3 cell viability. Abbreviations: NC: Negative Control (0.1% DMSO) for ABT-737 and NC: Negative Control (Growth medium) for ErPC3, *P<0.05.

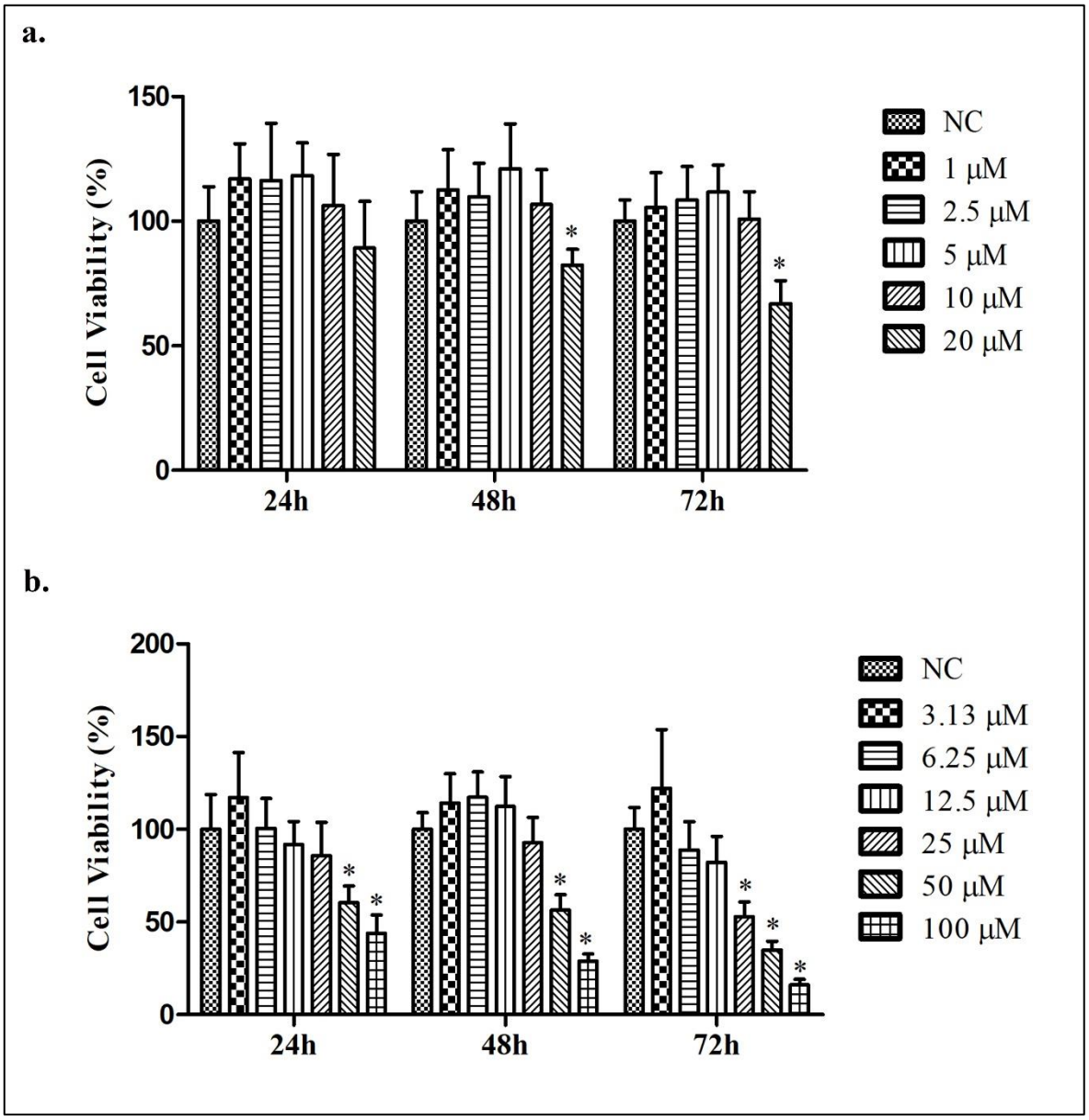

Figure 3.2. Effects of various concentrations of ABT-737 (a) and ErPC3 (b) on the cell viability of DU-145 cells. Abbreviations: NC: Negative Control (0.1% DMSO) for ABT-737 and NC: Negative Control (Growth medium) for ErPC3, *P<0.05.

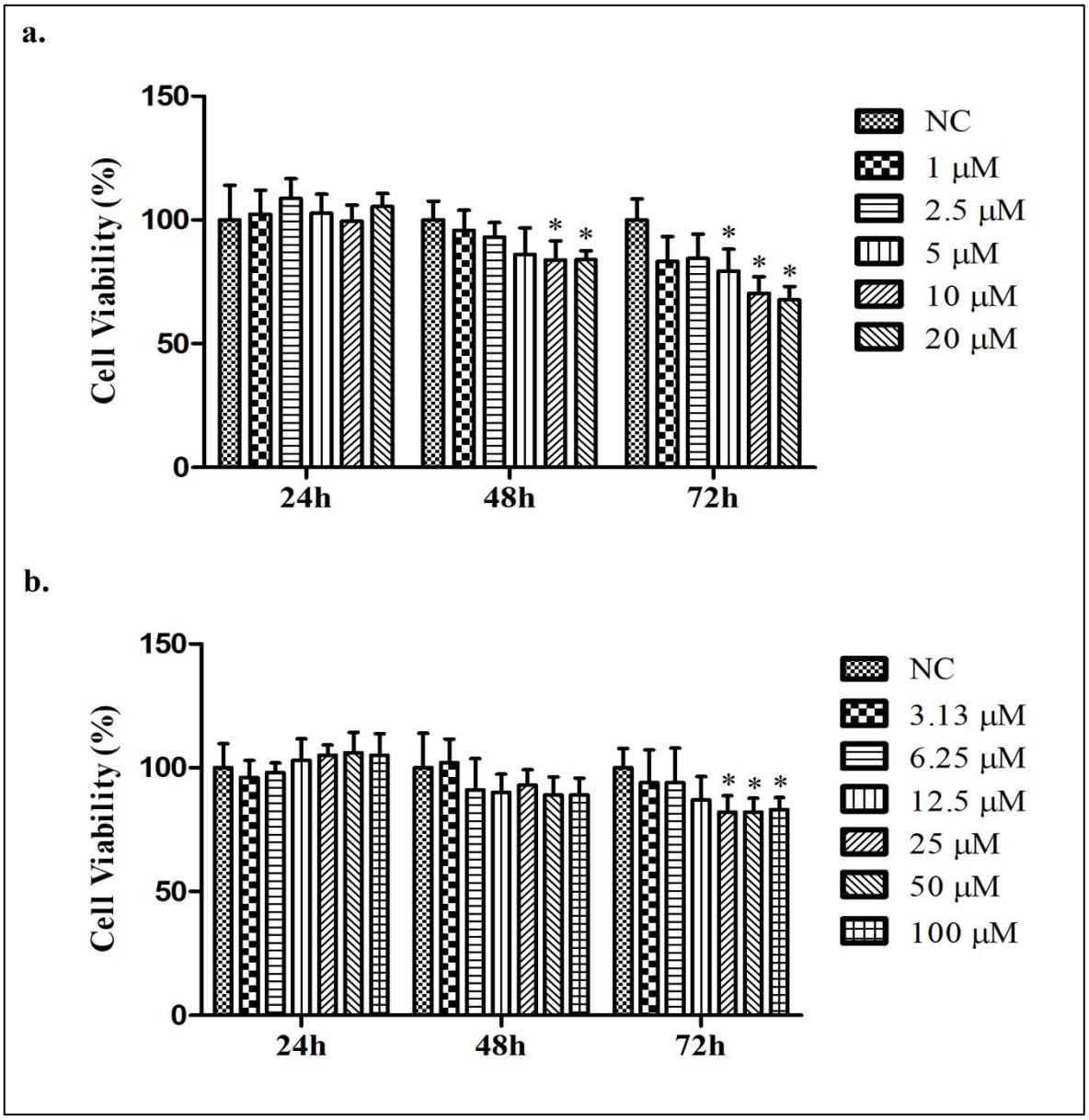

Figure 3.3. Effects of various concentrations of ABT-737 (a) and ErPC3 (b) on the cell viability of PNT-1A cells. Abbreviations: NC: Negative Control (0.1% DMSO) for ABT-737 and NC: Negative Control (Growth medium) for ErPC3, *P<0.05.

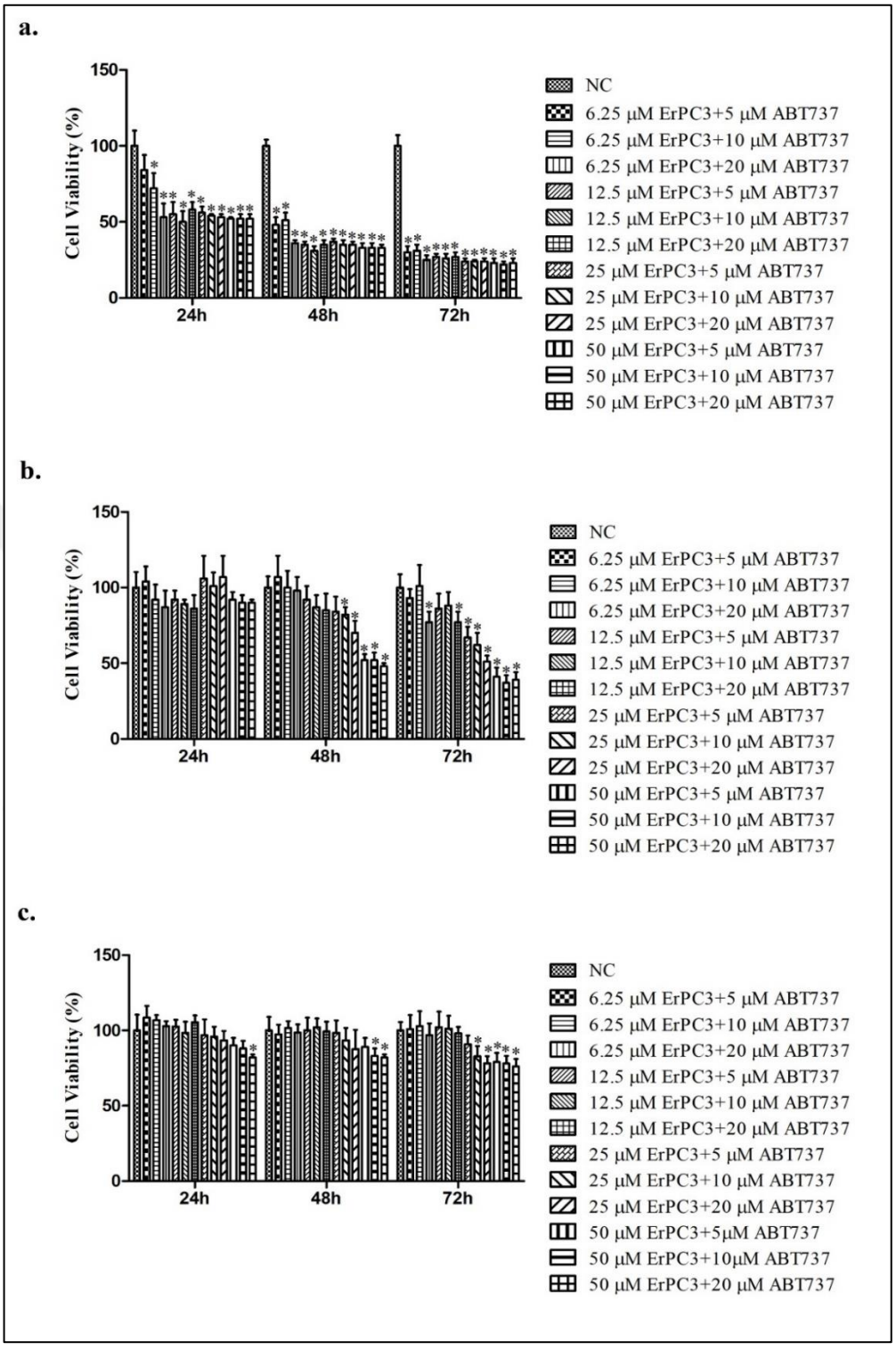

Figure 3.4. Effects of various concentrations of ErPC3 plus ABT-737 combinations on PC-3 (a), DU-145 (b) and PNT-1A (c) cell viability. Abbreviations: NC: Negative Control (Growth medium), DMSO: Dimethyl sulfoxide (0.1% v/v) containing growth medium, *P<0.05.

3.2. WOUND HEALING ASSAY

In vitro scratch assay was performed to evaluate whether ABT-737 and ErPC3 alone and in combination affect two dimensional cell migration capacity of PCa and healthy cell lines. According to the results obtained, ErPC3 and ABT-737 combinations reduced cell migration and decreased the closure rate of prostate cancer cells.

In PC-3 cells, both agents displayed a dose-dependent inhibitory effect on wound closure. ABT-737 at concentrations of 5, 10 and 20 μM significantly reduced wound closure, whereas 2.5 μM ABT-737 displayed no significant effect when compared to the control group. Following 24h, gap closure (%) in 20 μM ABT-737-treated cells were 26±6% when compared to 52±6%, and 42±4% in 5 μM and 10 μM ABT-737-treated cells (vs 65±6% in the control group) (Figure 3.5). ErPC3 at concentrations of 6.25, 12.5 and 25 μM also significantly reduced wound closure when compared to the control group. Following 24h, gap closure (%) in 25 μM ErPC3-treated cells were 26±5% when compared to 61±9%, and 46±5% in 6.25 μM and 12.5 μM ErPC3-treated cells, respectively (vs 64±6% in the control group) (Figure 3.6).

In PC-3 cells, concentrations of 5 μM ABT-737 plus 6.25 μM ErPC3 were used for combination testing, because at higher doses, cell death was more prominent, hence prevented detection of wound closure. Following 24h, gap closure (%) in the cells exposed to 5 μM ABT-737 plus 6.25 μM ErPC3 combination was 26±5% (Figure 3.7). The combination of 6.25 μM ErPC3 with 5 μM ABT-737 increased the inhibitory effect on wound closure, thus decreased the closure rate of the scratch area when compared to single agents.

In DU-145 cells, both agents displayed a dose-dependent inhibitory effect on wound closure. 20 μM ABT-737 was more effective than 5 μM and 10 μM. Following 24h, the gap closure (%) in the 20 μM ABT-737-treated cells were 7±3% when compared to 40±3%, and 15±2% in 5 μM and 10 μM ABT-737-treated cells (vs 51±2% in the control group) (Figure 3.8). On the other hand, ErPC3 (12.5, 25 and 50 μM) inhibited cell migration and decreased the closure rate of the scratched area when compared to the control group. However, 50 μM ErPC3 was significantly more effective than 12.5 μM and 25 μM ErPC3. Following 24h, gap closure (%) in the 50 μM ErPC3-treated cells was 6±4% when compared to 38±6%, and

22±6% in 12.5 μM and 25 μM ErPC3-treated cells, respectively (vs 53±3% in the control group) (Figure 3.9).

In DU-145 cells, concentrations of 12.5 μM ErPC3 plus 5 μM ABT-737 were chosen for combination testing, because at higher doses, cell death was more prominent, hence prevented detection of wound closure. Following 24h, the gap closure (%) in the 12.5 μM ErPC3 plus 5 μM ABT-737 combination-treated cells was 36±5% (Figure 3.10). According to these results, combination of ErPC3 with ABT-737 did not display significant difference when compared to the effects of single agents. The combination therapy remained ineffective on wound closure and the closure rate of the scratch.

In PNT-1A cells, ABT-737 at concentrations of 2.5, 5 and 10 μM displayed no significant effect, whereas 20 μM ABT-737significantly reduced wound closure when compared to the NC. After 24h, the gap closure (%) in the 20 μM ABT-737-treated cells were 38±1% when compared to 44±3%, 44±3% and 39±4% in 2,5, 5 and 10 μM ABT-737-treated cells (vs 44±3% in the control group) (Figure 3.11). ErPC3 at concentrations of 6.25, 12.5 and 25 μM weren't significantly different when compared to the NC group. Following 24h, gap closure (%) in 6.25, 12.5 and 25 μM ErPC3-treated cells were 45±11%, 43±3%, and 39±5%, respectively (vs 44±6% in the control group) (Figure 3.12).

In PNT-1A cells, concentrations of 5 μM ABT-737 plus 6.25 μM ErPC3 were used for combination testing, because at higher doses, cell death was more prominent, hence prevented detection of wound closure. Following 24h, gap closure (%) in the cells were exposed to 5 μM ABT-737 plus 6.25 μM ErPC3 combination was 44±10% (Figure 3.13). The combination of 6.25 μM ErPC3 with 5 μM ABT-737 did not display significant difference when compared to the effects of single agents.

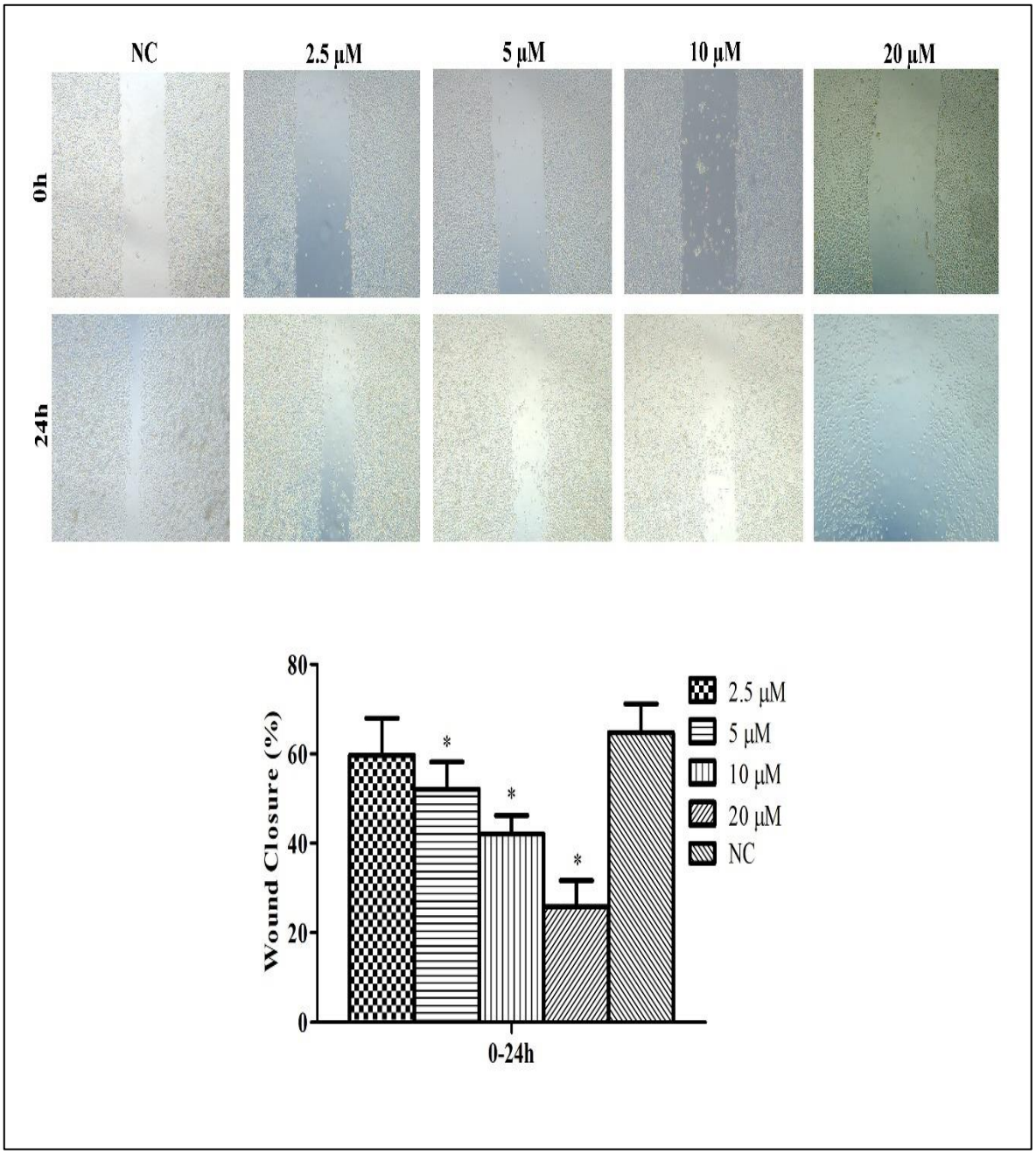

Figure 3.5. Wound healing assay following 24h treatment with ABT-737 in PC-3 cell line. Representative images of ABT-737 treated PC-3 scratches taken using inverted light microscope and wound closure rates of PC-3 cells after ABT-737 application. Abbreviations: NC: Negative Control (0.1% DMSO), *P<0.05, magnification: 40x.

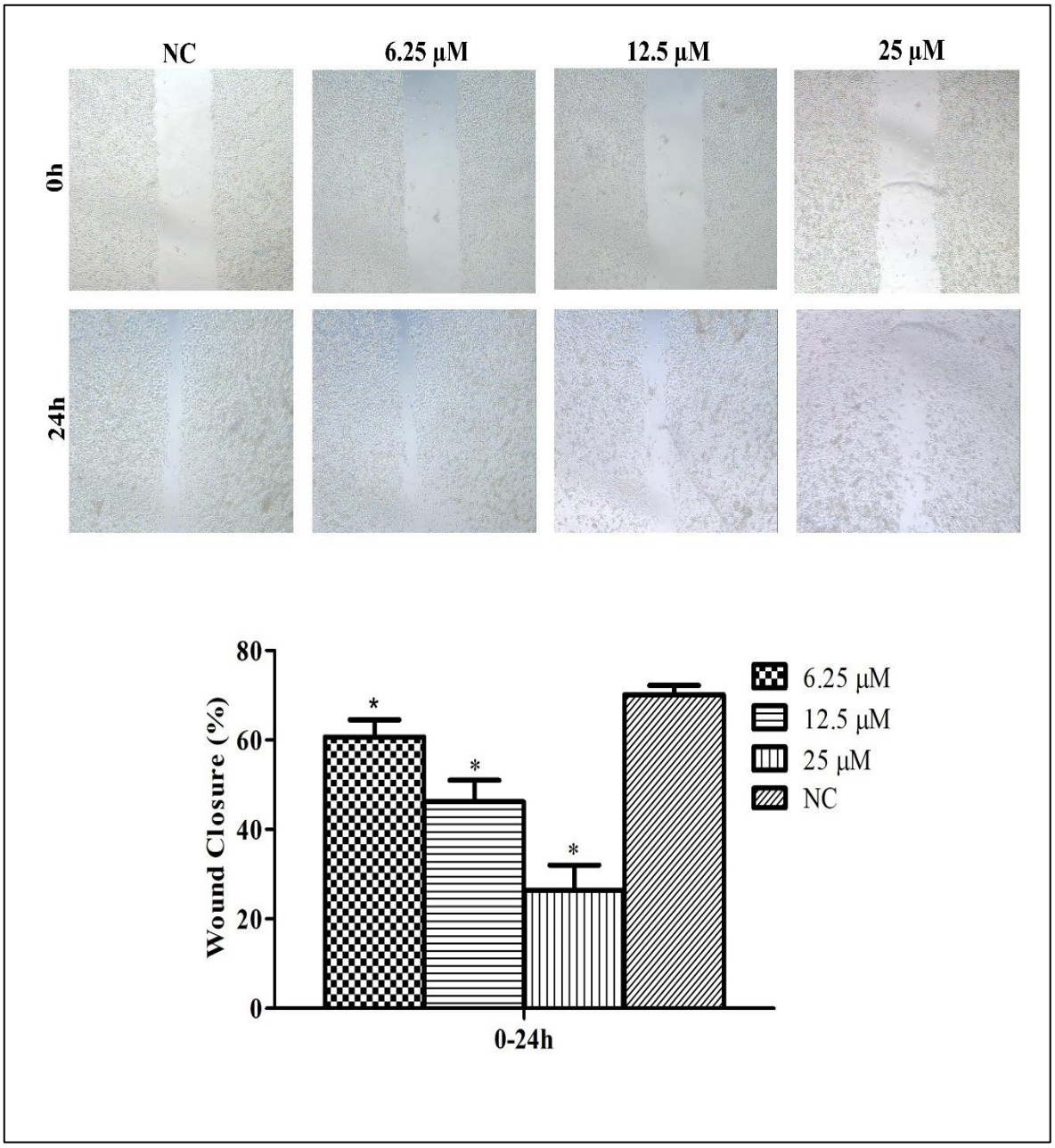

Figure 3.6. Wound healing assay following 24h treatment with ErPC3 in PC-3 cell line. Representative images of ErPC3 treated PC-3 scratches taken using inverted light microscope and wound closure rates of PC-3 cells after ErPC3 application. Abbreviations: NC: Negative Control (Growth medium), *P<0.05, magnification: 40x.

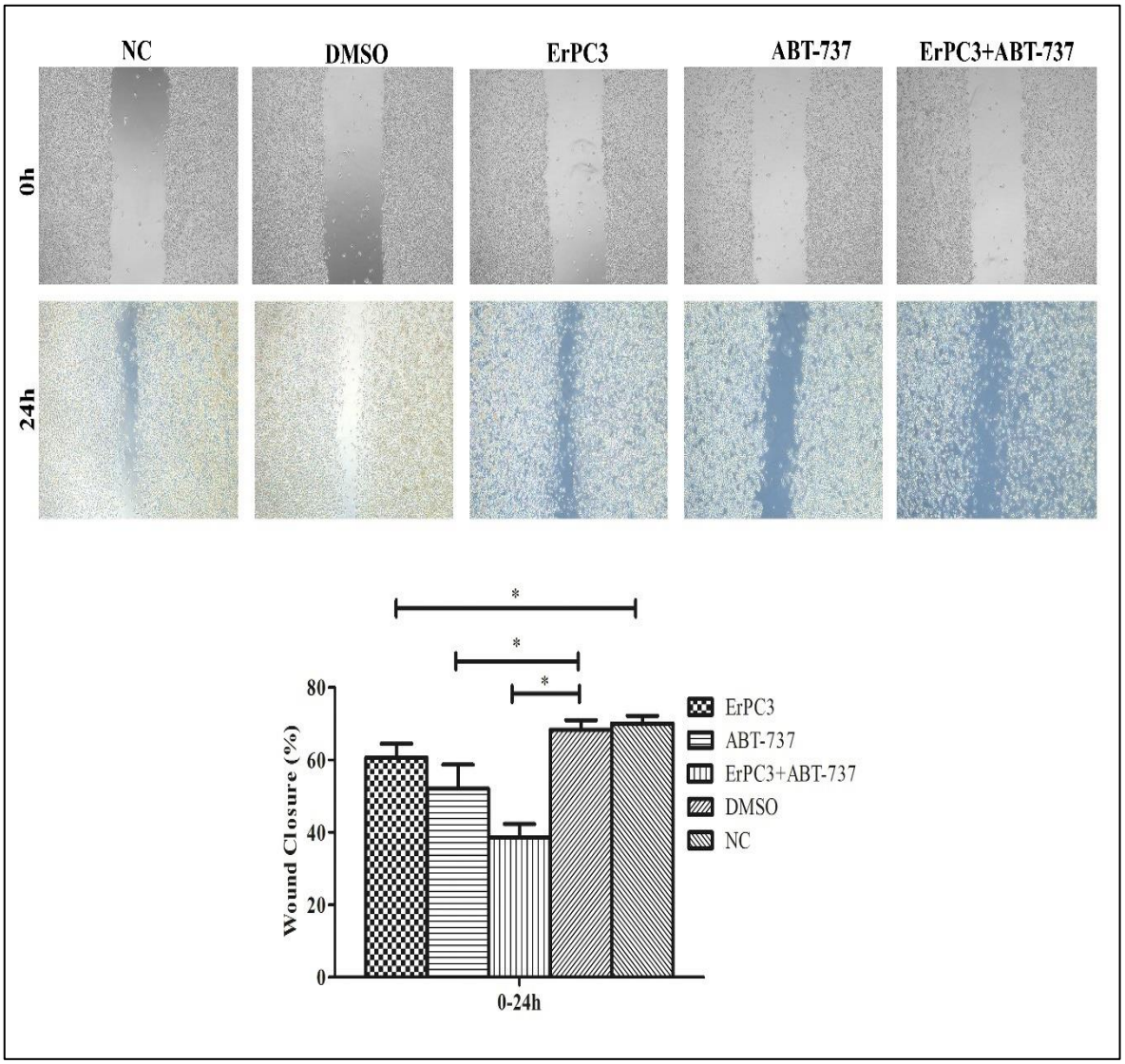

Figure 3.7. Wound healing assay following 24h treatment with ErPC3 (6.25 μM) and ABT-737 (5 μM), alone and in combination, in PC-3 cells. Representative images of ErPC3 and ABT-737 alone and in combination treated PC-3 scratches taken using inverted light microscope and wound closure rates of PC-3 cells after ErPC3 and ABT-737 alone and in combination applications. Abbreviations: NC: Negative Control (Growth medium), DMSO: Dimethyl sulfoxide (0.1% v/v) containing growth medium, *P<0.05, magnification: 40x.

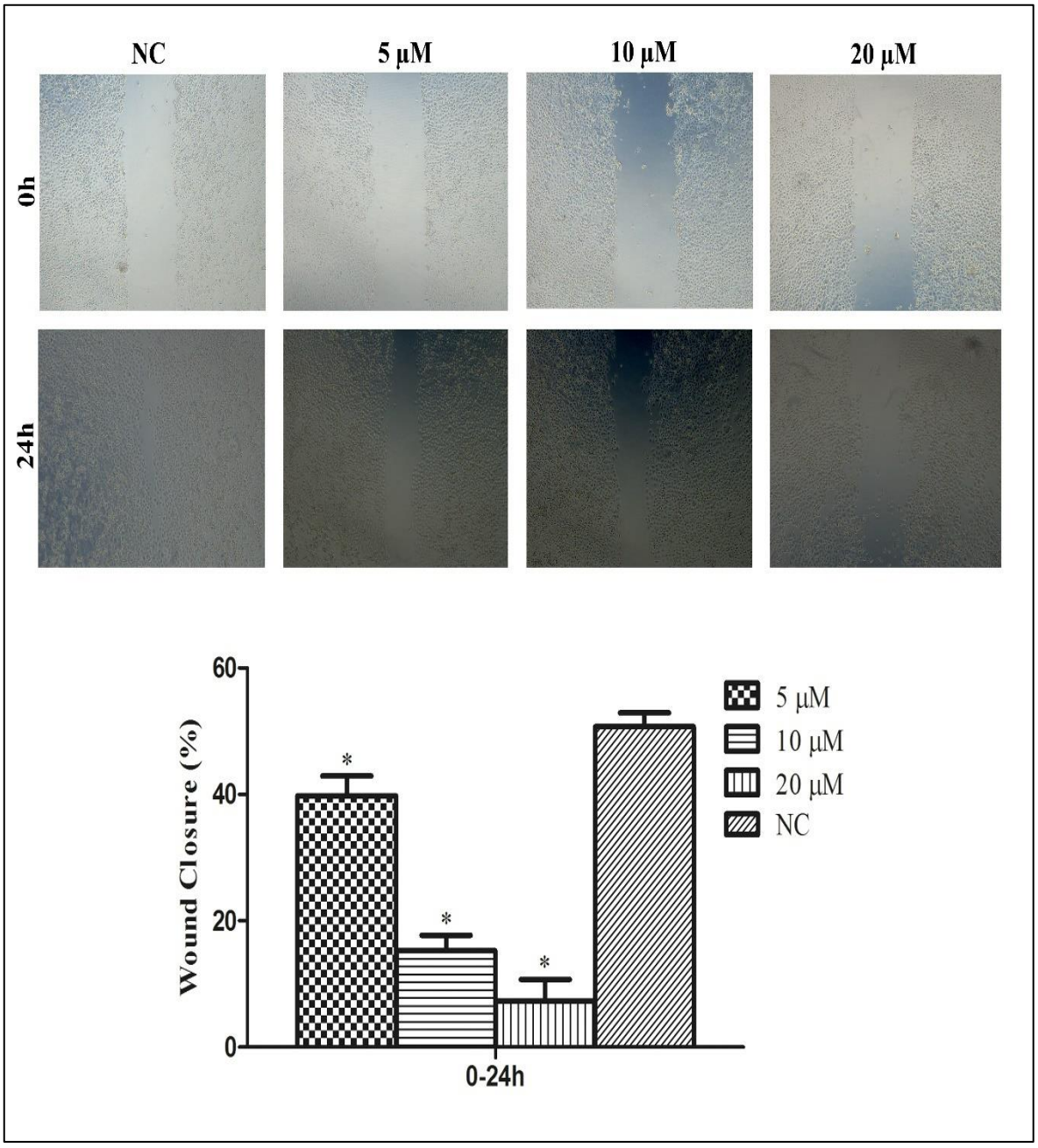

Figure 3.8. Wound healing assay following 24h treatment with ABT-737 in DU-145 cell line. Representative images of ABT-737 treated DU-145 scratches taken using inverted light microscope and wound closure rates of DU-145 cells after ABT-737 application. Abbreviations: NC: Negative Control (0.1% DMSO), *P<0.05, magnification: 40x.

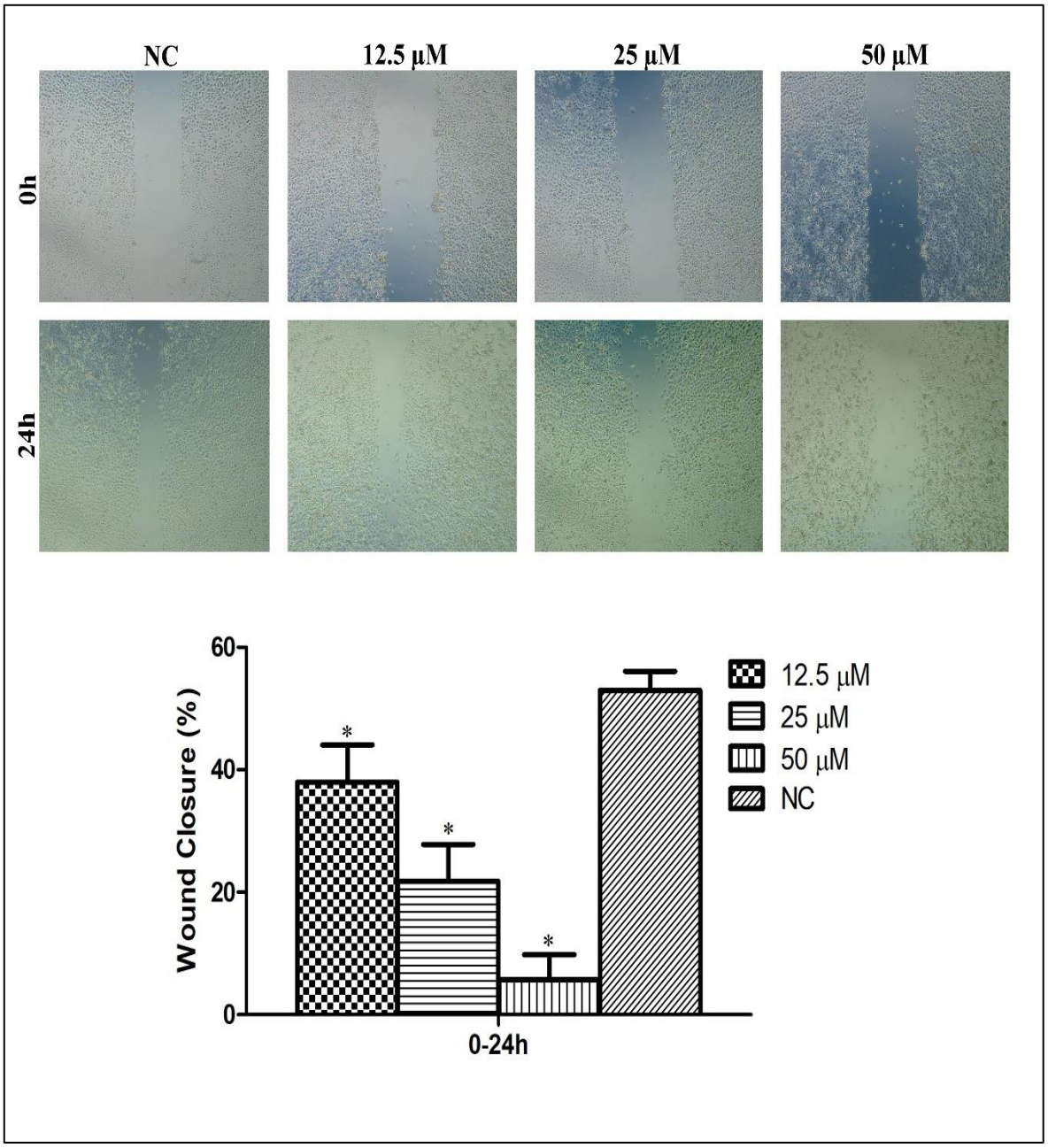

Figure 3.9. Wound healing assay following 24h treatment with ErPC3 in DU-145 cell line. Representative images of ErPC3 treated DU-145 scratches taken using inverted light microscope and wound closure rates of DU-145 cells after ErPC3 application. Abbreviations: NC: Negative Control (Growth medium), *P<0.05, magnification: 40x.

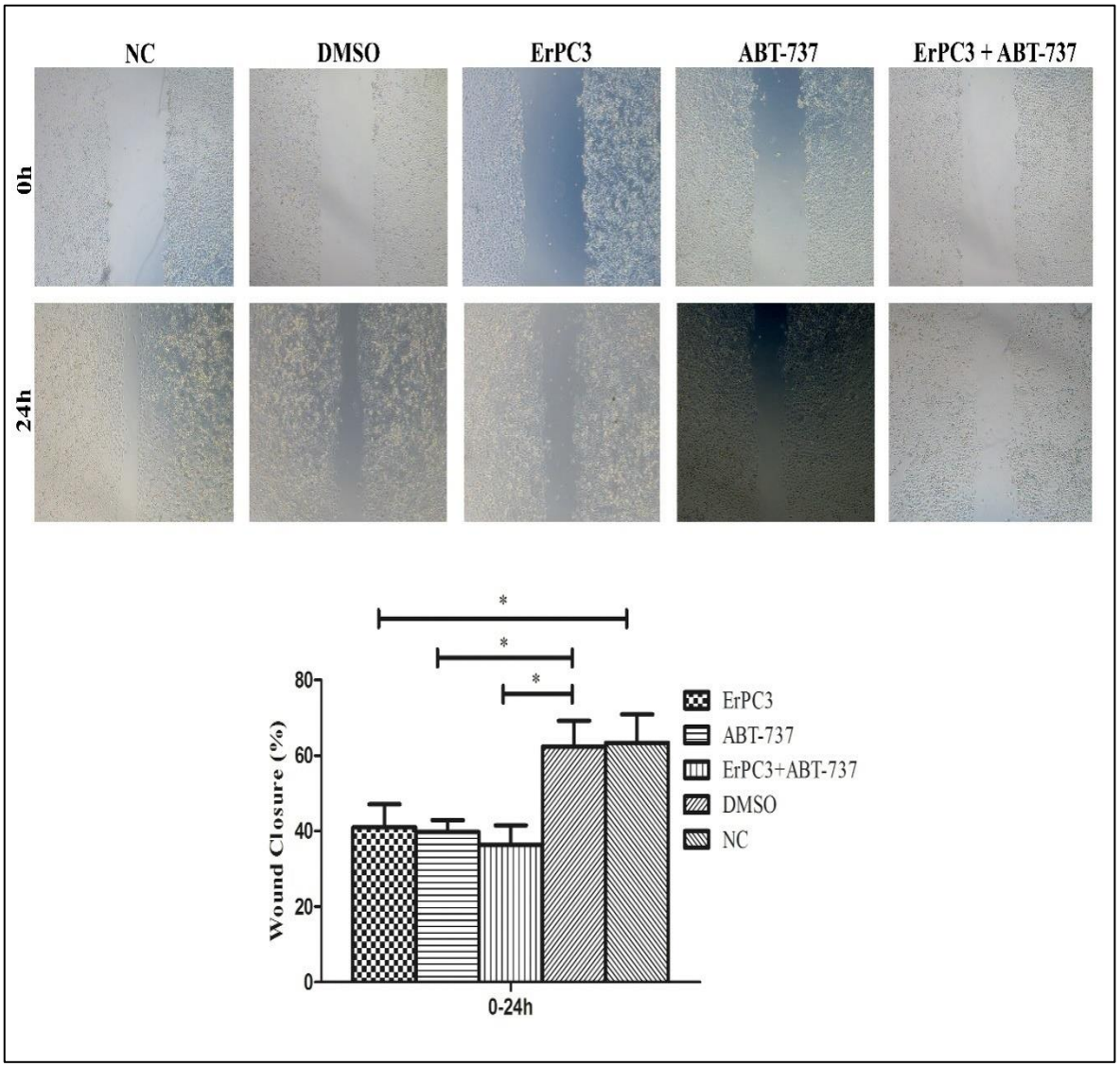

Figure 3.10. Wound healing assay following 24h treatment with ErPC3 (12.5 µM) and ABT-737 (5 µM), alone and in combination, in DU-145 cells. Representative images of ErPC3 and ABT-737 alone and in combination treated DU-145 scratches taken using inverted light microscope and wound closure rates of DU-145 cells after ErPC3 and ABT-737 alone and in combination applications. Abbreviations: NC: Negative Control (Growth medium), DMSO: Dimethyl sulfoxide (0.1% v/v) containing growth medium, *P<0.05, magnification: 40x.

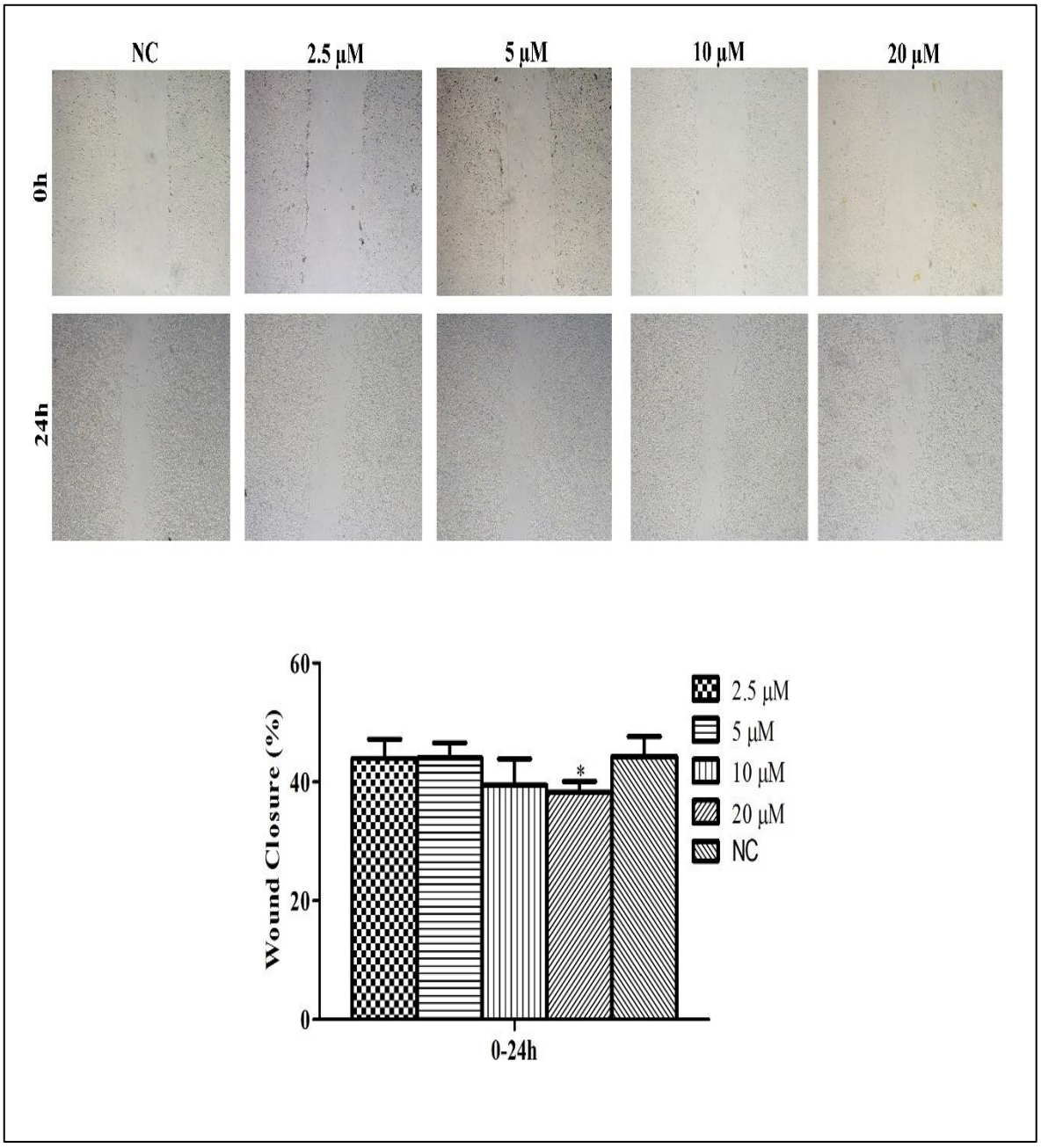

Figure 3.11. Wound healing assay following 24h treatment with ABT-737 in PNT-1A cell line. Representative images of ABT-737 treated PNT-1A scratches taken using inverted light microscope and wound closure rates of PNT-1A cells after ABT-737 application. Abbreviations: NC: Negative Control (0.1% DMSO), *P<0.05, magnification: 40x.

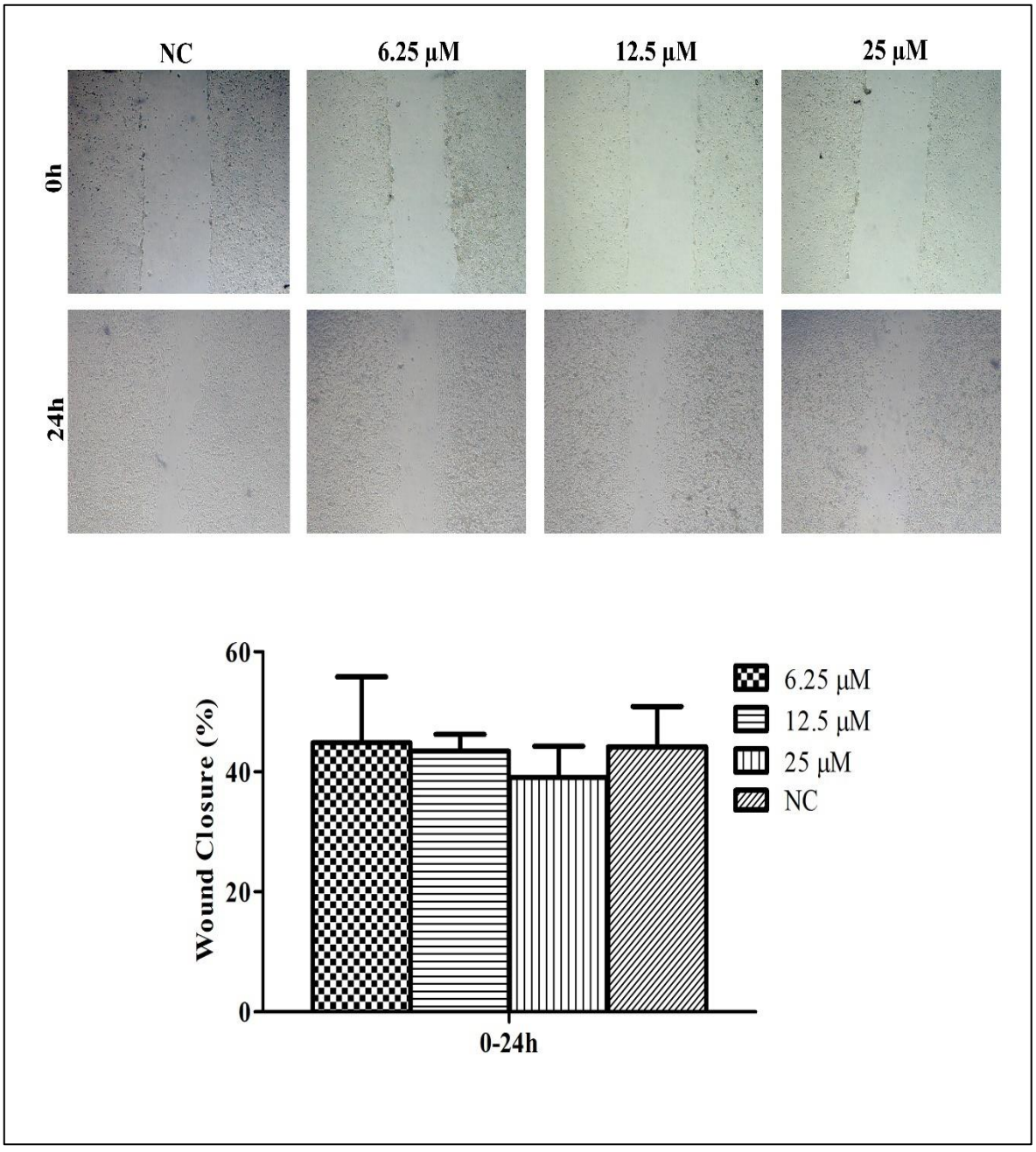

Figure 3.12. Wound healing assay following 24h treatment with ErPC3 in PNT-1A cell line. Representative images of ErPC3 treated PNT-1A scratches taken using inverted light microscope and wound closure rates of PNT-1A cells after ErPC3 application. Abbreviations: NC: Negative Control (Growth medium), *P<0.05, magnification: 40x.

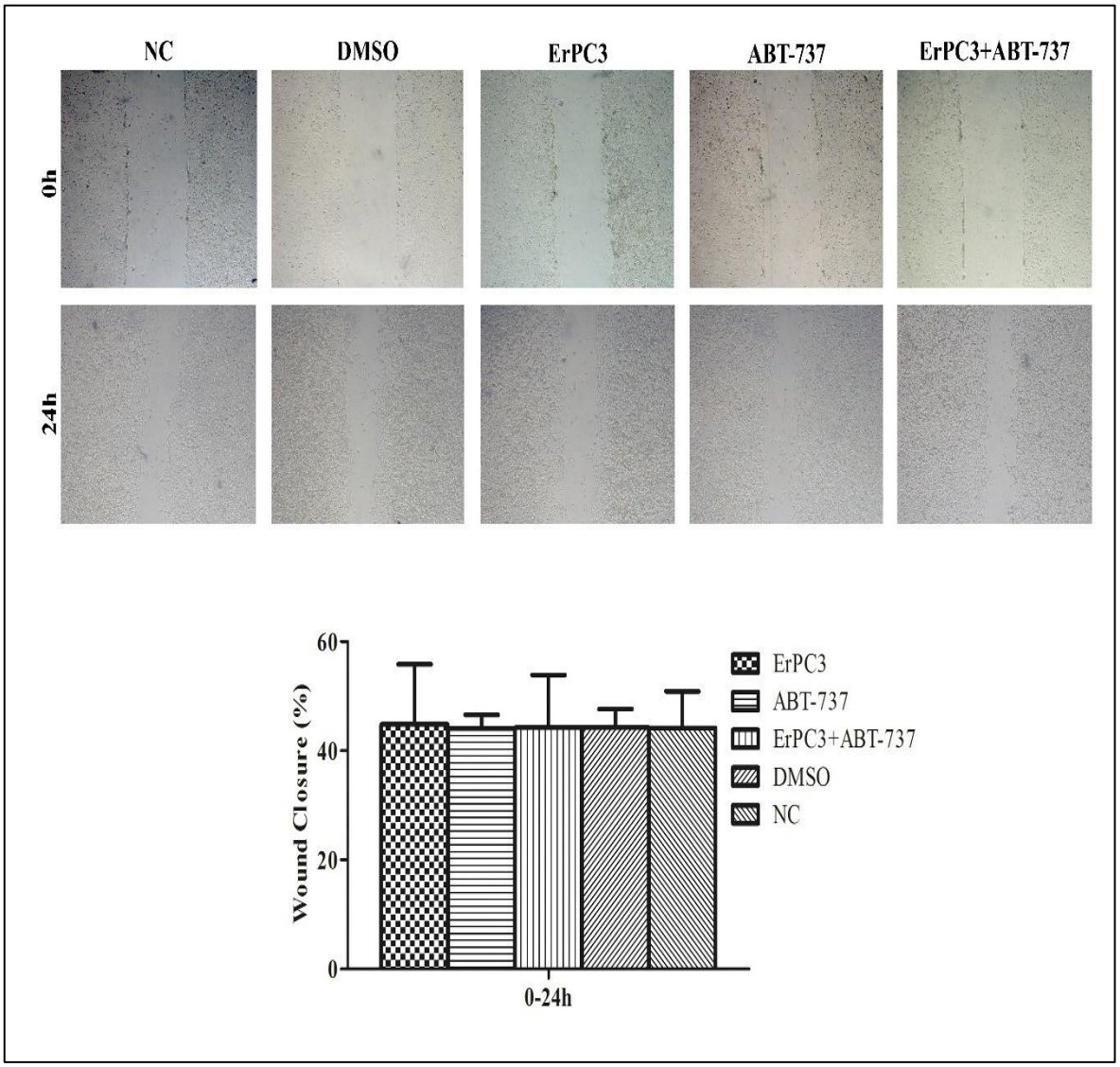

Figure 3.13. Wound healing assay following 24h treatment with ErPC3 (6.25 µM) and ABT-737 (5 µM), alone and in combination, in PNT-1A cells. Representative images of ErPC3 and ABT-737 alone and in combination treated PNT-1A scratches taken using inverted light microscope and wound closure rates of PNT-1A cells after ErPC3 and ABT-737 alone and in combination applications. Abbreviations: NC: Negative Control (Growth medium), DMSO: Dimethyl sulfoxide (0.1% v/v) containing growth medium, *P<0.05, magnification: 40x.

3.3. APOPTOSIS ANALYSIS

Apoptotic status of prostate cancer and healthy cell lines were established by Annexin V-PI assay. In PC-3 cells, following 12 and 24h of incubation, 5 μM ABT-737 elevated the percentage of total apoptotic cells to 8±2% and 30±6%, respectively, when compared to the DMSO (0.1%) group (3±2% and 6±4%, respectively). Similarly, the same incubation periods with ErPC3 at a concentration of 6.25 μM, increased the apoptotic cell percentage to 8±3% and 18±2%, respectively when compared to control group (1±1% and 0±3%, respectively). Therefore, following 12h of exposure, ABT-737 (5 μM) and ErPC3 (6.25 μM) alone showed similar effects. However, after 24h incubation period, ABT-737 (5 μM) was more effective than ErPC3 (6.25 μM). Following exposure to the combination of 6.25 μM ErPC3 and 5 μM ABT-737 for 12h and 24h, the percentage of total apoptotic cells (%) were 27±4% and 75±8%, respectively, when compared to the DMSO (0.1%) control group (3±2% and 6±4%, respectively) (Figure 3.14). In conclusion, the combination of 6.25 μM ErPC3 with 5 μM ABT-737 significantly increased the percentage of apoptotic cells as compared to the agents used individually and a synergistic effect on apoptosis was observed.

In DU-145 cells, after 12h/24h of incubation, 50 μM ErPC3, significantly elevated the percentage of total apoptotic cells to 16±2% / 42±2%, respectively (vs 6±1% / 0±2% control group). In addition, 5 μM ABT-737, and 50 μM ErPC3 plus 5 μM ABT-737 significantly elevated the percentage of total apoptotic cells to 5±2% / 9±3%, and 11±2% / 27±4%, respectively (vs 2±1% and 9±1% control group). Following 12h and 24h, 5 μM ABT-737 did not display any significant effect when compared to the DMSO (0.1%) group (2±1% and 9±1%), respectively (Figure 3.15). Therefore, after 12h and 24h, the combination of 5 μM ABT-737 plus 50 μM ErPC3 significantly elevated the total apoptotic cells compared to control group. These findings indicate that 50 μM ErPC3 treatment was more effective than 5 μM ABT-737 plus 50 μM ErPC3 combination treatment.

In PNT-1A cells, after 12h and 24h, 6.25 μM ErPC3 treatment elevated the percentage of total apoptotic cells to 6±2% and 1±0.3% compared to the NC group (0±0.4% and 0±0.5%), respectively. The same incubation periods, 5 μM ABT-737 significantly elevated the apoptotic cell percentage to 12±4% and 5±1, compared to the DMSO (0.1%) group (3±1% and 1±0.3%), respectively. Following 12h and 24h, the combination of 5 μM ABT-737 plus

6.25 µM ErPC3 significantly elevated the percentage of total apoptotic cells to 6 ±1% and 5±1% compared to control group, respectively (Figure 3.16). According to these results, after 12h, 5 µM ABT-737 had a higher apoptotic effect than the other groups did. After 24h, ABT-737 treatment and ABT-737 / ErPC3 combination showed similar effects and their apoptotic effects were greater than 6.25 µM ErPC3.

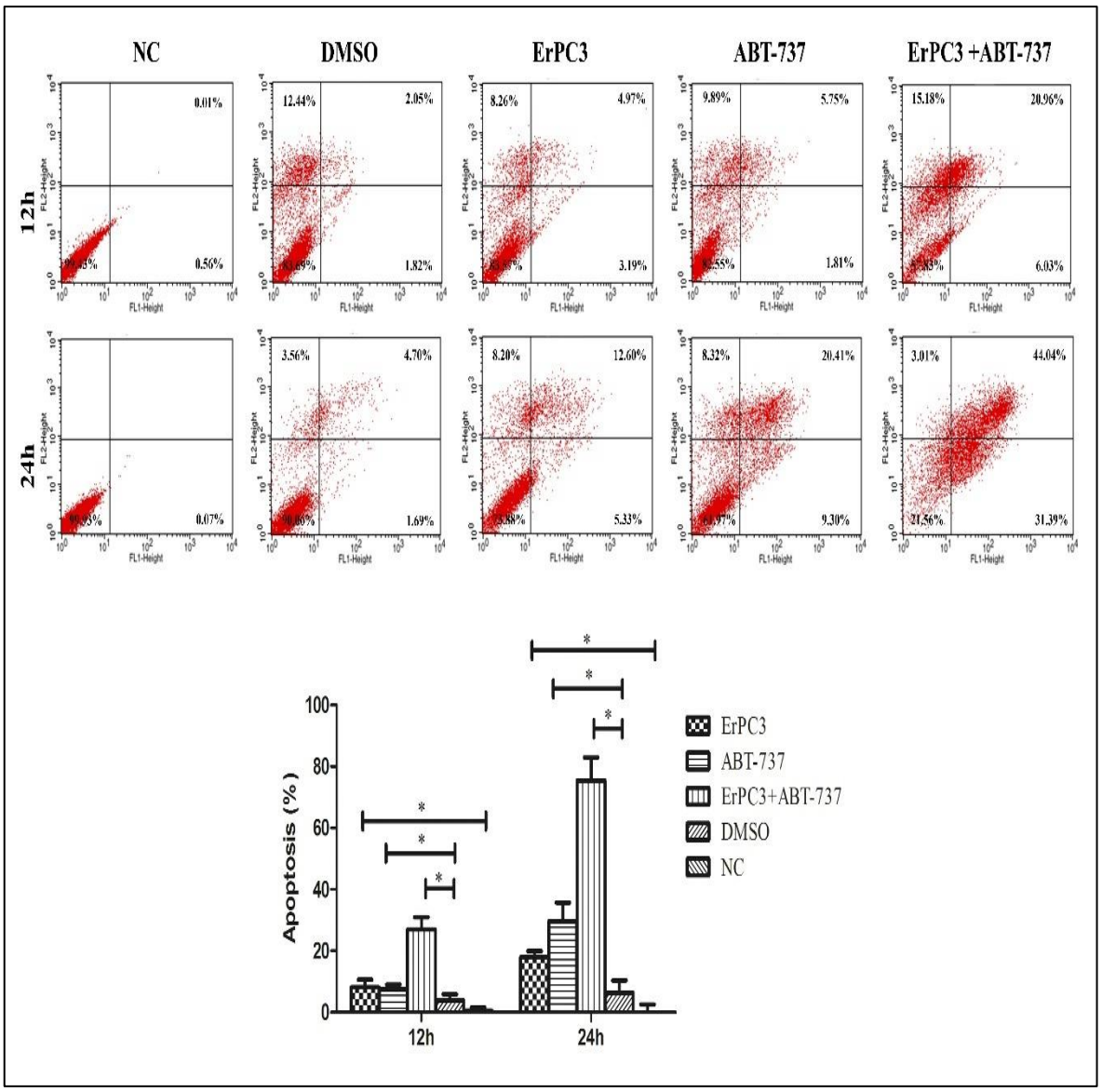

Figure 3.14. Apoptosis analysis by Annexin-V assay following 12h and 24h exposure to ErPC3 (6.25 µM) and ABT-737 (5 µM), alone and in combination in PC-3 cell line. Abbreviations: NC: negative control (growth medium), DMSO: dimethyl sulfoxide (0.1% v/v) containing growth medium, *P<0.05.

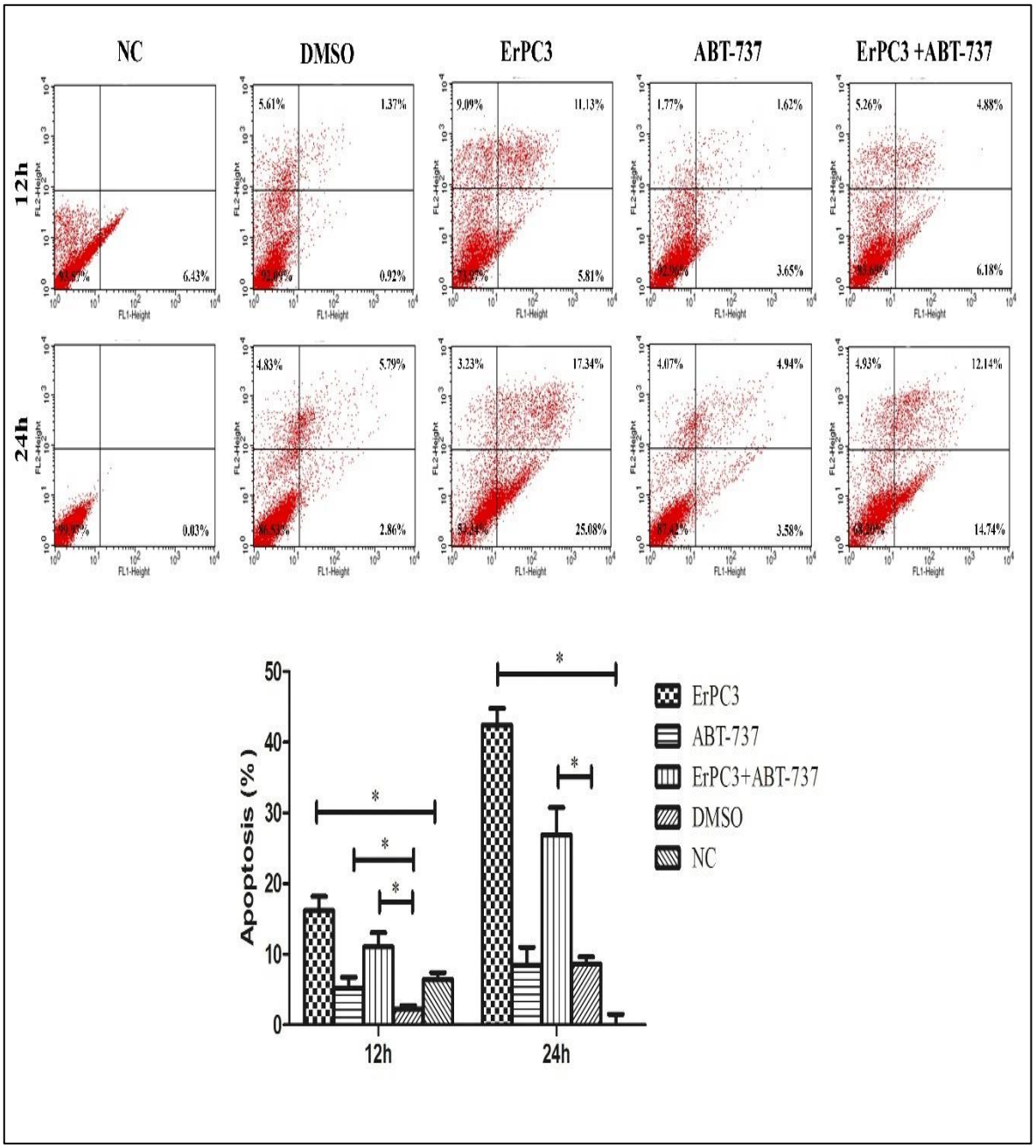

Figure 3.15. Apoptosis analysis by Annexin-V assay following 12h and 24h exposure to ErPC3 (50 µM) and ABT-737 (5 µM), alone and in combination in DU-145 cell line. Abbreviations: NC: Negative Control (Growth medium), DMSO: Dimethyl sulfoxide (0.1% v/v) containing growth medium, *P<0.05.

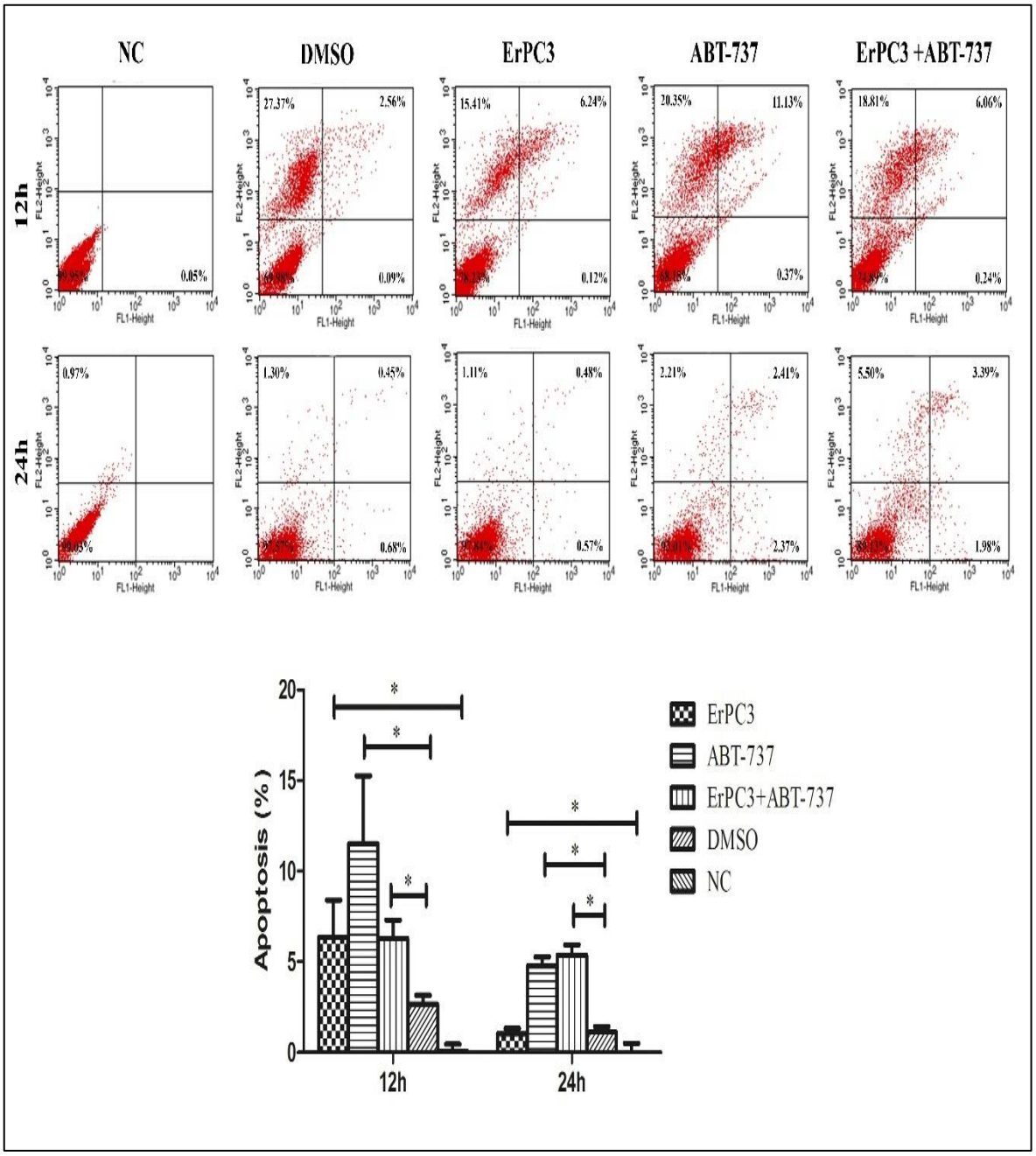

Figure 3.16. Apoptosis analysis by Annexin-V assay following 12h and 24h exposure to ErPC3 (6.25 μM) and ABT-737 (5 μM), alone and in combination in PNT-1A cell line. Abbreviations: NC: Negative Control (Growth medium), DMSO: Dimethyl sulfoxide (0.1% v/v) containing growth medium, *P<0.05.

3.4. CELL CYCLE ANALYSIS

To examine the cell cycle phase distribution in prostate cancer and healthy cells following exposed to ErPC3, ABT-737 alone and in combination for 24h, flow cytometry was performed.

In PC-3 cells, 6.25 μM ErPC3 treated cells had 35.38±0.5% of cells in G0/G1, 9.36±1% of cells in S and 55.26±1.5% of cells in G2/M phases (vs the control group: 54.66±2% of cells in G0/G1, 13.48±1% of cells in S and 31.86±1% of cells in G2/M phases). 6.25 μM ErPC3 decreased the percentage of cells in the G0/G1 and S phases and increased the percentage of cells in the G2/M phase. 5 μM ABT-737 treated cells had 52.60±0.6% of cells in G0/G1, 13.65±0.6% of cells in S and 33.75±0.7% of cells in G2/M phases (vs the DMSO 0.1% control group 48.33±1% of cells in G0/G1, 14.10±0.1% of cells in S and 37.56±1% of cells in G2/M phases). 5 μM ABT-737 decreased the percentage of cells in the S and G2/M phases and elevated the percentage of cells in the G0/G1 phase. Cells were treated with the combination of 6.25 μM ErPC3 plus 5 μM ABT-737, had 43.78±1%, of cells in G0/G1, 16.30±0.5% of cells in S and 39.92±0.2% of cells in G2/M phases when compared to the control group (vs the DMSO 0.1% control group 48.33±1%, 14.10±0.1%, and 37.56±1% of cells in G0/G1, S and G2/M phases, respectively) (Figure 3.17). According to these results, ABT-737 induced the accumulation of cells at the G0/G1 phase, whereas ErPC3 caused G2/M cell cycle arrest. However, ErPC3 is more effective on cell cycle phase distribution when compared to the combination of ABT-737 plus ErPC3 in PC-3 cells.

In DU-145 cells, 50 μM ErPC3 treated cells had 41.70±1% of cells in G0/G1, 8.79±1% of cells in S, and 49.51±2% of cells in G2/M phases (vs the control group: 57.10±2% of cells in G0/G1, 17.01±1% of cells in S and 25.88±2% of cells in G2/M phases). 50 μM ErPC3 decreased the percentage of cells in the G0/G1 and S phases and increased the percentage of cells in the G2/M phase. 5 μM ABT-737 treated cells had 54.8±1% of cells in G0/G1, 13.5±0.3% of cells in S and 31.92±0.5% of cells in G2/M phases (vs the DMSO 0.1% control group 49.68±1% of cells in G0/G1, 16.32±0.5% of cells in S and 34±0.5% of cells in G2/M phases). 5 μM ABT-737 decreased the percentage of cells in the S and G2/M phases and elevated the percentage of cells in the G0/G1 phase. Cells were treated with the combination of 50 μM ErPC3 plus 5 μM ABT-737, had 35.78±0.5% of cells in G0/G1, 8.58±1% of cells

in S and 55.64±1.5% of cells in G2/M phases when compared to the control group (vs the DMSO (0.1%) control group) (Figure 3.18). According to these results, ABT-737 triggered accumulation of cells at the G0/G1 phase, whereas ErPC3 caused G2/M cell cycle arrest. The combination of ABT-737 plus ErPC3 significantly decreased cells in the G0/G1 phase but induced accumulation of cells in the G2/M phase when compared to ErPC3 alone. These results point that ABT-737 plus ErPC3 combination enhances cell cycle arrest in the G2/M phase in DU-145 cells.

In PNT-1A cells exposed to 6.25 μM ErPC3, 50.11±1% of cells in G0/G1, 15.85±0.2% of cells in S and 34.04±0.5% of cells in G2/M phases (vs the control group: 51.88±2% of cells in G0/G1, 17.60±0.5% of cells in S and 29.12±1% of cells in G2/M phases). 6.25 μM ErPC3 reduced the percentage of cells in the S phase and elevated the percentage of cells in the G2/M phase. 5 μM ABT-737 displayed no significant effect in PNT-1A cells. 5 μM ABT-737 treated cells had 49.91±2.5% of cells in G0/G1, 19.31±2% of cells in S and 30.78±1% of cells in G2/M phases (vs the DMSO 0.1% group 51.50±2% of cells in G0/G1, 15.26±2.5% of cells in S and 34.23±3% of cells in G2/M phases). The combination of 6.25 μM ErPC3 plus 5 μM ABT-737 cells had 49.59±1% of cells in G0/G1, 16.42±1% of cells in S and 33.99±1.5% of cells in G2/M phases when compared to control group (vs the DMSO (0.1%) group) (Figure 3.19). According to the overall results, ErPC3 triggered cell accumulation at G2/M phase whereas ABT-737 and ABT-737 plus ErPC3 had no influence on cell cycle phase distribution in PNT-1A cells.

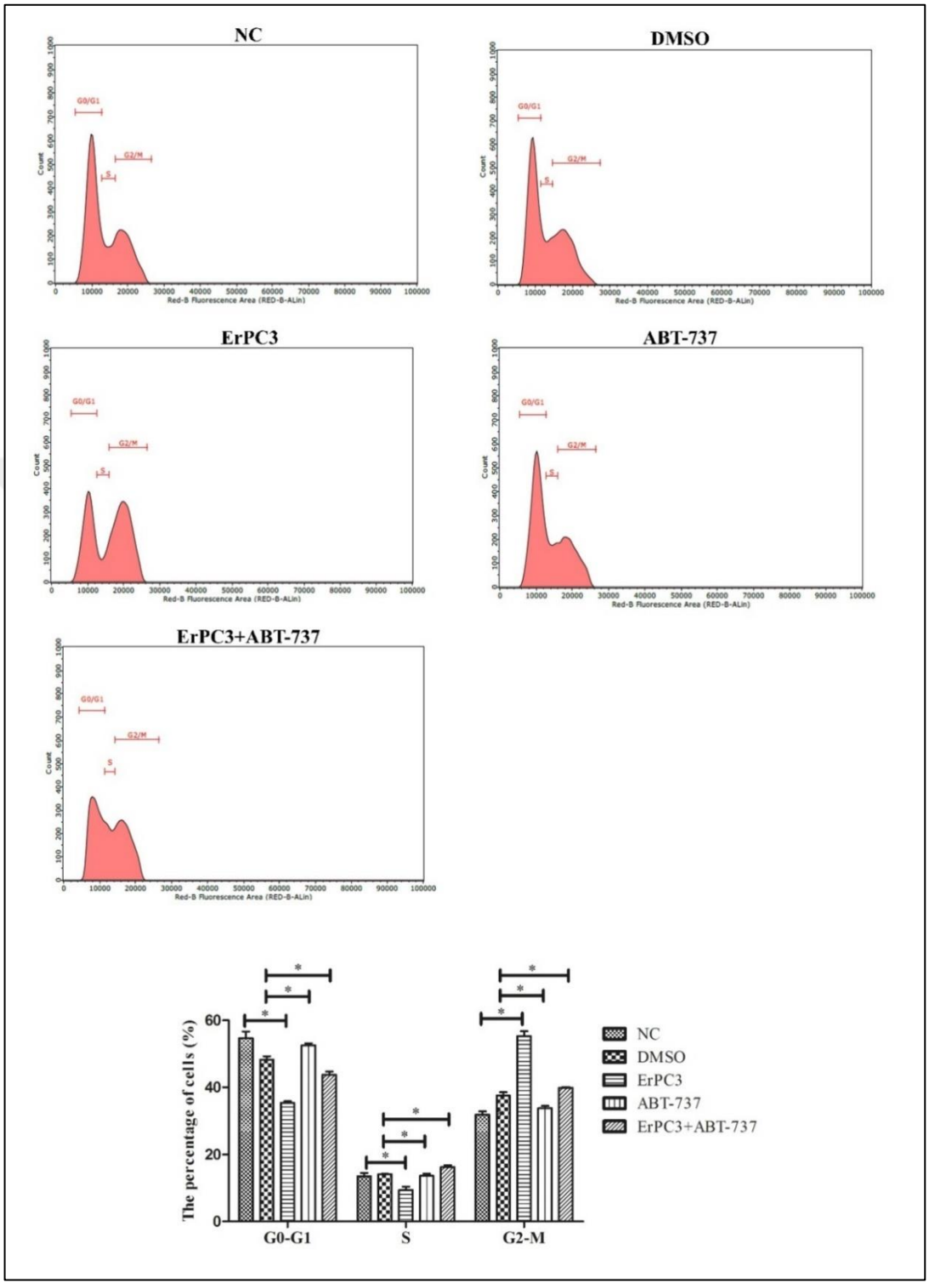

Figure 3.17. Cell cycle phase distribution following 24h treatment with ErPC3 (6.25 µM) and ABT-737 (5 µM) alone and in combination in PC-3 cell line. Abbreviations: NC: Negative Control (Growth medium), DMSO: Dimethyl sulfoxide (0.1% v/v) containing growth medium, *P<0.05.

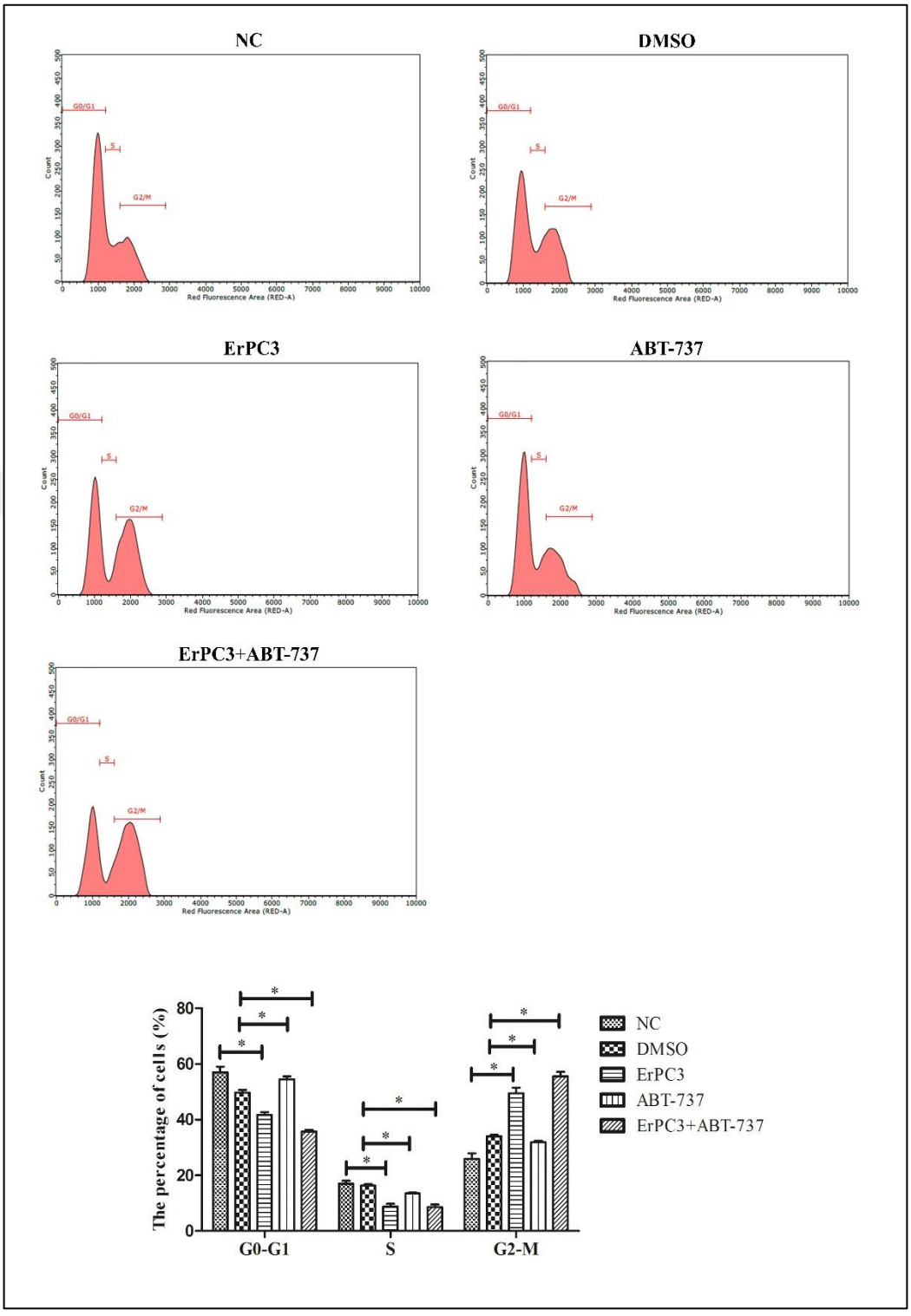

Figure 3.18. Cell cycle phase distribution following 24h treatment with ErPC3 (50 µM) and ABT-737 (5 µM) alone and in combination in DU-145 cell line. Abbreviations: NC: Negative Control (Growth medium), DMSO: Dimethyl sulfoxide (0.1% v/v) containing growth medium, *P<0.05.

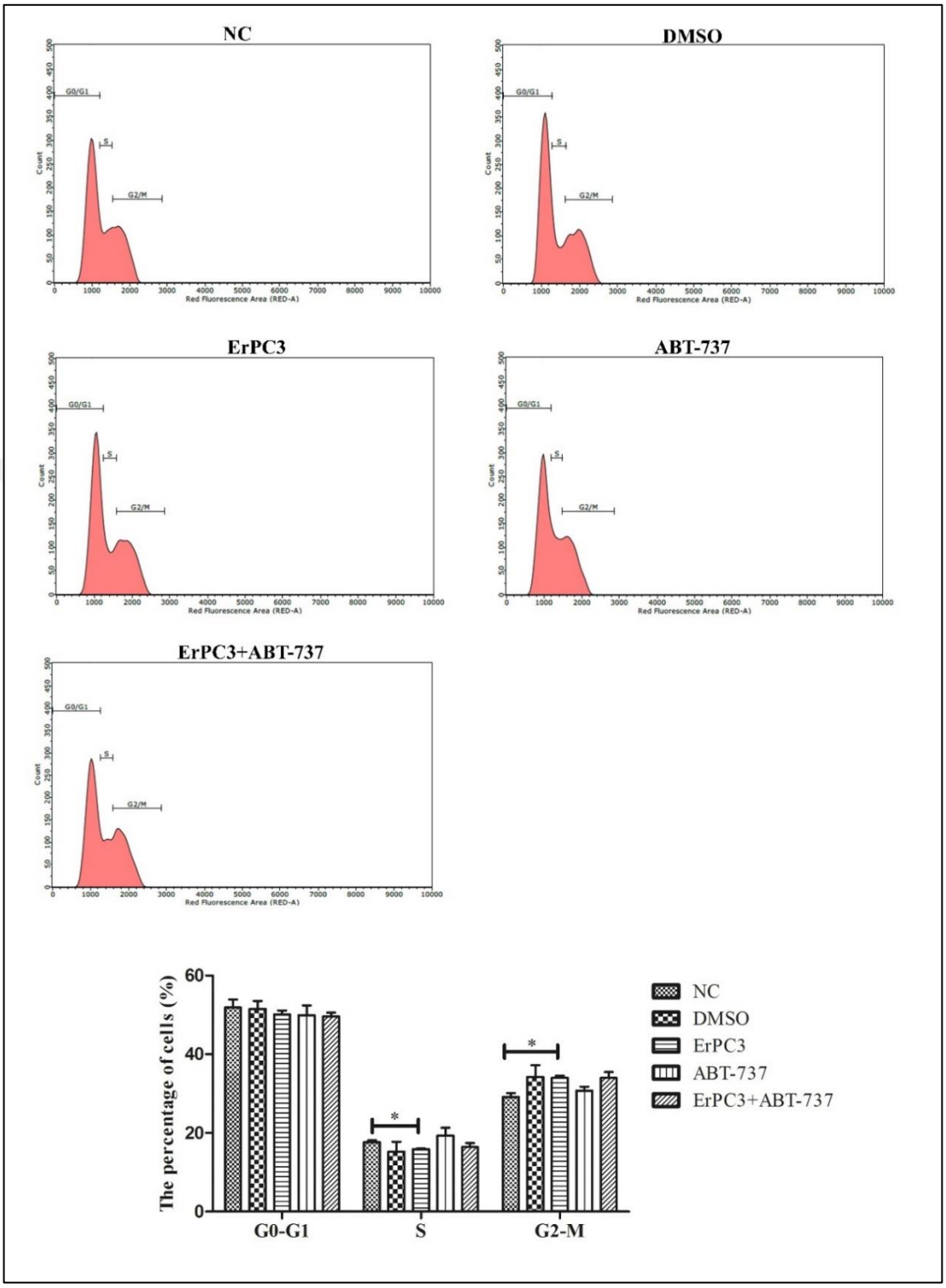

Figure 3.19. Effects of various concentrations of ErPC3 (6.25 μM) and ABT-737 (5 μM) on the cell cycle phase distribution analysis of PNT-1A at 24h. Abbreviations: NC: Negative Control (Growth medium), DMSO: Dimethyl sulfoxide (0.1% v/v) containing growth medium, *P<0.05.

3.5. REAL TIME PCR (RT-PCR) ANALYSIS

PC-3, DU-145 and PNT-1A cells were treated with ABT-737, ErPC3 and their combinations in order to check gene expression levels of apoptotic markers.

In PC-3 cells, Akt mRNA levels reduced in 6.25 μM ErPC3 and 5 μM ABT-737 plus 6.25 μM ErPC3-treated groups whereas high AKT expression was detected in 5 μM ABT-737-treated group (≈1.5-fold). Bcl-2 mRNA levels reduced in 5 μM ABT-737 and 5 μM ABT-737 plus 6.25 μM ErPC3-treated groups whereas high BCL-2 expression was detected in 6.25 μM ErPC3-treated group (≈1.5-fold). On the other hand, 6.25 μM ErPC3, 5 μM ABT-737 and combining ABT-737 with ErPC3 decreased AKT, BCL-2 and NF-κB gene expression levels (Figure 3.20).

In DU-145 cells, RT-PCR assay results showed that AKT gene levels significantly decreased in 50 μM ErPC3 (≈2.5-fold) and 5 μM ABT-737 plus 50 μM ErPC3-treated groups (≈1.5-fold) and increased in 5 μM ABT-737 treated group when compared to control group. BCL-2 gene level enhanced in 50 μM ErPC3-treated group for an approximately ≈2.5-fold, while 5 μM ABT-737 application reduced BCL-2 mRNA levels. 5 μM ABT-737 plus 50 μM ErPC3 application did not significantly change BCL-2 gene expression level. NF-κB gene expression level significantly decreased ≈2-fold in 5 μM ABT-737 group. 50 μM ErPC3 and 5 μM ABT-737 plus 50 μM ErPC3 treatments did not significantly differ NF-κB mRNA levels (Figure 3.21).

In PNT-1A cells, AKT, BCL-2 and NF-κB gene levels in all experimental groups did not significantly different from control group (Figure 3.22).

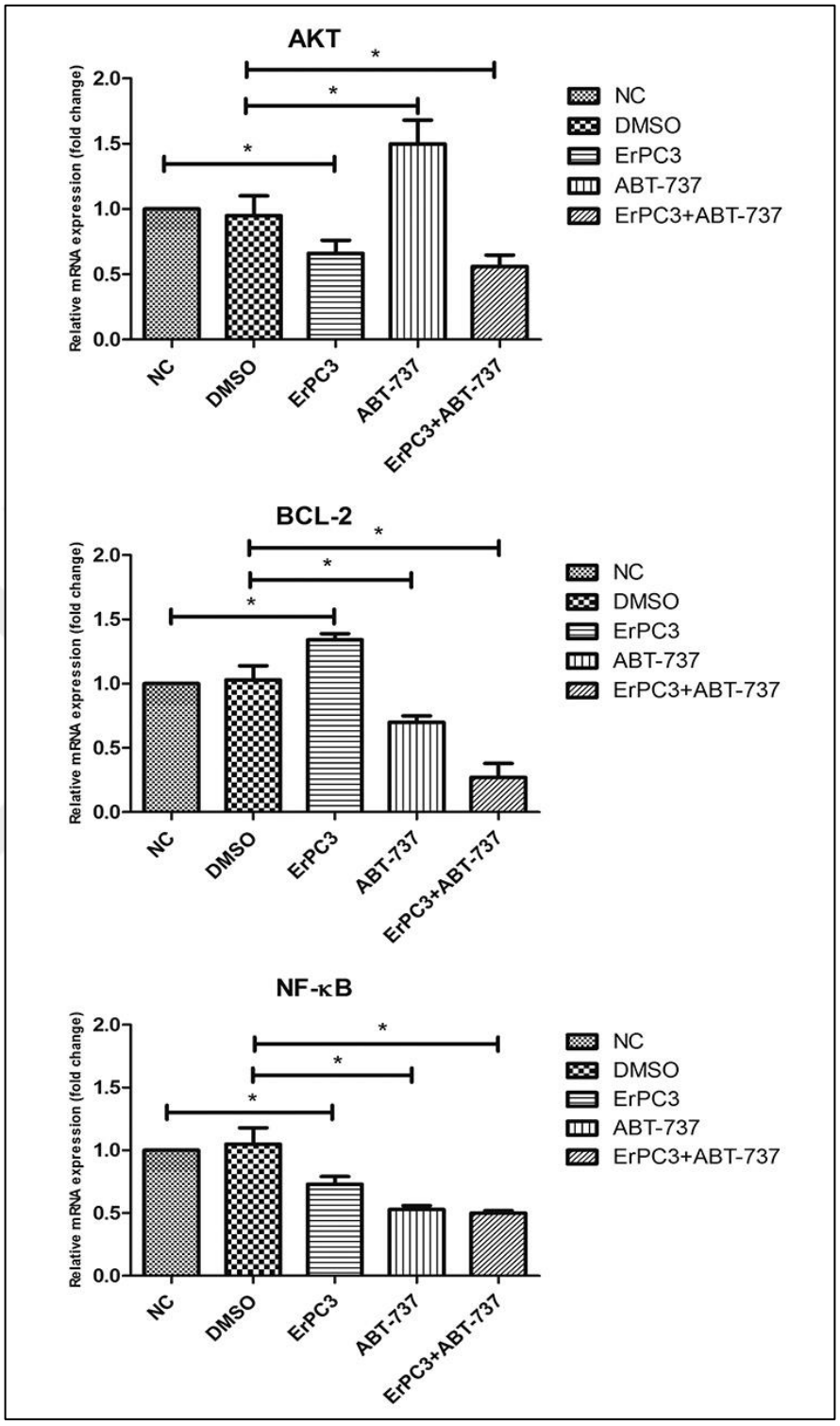

Figure 3. 20. Effects of various concentrations of ErPC3 (6.25 μM) and ABT-737 (5 μM) on gene expression levels of PC-3 cells at 12h. Abbreviations: NC: Negative Control (Growth medium), DMSO: Dimethyl sulfoxide (0.1% v/v) containing growth medium, *P<0.05.

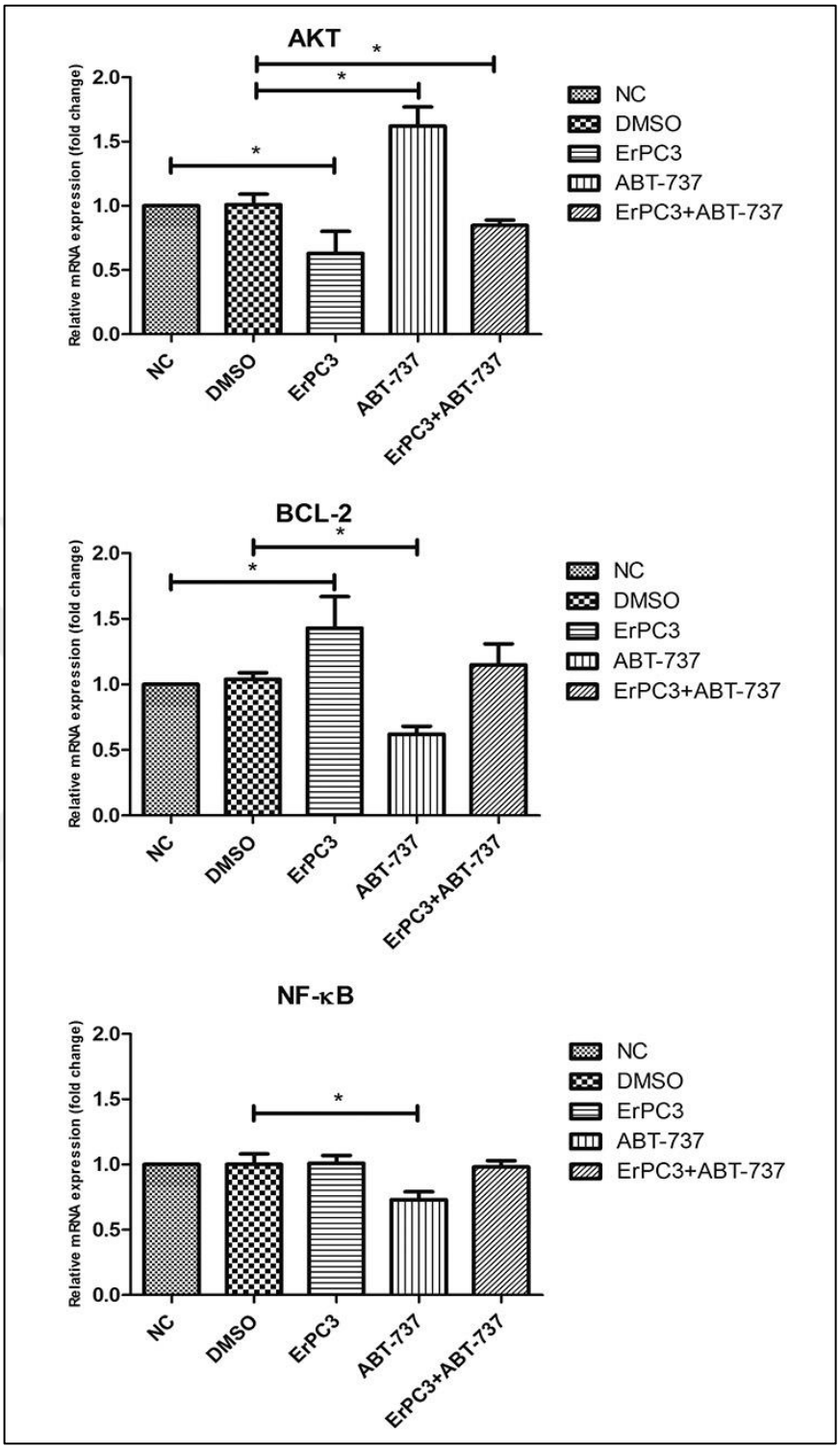

Figure 3. 21. Effects of various concentrations of ErPC3 (50 μM) and ABT-737 (5 μM) on gene expression levels of DU-145 cells at 12h. Abbreviations: NC: Negative Control (Growth medium), DMSO: Dimethyl sulfoxide (0.1% v/v) containing growth medium, *P<0.05.

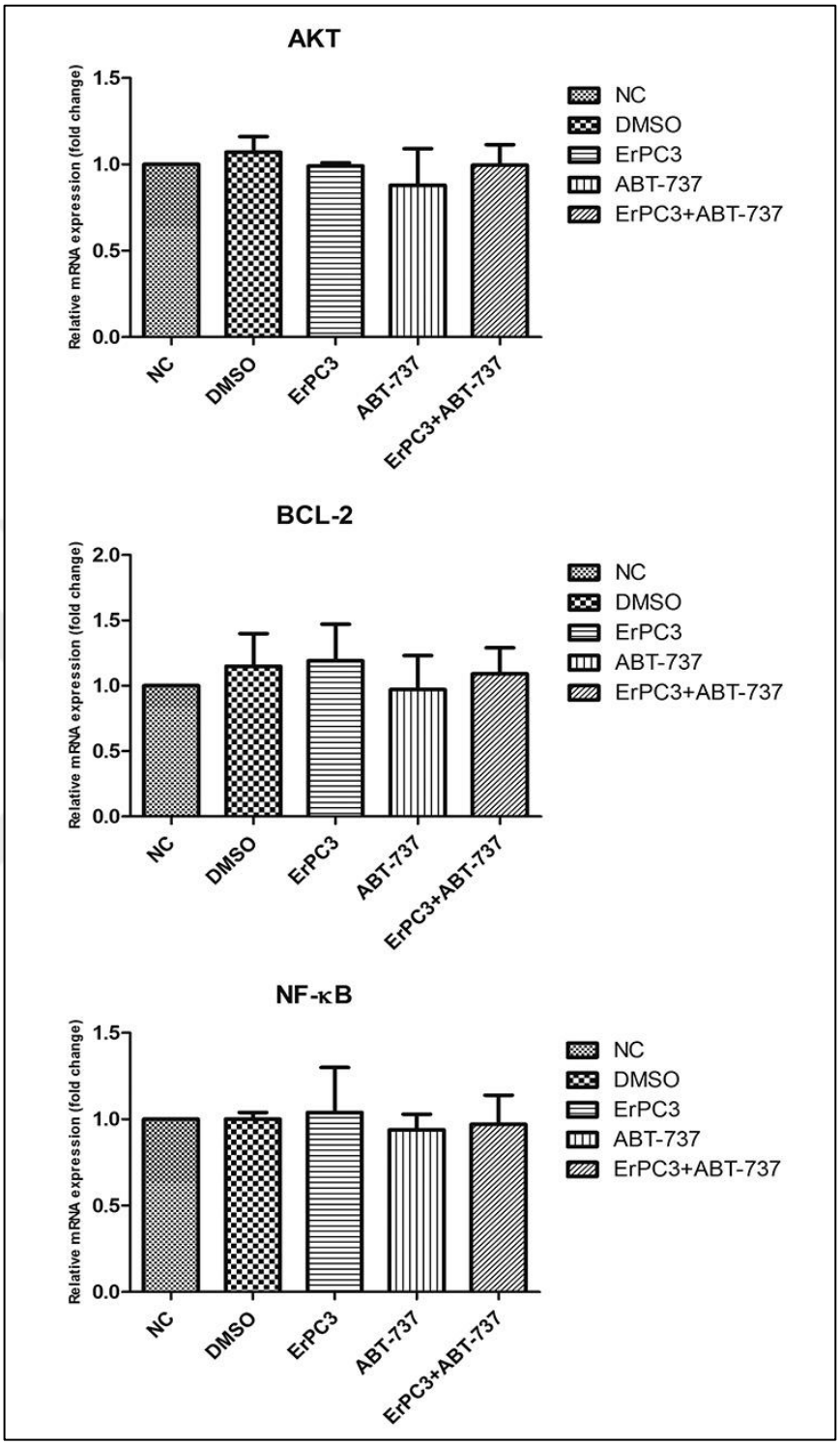

Figure 3. 22. Effects of various concentrations of ErPC3 (6.25 μM) and ABT-737 (5 μM) on gene expression levels of PNT-1A cells at 12h. Abbreviations: NC: Negative Control (Growth medium), DMSO: Dimethyl sulfoxide (0.1% v/v) containing growth medium, *P<0.05.

3.6. WESTERN BLOT ANALYSIS

Bcl-2, Bcl-xL, p-NF-κB Mcl-1, Bak, c-parp, c-caspase 3, c-caspase 9, Akt and p-Akt protein levels were determined in prostate cancer and healthy cell lines for 12h treatment with ErPC3, ABT-737 alone and in combination by using western blot analysis.

In PC-3 cells, following 12h of incubation, Bcl-2 protein level significantly decreased after 6.25 μM ErPC3 (~0.2-fold), 5 μM ABT-737 (~0.5-fold) and 6.25 μM ErPC3 plus 5 μM ABT-737 (~0.7-fold) treatment. Bcl-2 protein level in 6.25 μM ErPC3 plus 5 μM ABT-737 treated cells was significantly lower than control (DMSO 0.1%), ErPC3 and ABT-737 groups. Bcl-xL protein level significantly decreased in 5 μM ABT-737 (~0.1-fold) alone and 6.25 μM ErPC3 plus 5 μM ABT-737 (~0.1-fold)-treated cells but no significant change was observed in 6.25 μM ErPC3-treated cells when compared to the NC group. Mcl-1 level significantly reduced in 6.25 μM ErPC3 (~0.3-fold) and 6.25 μM ErPC3 plus 5 μM ABT-737 (~0.4-fold)-treated cells when compared to 5 μM ABT-737 and control group. p-NF-κB protein level significantly decreased after 6.25 μM ErPC3 (~0.1-fold), 5 μM ABT-737 (~0.2-fold) and 6.25 μM ErPC3 plus 5 μM ABT-737(~0.4-fold) treatment. p-NF-κB expression in 6.25 μM ErPC3 plus 5 μM ABT-737 treated cells was significantly lower than control (DMSO 0.1%), ErPC3 and ABT-737 groups (Figure 3.23).

Bak, c-caspase 9 and cleaved PARP protein levels did not change significantly in PC-3 cells treated with 6.25 μM ErPC3, 5 μM ABT-737, and 6.25 μM ErPC3 plus 5 μM ABT-737 when compared to the NC group. c-caspase 3 expression in ABT-737 and ErPC3 treated cells was not significantly different from control group. However, caspase 3 protein level significantly decreased 0.5-fold on average by ABT-737 plus ErPC3 combination treatment (Figure 3.24).

Akt and p-Akt protein levels were significantly reduced in 6.25 μM ErPC3 and 6.25 μM ErPC3 plus 5 μM ABT-737-treated cells when compared to the control group. Akt protein level decreased approximately by ~0.3-fold and ~0.5-fold after 6.25 μM ErPC3 and 6.25 μM ErPC3 plus 5 μM ABT-737 treatments, respectively, when compared to the NC group. p-Akt protein level was significantly decreased in 6.25 μM ErPC3 (~0.4-fold) and 6.25 μM ErPC3 plus 5 μM ABT-737 (~0.3-fold)-treated cells, respectively, when compared to the control group. 6.25 μM ErPC3 significantly reduced p-Akt level when compared to 6.25 μM

ErPC3 plus 5 μM ABT-737. 5 μM ABT-737 alone did not change Akt and p-Akt protein levels (Figure 3.25).

In DU-145 cells, following 12h of incubation, Bcl-2 protein level significantly decreased by 50 μM ErPC3 plus 5 μM ABT-737 (~0.8-fold) treatment when compared to the control group (DMSO 0.1%). Bcl-2 protein level did not change in 50 μM ErPC3 and 5 μM ABT-737 treated cells. Bcl-xL protein level increased in 5 μM ABT-737 (~0.1-fold)-treated cells and did not change significantly in 50 μM ErPC3 and 50 μM ErPC3 plus 5 μM ABT-737-treated cells when compared to the NC group. Mcl-1 level significantly elevated in 50 μM ErPC3 (~4-fold) and 50 μM ErPC3 plus 5 μM ABT-737 (~4-fold)-treated cells and did not change significantly in 5 μM ABT-737 when compared to the control group. p-NF-κB protein level did not significantly different from the 50 μM ErPC3, 5 μM ABT-737, and 50 μM ErPC3 plus 5 μM ABT-737 groups when compared to the control group (Figure 3.26).

Bak protein level significantly increased in 50 μM ErPC3 (~0.1-fold), 50 μM ErPC3 (~0.4-fold) and 50 μM ErPC3 plus 5 μM ABT-737 (~0.3-fold)-treated cells when compared to the NC group. Cleaved PARP level significantly increased in 5 μM ABT-737 (~0.1-fold) and 50 μM ErPC3 plus 5 μM ABT-737 (~0.4-fold)-treated cells and decreased in 50 μM ErPC3 (~0.3-fold) when compared to the control group. Cleaved caspase 3 expression significantly decreased in 50 μM ErPC3 (~0.3-fold), 5 μM ABT-737 (~0.2-fold) and 50 μM ErPC3 plus 5 μM ABT-737 (~0.3-fold)-treated cells when compared to the NC group. Cleaved caspase 9 level significantly increased in 50 μM ErPC3 plus 5 μM ABT-737 (~0.1-fold)-treated cells and did not change significantly in 50 μM ErPC3 and 5 μM ABT-737 when compared to the control group (Figure 3.27).

Akt level significantly decreased approximately by ~0.8-fold and ~0.3-fold following 50 μM ErPC3 and 50 μM ErPC3 plus 5 μM ABT-737 treatments, respectively and significantly increased in 5 μM ABT-737 (~0.4-fold) when compared to the NC group. p-Akt level significantly reduced in 50 μM ErPC3 (~0.6-fold)-treated cells, when compared to the control group. 5 μM ABT-737 and 50 μM ErPC3 plus 5 μM ABT-737 did not change p-Akt level significantly (Figure 3.28).

In PNT-1A cells, following 12h of incubation, Bcl-2 and p-NF-κB protein levels did not change in 50 μM ErPC3, 5 μM ABT-737 and combined drug-treated cells. Bcl-xL protein

level significantly decreased in 5 μM ABT-737 (~0.3-fold)-treated cells and did not change in 6.25 μM ErPC3 and 6.25 μM ErPC3 plus 5 μM ABT-737-treated cells when compared to the NC group. Mcl-1 level significantly decreased in 6.25 μM ErPC3 (~0.3-fold) and 5 μM ABT-737 (~0.4-fold)-treated cells and did not change significantly in combined drug application when compared to the NC group (Figure 3.29).

Bak protein level significantly decreased in 6.25 μM ErPC3 (~0.2-fold) and 5 μM ABT-737 (~0.3-fold)-treated cells when compared to the control group. c-PARP expression was about ~0.3-fold higher in 6.25 μM ErPC3 when compared to the NC group. c-caspase 3 significantly reduced in 5 μM ABT-737 (~0.1-fold) and increased in 6.25 μM ErPC3 (~0.2-fold)-treated cells when compared to the NC group. c-caspase 9 level significantly decreased in 6.25 μM ErPC3 (~0.3-fold)-, 5 μM ABT-737 (~0.2-fold)- and 6.25 μM ErPC3 plus 5 μM ABT-737 (~0.2-fold)-treated cells when compared to the NC group (Figure 3.30).

Akt protein level in 6.25 μM ErPC3, 5 μM ABT-737 and 6.25 μM ErPC3 plus 5 μM ABT-737-treated cells did not significantly different from control group. p-Akt protein level significantly decreased in 6.25 μM ErPC3 plus 5 μM ABT-737 (~0.3-fold)-treated cells, when compared to the control group. 5 μM ABT-737 and 6.25 μM ErPC3 did not change p-Akt protein level significantly (Figure 3.31).

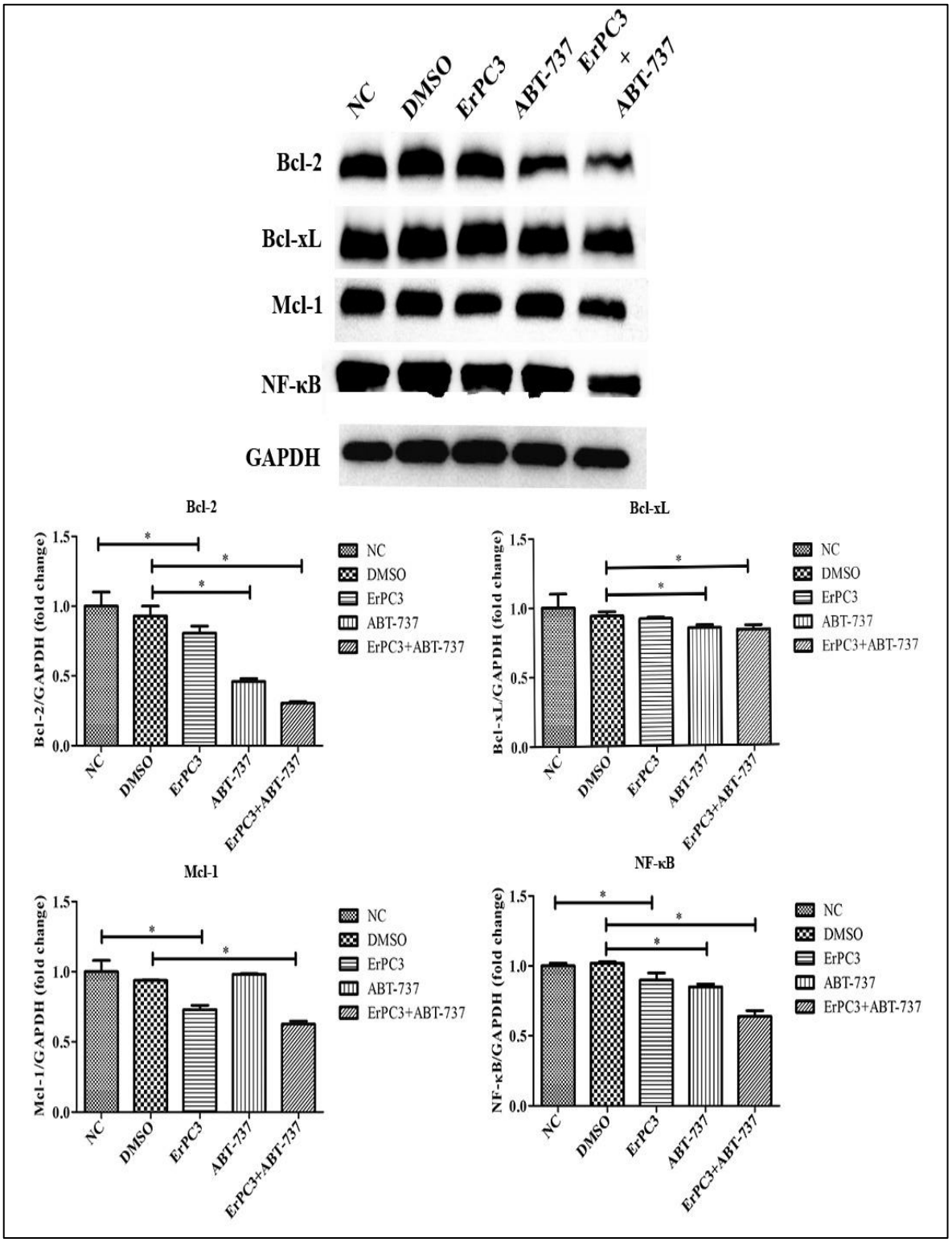

Figure 3. 23. Effects of various concentrations of ErPC3 (6.25 μM) and ABT-737 (5 μM) on the western blot analysis of PC-3 at 12h. Abbreviations: NC: Negative Control (Growth medium), DMSO: Dimethyl sulfoxide (0.1% v/v) containing growth medium, *P<0.05.

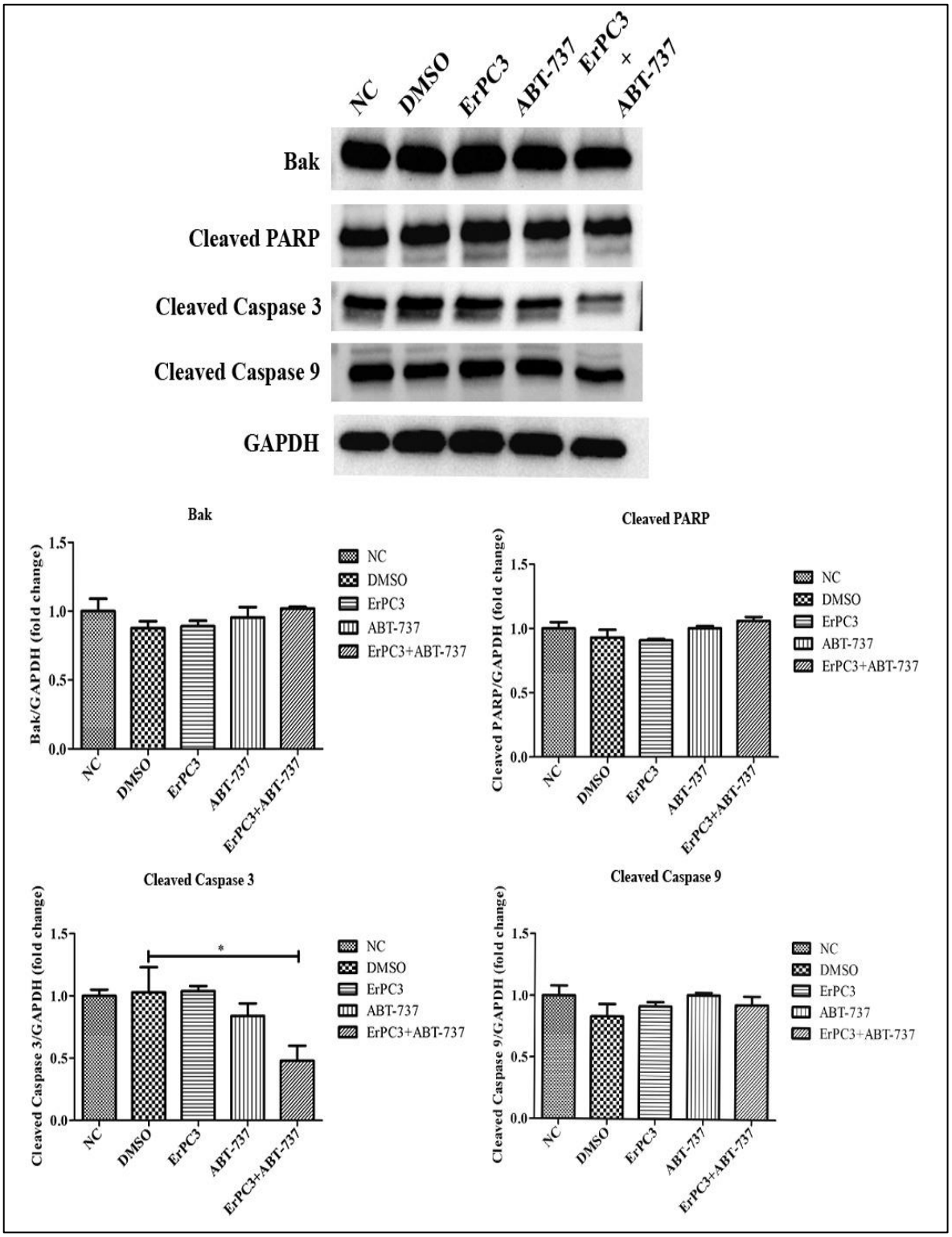

Figure 3. 24. Effects of various concentrations of ErPC3 (6.25 μM) and ABT-737 (5 μM) on the western blot analysis of PC-3 at 12h. Abbreviations: NC: Negative Control (Growth medium), DMSO: Dimethyl sulfoxide (0.1% v/v) containing growth medium, *P<0.05.

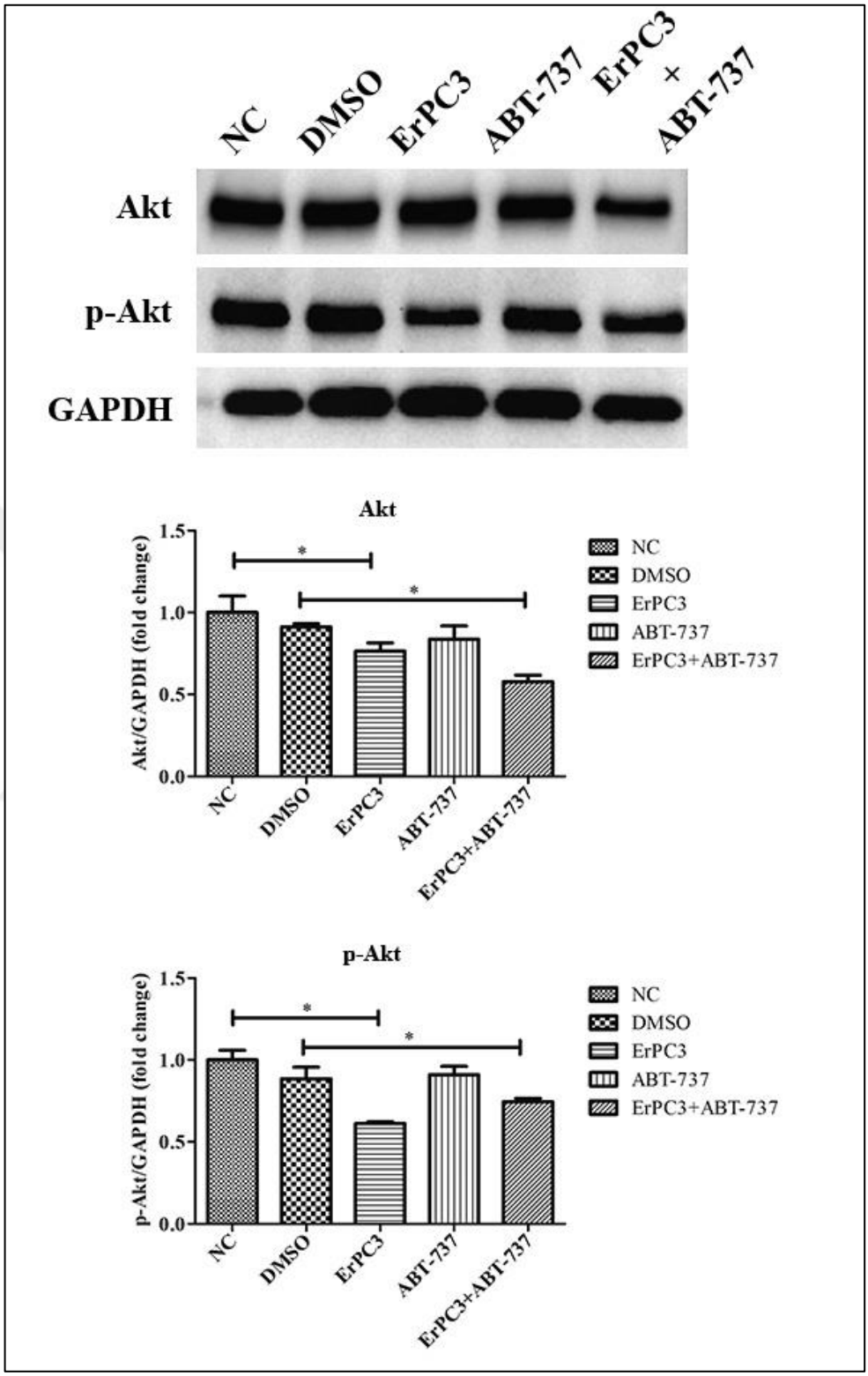

Figure 3. 25. Effects of various concentrations of ErPC3 (6.25 µM) and ABT-737 (5 µM) on the western blot analysis of PC-3 at 12h. Abbreviations: NC: Negative Control (Growth medium), DMSO: Dimethyl sulfoxide (0.1% v/v) containing growth medium, *P<0.05.

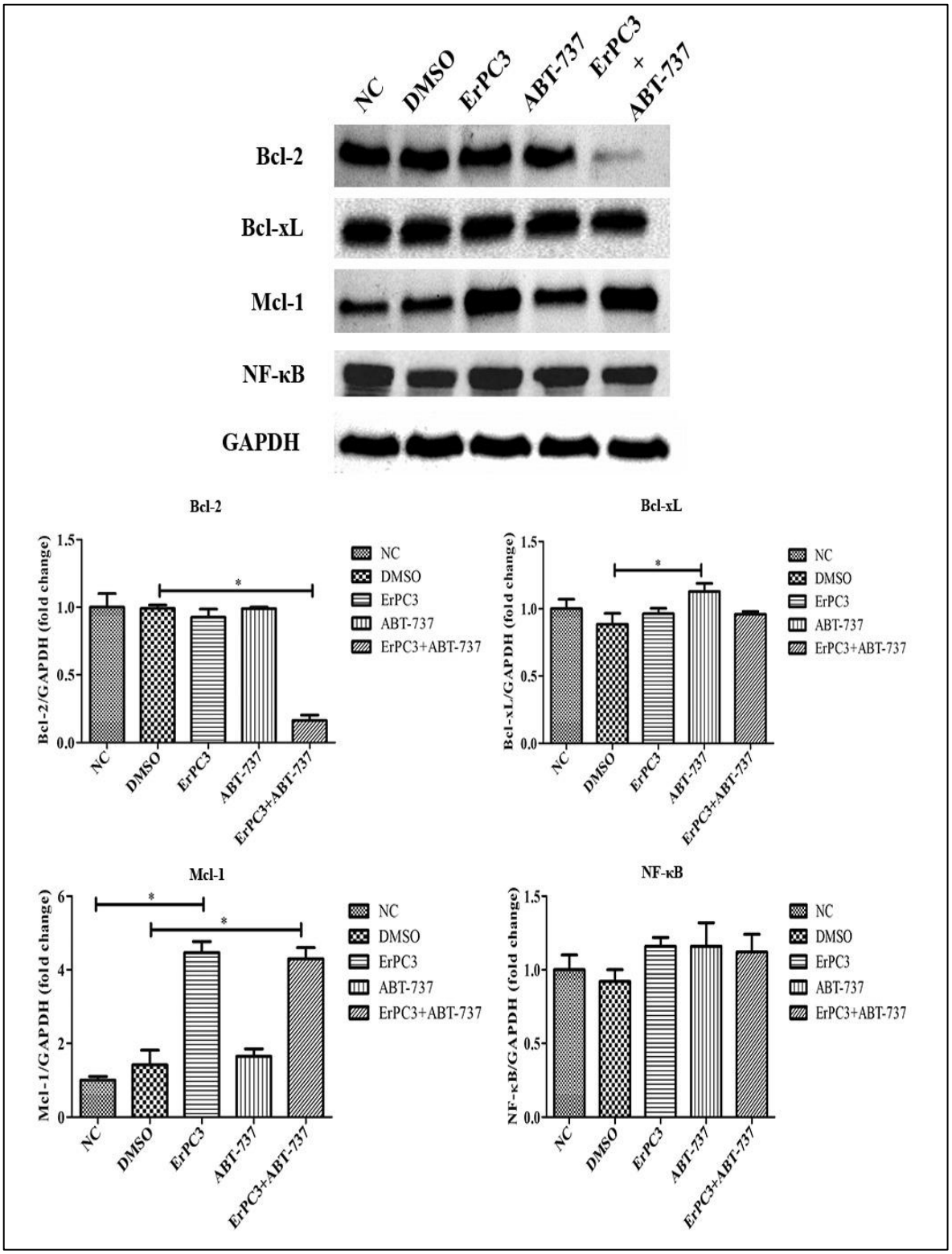

Figure 3. 26. Effects of various concentrations of ErPC3 (50 μM) and ABT-737 (5 μM) on the western blot analysis of DU-145 at 12h. Abbreviations: NC: Negative Control (Growth medium), DMSO: Dimethyl sulfoxide (0.1% v/v) containing growth medium, *P<0.05.

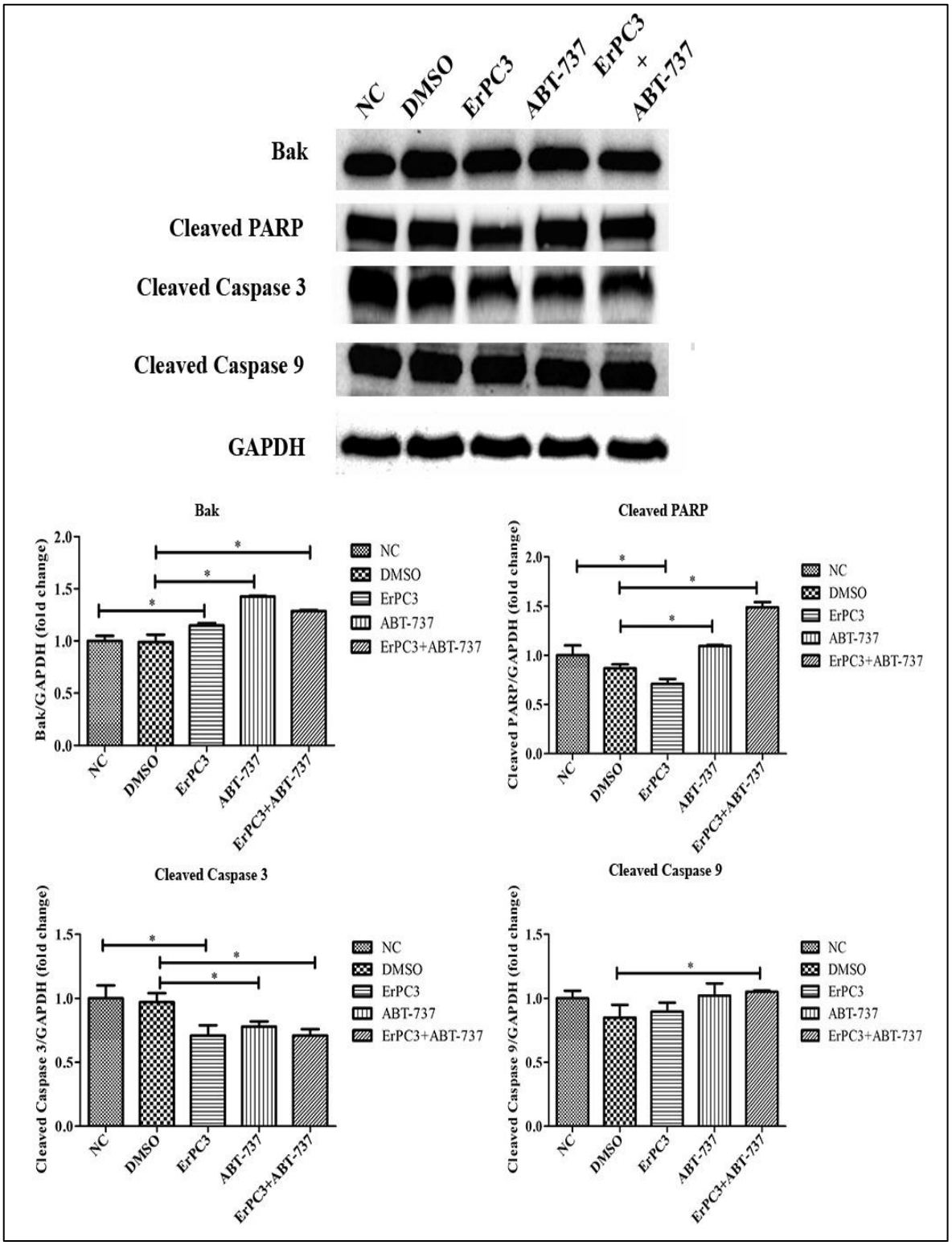

Figure 3. 27. Effects of various concentrations of ErPC3 (50 µM) and ABT-737 (5 µM) on the western blot analysis of DU-145 at 12h. Abbreviations: NC: Negative Control (Growth medium), DMSO: Dimethyl sulfoxide (0.1% v/v) containing growth medium, *P<0.05.

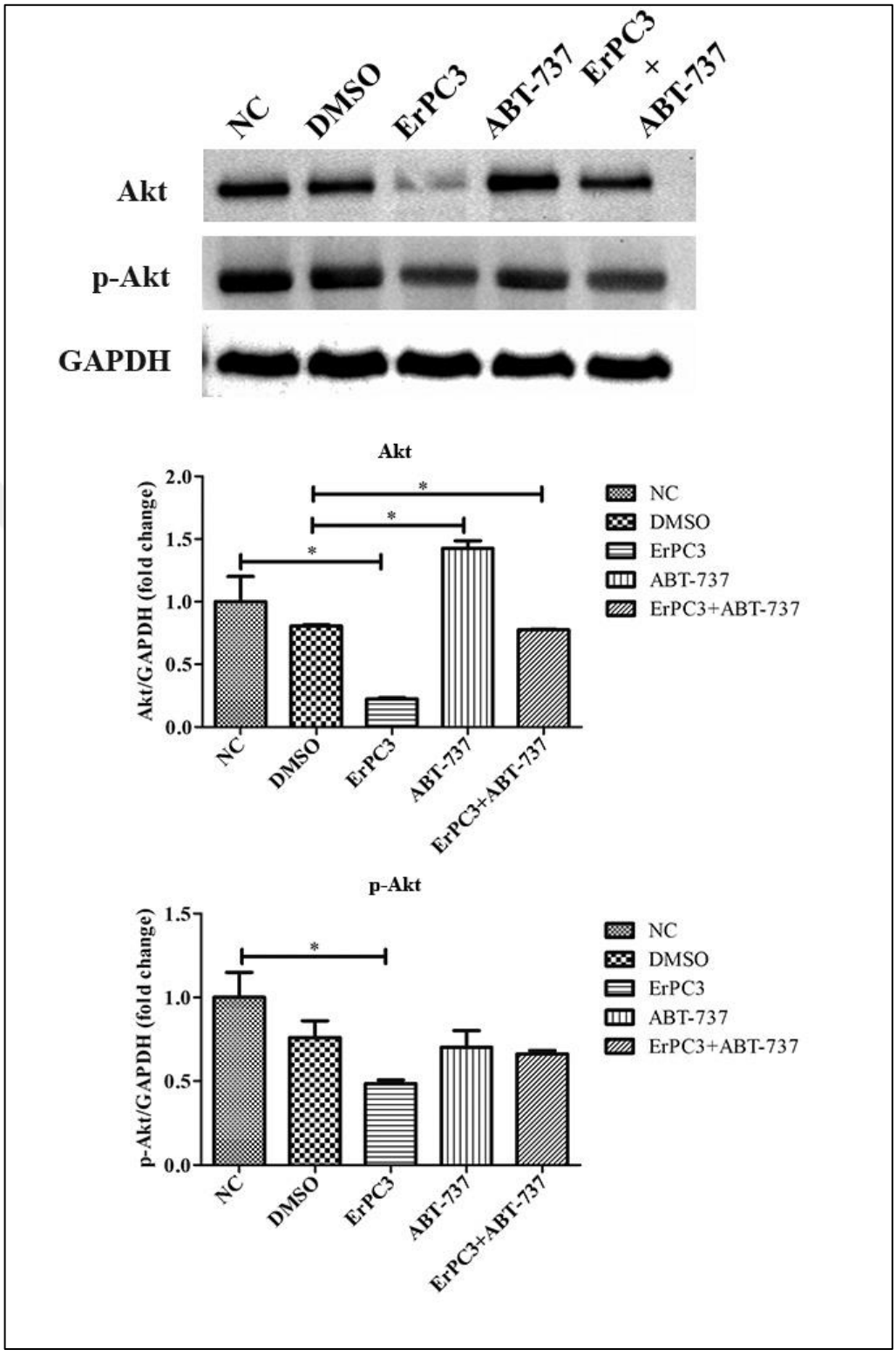

Figure 3. 28. Effects of various concentrations of ErPC3 (50 μM) and ABT-737 (5 μM) on the western blot analysis of DU-145 at 12h. Abbreviations: NC: Negative Control (Growth medium), DMSO: Dimethyl sulfoxide (0.1% v/v) containing growth medium, *P<0.05.

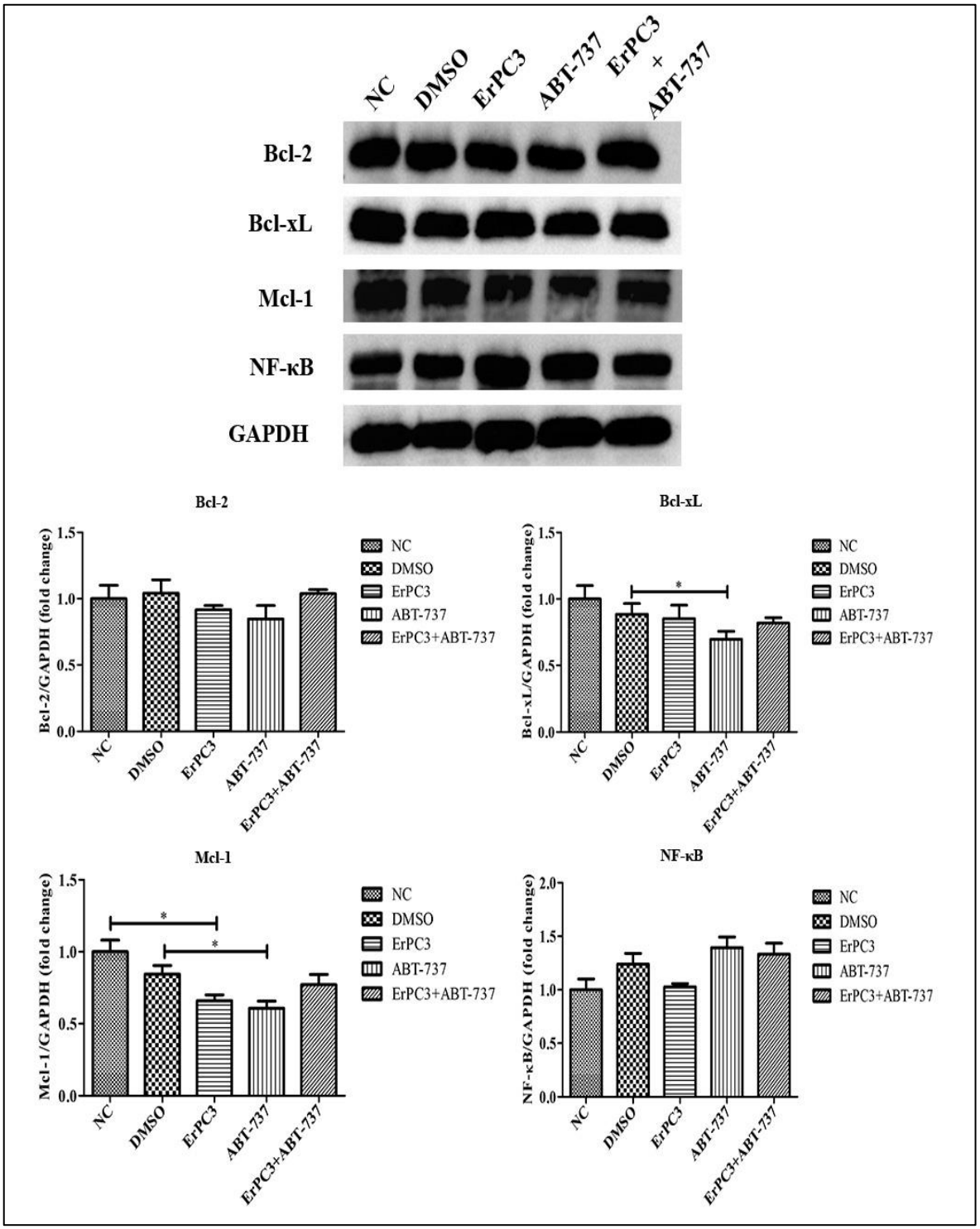

Figure 3. 29. Effects of various concentrations of ErPC3 (6.25 μM) and ABT-737 (5 μM) on the western blot analysis of PNT-1A at 12h. Abbreviations: NC: Negative Control (Growth medium), DMSO: Dimethyl sulfoxide (0.1% v/v) containing growth medium, *P<0.05.

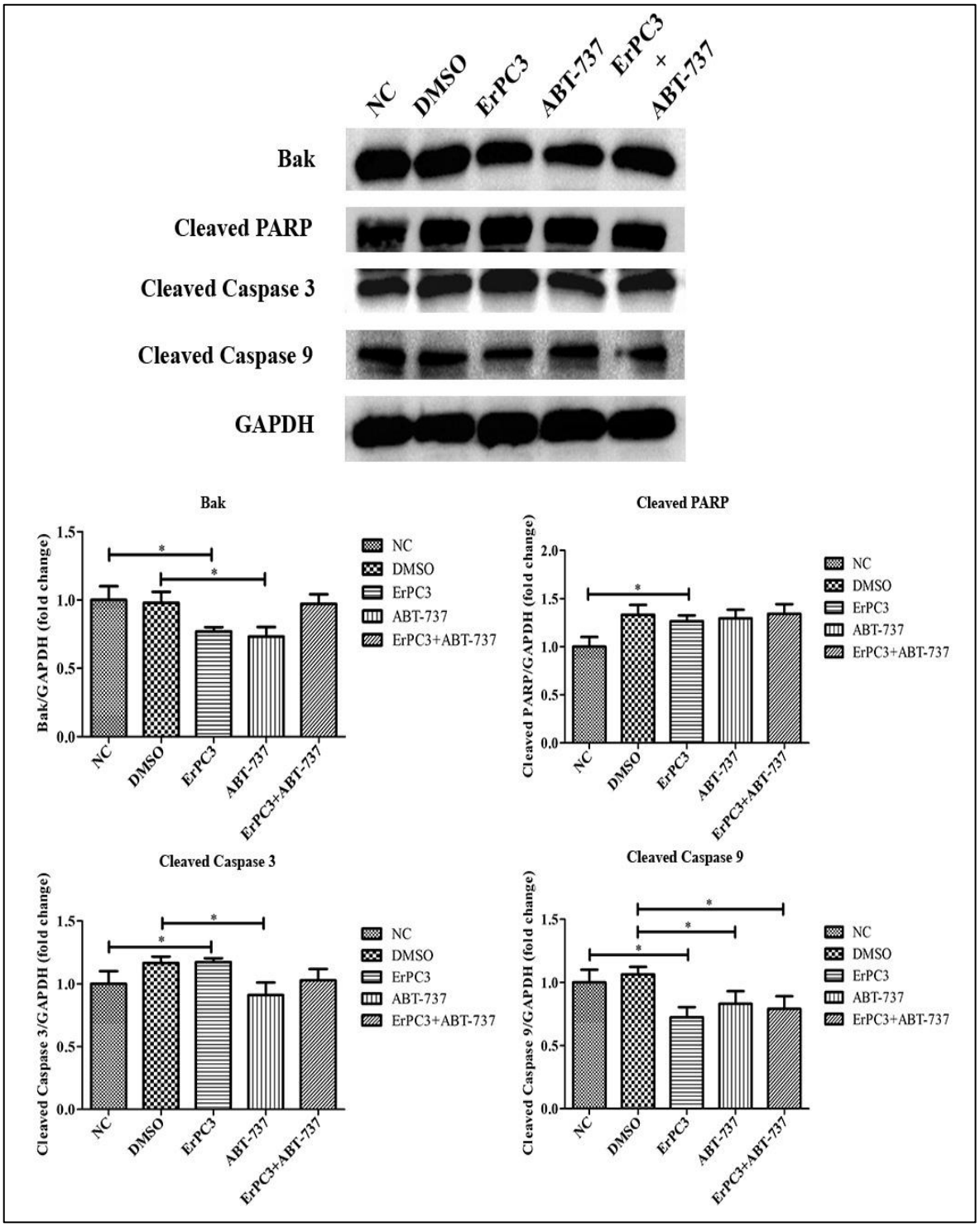

Figure 3. 30. Effects of various concentrations of ErPC3 (6.25 μM) and ABT-737 (5 μM) on the western blot analysis of PNT-1A at 12h. Abbreviations: NC: Negative Control (Growth medium), DMSO: Dimethyl sulfoxide (0.1% v/v) containing growth medium, *P<0.05.

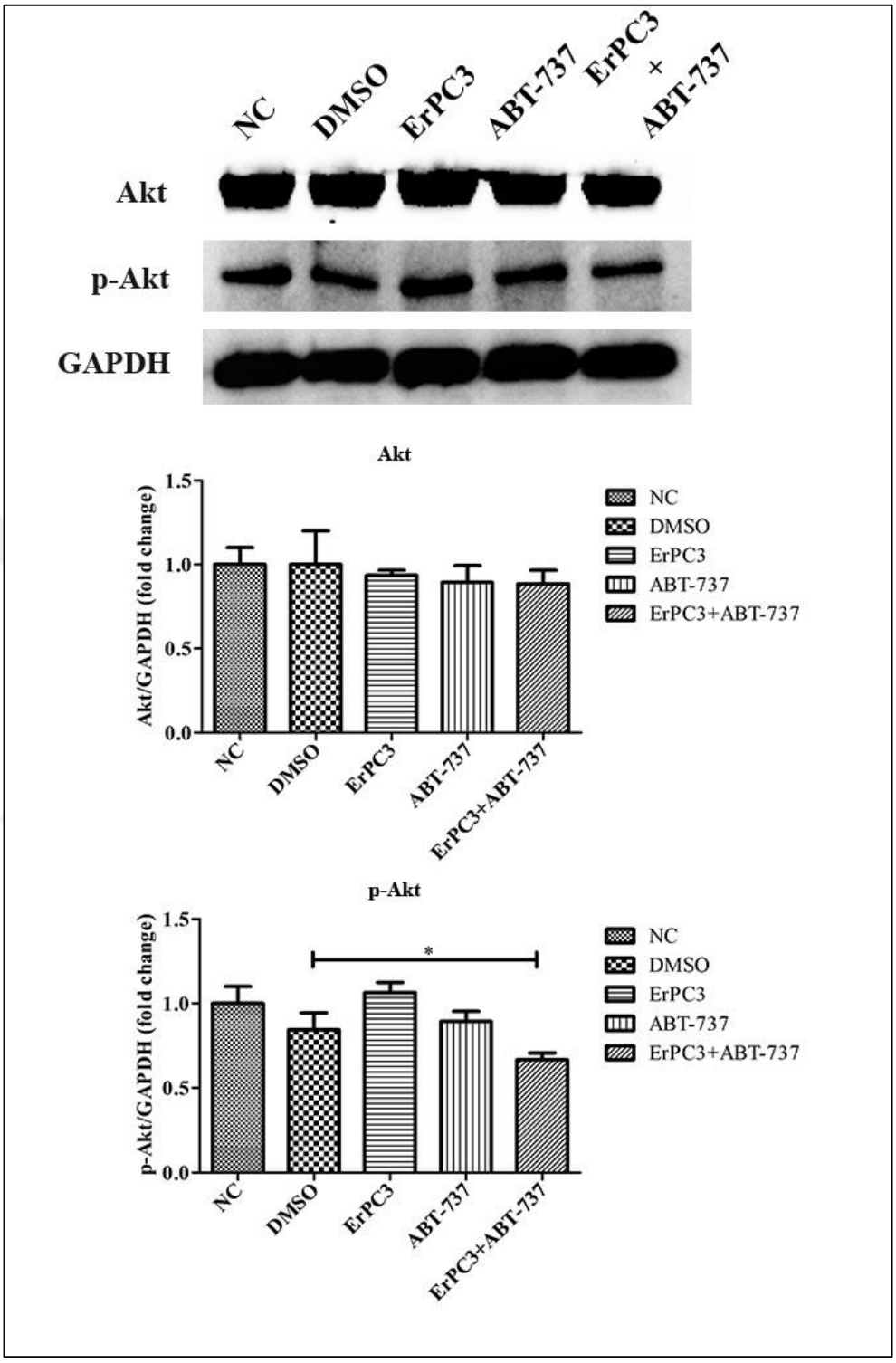

Figure 3. 31. Effects of various concentrations of ErPC3 (6.25 µM) and ABT-737 (5 µM) on the western blot analysis of PNT-1A at 12h. Abbreviations: NC: Negative Control (Growth medium), DMSO: Dimethyl sulfoxide (0.1% v/v) containing growth medium, *P<0.05.

4. DISCUSSION

PCa is a hormone-dependent disease but may develop into a phenotype which is resistant against hormone therapy, in another words androgen-independent prostate cancer (castration-resistant prostate cancer, CRPC) [103, 104]. For this reason, currently available treatment methods have been deemed ineffective especially in CRPC [105] which is a progressive and may lead to debilitating consequences. Although increased overall survival rates have been obtained by the advent of noverapeutics, optimal clinical outcome has not yet been achieved. On the other hand, the lack of reliable prognostic biomarkers may also delay CRPC treatment results [106].

Several genetic alterations are known to induce the progression of prostate cancer. BCL-2 is an important target especially for CRPC progression. Recent studies have shown that Bcl-2 signaling pathway is closely associated with the development of chemoresistance and progression of PCa [107]. Anti-apoptotic proteins Bcl-2, Bcl-xL and Mcl-1 are overexpressed in CRPC [80]. The Bcl-2 inhibitor, ABT-737 interact to Bcl-2, Bcl-xL and Bcl-w (but not Mcl-1) and inhibits their anti-apoptotic activity. ABT-737 also stimulates Akt/Bad phosphorylation and diminishes pro-apoptotic signals. Prostate cancer cell lines which overexpress Mcl-1 decreases the pro-apoptotic function of ABT-737 [107] so, Bcl-2 signaling pathway is not a single target for the treatment of CRPC. Therefore, combination therapy is recommended against Bcl-2 and its related pathways for effective clinical trials [105].

On the other hand, PI3K/Akt/mTOR signaling pathway is one of famous pathways in PCa, therefore attractive therapeutic targets in cancer therapy. Many prostate tumors displayed mutations which activates the PI3K/Akt/mTOR signaling pathway. The Akt inhibitor, ErPC3, inhibits both extrinsic and intrinsic pathways of apoptosis. Combination therapy with PI3K/Akt/mTOR pathway inhibitors can inhibit multiple nodes in other parallel pathways, hence it’s an effective therapeutic approach in the treatment of PCa [108].

This study was designed on the basis of the above highlighted data, and demonstrated that ABT-737 and ErPC3 combination displayed differential anticancer effects and interference with the apoptotic signaling pathways in PC-3, DU 145 and PNT-1A cell lines.

Cell viability analysis

In PC-3 cells, ABT-737 alone and in combination exhibited time and dose dependent cytotoxicity over 72-hours of incubation. The low concentrations of ABT-737 displayed no significant cytotoxic effect when compared to the NC group, following 24, 48 and 72h of incubation periods. At higher concentrations, ABT-737 (≥5μM) significantly decreased the cell viability after 72h. Following 72h of incubation, 5μM ABT-737 reduced cell viability to 86% (C %). Dash et al. tested cell viability of PC-3 cells were treated with ABT-737 (0.005-50 μM) for 48h. They reported a dose dependent inhibitory effect and an IC_{50} value of 12 μM at 48h, which is close to the value in our study (17 μM). Following 48h, a similar inhibitory effect was observed with 12.5 μM ABT-737 as compared to our study, at 10 μM ABT-737 (65 vs 69%) [109]. In another study, ABT-737 (2.5-20 μM) was applied to PC-3 cells for 48h. ABT-737 induced cytotoxicity was time and dose dependent. Following 48h, a similar inhibitory effect was observed with 5 μM ABT-737 treatment (90 vs 95%) [110]. Tamaki et al. examined the sensitizing effect of the Bcl-2 family inhibitors ABT-263 and ABT-737 on PC-3 cells. In this study, ABT-737 (0-10 μM) was applied to PC-3 cells for 48h. After the incubation period, 5 μM and 10 μM ABT-737 inhibited cell proliferation approximately by 20% and 40%, respectively. They demonstrated similar inhibitory effects with ABT-737 as compared to our study, at 10 μM concentration (40% vs 30%), but not with 5 μM (20% vs 5%), which may be due to the differences in experimental setting such as medium ingredients, number of wells used for each test concentration (3 vs 8) and unspecified solvent concentrations [111]. On the other hand, Hao et al. reported a decrease of cell viability by 7% when PC-3 cells were treated with ABT-737 (0.4 μM) for 48h, whereas a synergistic inhibition (80%) of cell viability was noted in combination with docetaxel (20 nmol/L) [112]. Zhang et al. demonstrated that ABT-737, displayed dose dependent inhibition on proliferation of PC-3 cells at 2 μM and 4 μM at 72h. After 72 hours exposure, they observed an inconsistently high cytotoxic effect (50%) [113].

ErPC3 alone and in combination exhibited time and dose dependent cytotoxicity over 72-hours of incubation. The low concentrations of ErPC3 displayed no significant cytotoxic effect when compared to the NC group, following 24, 48 and 72h of incubation periods. At higher concentrations, ErPC3 (≥6.25 μM) significantly decreased the cell viability after 72h. Following 72h of incubation, 6.25 μM ErPC3 reduced cell viability to 69% (C %). PC-3

cells were highly sensitive to Akt inhibitor, ErPC3. Rudner et al. treated PC-3 cells with 0-100 μM ErPC3 for 48h. Following 48h, although a higher survival rate was observed in Rudner's study at 12.5 μM (80% vs 60%), survival rates were quite similar at 25 μM concentration (50% vs 59%) when compared to our results [114].

After 72h, a ceiling effect was observed with ABT-737 and ErPC3 combination at concentrations equal to and greater than 5 μM and 6.25 μM, respectively. The combination of ABT-737 plus ErPC3 displayed a synergistic cytotoxic effect in PC-3. The cell viability falling to 30% after 72 hours of incubation, when ABT-737 (5 μM) and ErPC3 (6.25 μM) were combined. Saleem et al. tested cell viability of PC-3 cells were treated with ABT-737 (2.5-20 μM) with the autophagy inhibitor, hydroxychloroquine (HCQ) combination for 48h. They showed that ABT-737 with HCQ inhibited cell viability approximately by 40%. Adding HCQ to ABT-737 enhanced the anti-proliferative effect of ABT-737, but increasing the concentration of HCQ provided no further benefit at each ABT-737 concentration and a ceiling effect was evident in this regard [110]. A ceiling effect was observed with ABT-737 (2.5-10 μM) and docetaxel (≥5 μM) combination. ABT-737 with docetaxel combination synergistically reduced the viability to approximately 30% after 48 hours. Since Hiroki et. al. did not provide 72h results following ABT-737 plus docetaxel exposure, it's not possible to negotiate whether a ceiling effect is reached at 72h, hence compare with ABT-737 and ErPC3 combination [111]. Zhang et al. demonstrated that ABT-737, as a single agent, displayed dose dependent inhibition on proliferation of PC-3 cells at 2 μM and 4 μM at 72h. After 72 hours exposure, they observed an inconsistently high cytotoxic effect (50%), which increased to 90% with ABT-737 plus gemcitabine (both 4 μM) [113]. In Song et al.'s study, ABT-737 (0.5 μM) when combined with Pim serine/threonine kinase inhibitor, SMI-4a, decreased cell viability in PC-3 cells (~80%) after 24h [107]. The combination of ErPC3 (12.5 μM) with irradiation did not significantly increase the anti-neoplastic effects when compared to ErPC3 alone [114].

DU-145 cells exhibited a relatively more resistant phenotype as compared to PC-3 cells. In DU-145 cells, a significant cytotoxic effect with ABT-737 was observed at the highest concentration (20 μM) and this effect was time dependent. After 24h, no significant difference was observed between the NC group and all concentrations of ABT-737; whereas after 48 and 72h, only the highest concentration of ABT-737 reduced cell survival to

approximately 89%, and 70% (C%), respectively. Higher concentrations of and longer exposure times to ABT-737 was reported to be effective in Bax-deficient DU-145 cells [115]. Parrondo et al. investigated the cytotoxic effects of ABT-737 (1-10 μM) in DU-145 cells for 72h. Following incubation with 5 μM and 10 μM ABT-737, cell survival rates were approximately 80% and 60%, respectively, which were lower than the rates demonstrated in our study (108% and 70%, respectively) [80].

On the other hand, high doses (50 μM and 100 μM) of ErPC3 showed a dose and time dependent cytotoxic effect following all the incubation periods. Exposure to 50 μM ErPC3 alone decreased survival rate to 40% (C %) after 72h. Rudner also reported a significant cytotoxic effect only at concentrations of ≥50 μM and cell survival rate was approximately 60% after 72h [114].

The combination of 50 μM ErPC3 with 5 μM ABT-737 was more effective than other combination treatments. A ceiling effect was reached with 50 μM ErPC3 combined with equal to or greater than 5 μM ABT-737. When 5 μM ABT-737 and 50 μM ErPC3 were applied alone, survival rates were 108% and 40% of the control group, respectively after 72h. However, 5 μM ABT-737 plus 50 μM ErPC3 combination treatment for 72h, resulted in a survival rate of 41%. These results indicate that combining ABT-737 with ErPC3 exerted similar effect compared to ErPC3 alone. Rudner et al. studied the combination of ErPC3 (12.5 μM) with ionizing radiation which did not significantly increase the anti-neoplastic effects compared to ErPC3 alone in DU-145 cells [114].

Scratch Assay

This is the first study demonstrating wound-healing inhibitory properties of ABT-737 and ErPC3 alone and in combination. Following 24h incubation periods, ABT-737 and ErPC3 alone displayed a dose-dependent inhibitory effect on wound closure in both cell lines. ABT-737 (5, 10 and 20 μM) and ErPC3 (6.25, 12.5 and 25 μM) alone significantly reduced wound closure when compared to the control group. At higher doses, cell death was more prominent which prevented the follow-up of wound healing. Therefore, concentrations of both agents for combinations were chosen accordingly. Concentrations of 6.25 μM ErPC3 plus 5 μM ABT-737 were chosen for combination testing in PC-3 cells. Gap closure (%) in the PC-3

cells treated with 5 μM ABT-737, 6.25 μM ErPC3 and 5 μM ABT-737 plus 6.25 μM ErPC3 combination was 52%, 61% and 26%, respectively. Combination treatment significantly decreased the closure rate of the scratch area when compared to single agents. Concentrations of 12.5 μM ErPC3 plus 5 μM ABT-737 were chosen for combination testing in DU-145 cells. Gap closure (%) in the DU-145 cells exposed to 5 μM ABT-737, 12.5 μM ErPC3 and 5 μM ABT-737 plus 12.5 μM ErPC3 combination was 40%, 38% and 36%, respectively. Consequently, combination therapy remained ineffective on wound closure and the closure rate of the scratch in DU-145.

Apoptosis Analysis

In PC-3 cells, following 12 and 24h of incubation with 5 μM ABT-737, the percentages of total apoptotic cells to 8% and 30%, respectively. ABT-737 significantly increased apoptotic cells when compared to the NC group. Parrondo et al. utilized a lower dose of ABT-737 (1 μM) for 72h which increased the percentage of cell death approximately to 30% [80]. A longer incubation period of 48h was associated with significantly higher percentage of apoptotic cell death, with 34% apoptotic cell death following incubation with 2.5 μM ABT-737 [116].

In PC-3 cells, following 12 and 24h of incubation with 6.25 μM ErPC3, the percentages of total apoptotic cells to 8% and 18%, respectively. ABT-737 (5 μM) and ErPC3 (6.25 μM) alone showed similar effects on apoptosis, following 12h incubation period, whereas ABT-737 (5 μM) was more effective than ErPC3 (6.25 μM) after 24h incubation period.

In PC-3 cells, following 12 and 24h, 5 μM ABT-737 plus 6.25 μM ErPC3 significantly increased the percentages of total apoptotic cells to 27% and 75%, respectively as compared to the single agents and a synergistic effect on apoptosis was observed. The combination of 1 μM ABT-737 with docetaxel elevated the percentage of cell death (~60%) for 72h [80]. A significant increase in apoptotic cell death (~77%) after 48h was also observed with the combination of ABT-737 (5 μM) and pseudolaric acid B (2 μM) when compared to single agents [116].

In DU-145 cells, after 12 and 24h of incubation with 5 μM ABT-737, the percentages of total apoptotic cells were 5% and 9%, respectively. Therefore, ABT-737 did not display any

significant effect on apoptosis when compared to the NC group. 24h incubation with a higher concentration, 10 μM, ABT-737 elevated the percentage of cell death approximately to 6% [107]. A longer incubation period of 48h was associated with significantly higher percentage of apoptotic cell death, with 15% and 8% apoptotic cell death following incubation with 5 μM and 15 μM ABT-737, respectively [115, 116]. Lower doses for 48 and 72 hours led to insignificant effects. Parrondo et al. utilized a lower dose of ABT-737 (1 μM) for 72h which showed no significant effect with regard to apoptotic cell percentage when compared to the NC group [80]. Pandit et al. investigated the anti-apoptotic effect of even a much lower dose (0.35 μM) of ABT-737 for 48 hours and showed that the percentage of DU-145 undergoing apoptosis was approximately 2%, hence there is no significant difference from the control group [117].

In DU-145 cells, following 12 and 24h of incubation, 50 μM ErPC3 significantly increased the percentages of total apoptotic cells to approximately 16% and 42%, respectively in DU-145 cells. Wnetrzak et al. incubated DU-145 cells with ErPC3 at concentrations ranging between 12.5-50 μM for 24 and 48h. Number of cells undergoing apoptosis was ErPC3 concentration-dependent; the highest amount of apoptotic cells (60-70%) were detected in population treated with 50 μM. The results indicated an increase of therapeutic effect, which is related to prolonged agent treatment time and the higher drug concentration [118].

Combination of ABT-737 with other antineoplastic agents significantly increased apoptotic cell death. In DU-145 cells, following 12 and 24h of incubation, 5 μM ABT-737 plus 50 μM ErPC3 significantly elevated the percentage of total apoptotic cells to 11% and 27%, respectively. These findings indicate that ErPC3 treatment alone is more effective than its combination with ABT-737. A significant increase of apoptotic cell death (~40%) after 72h was also observed with ABT-737 (1 μM) and docetaxel (1 nM) combination compared to ABT-737 alone but the effect was similar when compared to docetaxel alone [80]. The combination of 5 μM ABT-737 with pseudolaric acid B (2 μM) increased the percentage of cell death (~38%) when compared to single agents [116]. The percentage of DU-145 cells undergoing apoptosis after treatment for 48h with a combination of a global transcription inhibitor ARC and ABT-737 significantly increased by nearly nine-fold to 27% when compared to the control group [117]. The methylseleninic acid (3 μM) with ABT-737 (15 μM) combination significantly increased the apoptotic effect in DU-145 cells (40.6%) [115].

However, combining ABT-737 with TRAIL showed no favorable effect as compared to single agents [107].

Cell Cycle Analysis

In PC-3 cells, ABT-737 caused G0/G1 phase arrest, whereas ErPC3 induced G2/M phase arrest. Following 24h of incubation with 5 μM ABT-737, the ratio of cells which accumulated in G0/G1 phase was 52% versus 48% in the control group. ABT-737 (1 μM) was shown to accumulate thyroid carcinoma cell lines in G0/G1 phase after 24h [119]. 6.25 μM ErPC3-induced accumulation of cells in G2/M phase was 55% versus 32% in the control group. G2/M phase arrest with ErPC3 was also reported in squamous carcinoma [120] and leukemic T cell lines [121]. ABT-737 with ErPC3 combination induced distribution of cells in G0/G1 and G2/M phases were 43% and 39%, respectively. This result demonstrates that ABT-737 and ErPC3 combination redistributes and decreases G0/G1 and G2/M phase accumulation when compared to single agents. Rudner et al. reported, ErPC3 (5 μM) alone and the combination of ErPC3 with irradiation for 48h induced of cells accumulated in G0/G1 phase [114]. In another study, ABT-737 (0.35 μM) plus docetaxel combination induced of cells accumulated in the G0/G1 phase [112].

In DU-145 cells, following 24h, 5 μM ABT-737 accumulated cells in G0/G1 phase was 54%. 50 μM ErPC3 induced distribution of cells in the G2/M phase was 49%. ABT-737 with ErPC3 combination induced 35% and 55% of cells in G0/G1 and G2/M phases, respectively. These results indicated that ABT-737 plus ErPC3 combination enhances cell cycle arrest in the G2/M phase when compared to single agents. No comparable report is yet available on cell cycle analysis following ABT-737 and ErPC3 alone and in combination in DU-145 cells.

RT-PCR and Western Blot Analysis

In PC-3 cells, after the administration of ABT-737, ErPC3 and ABT-737 plus ErPC3 combination, for understanding the possible molecular mechanisms, gene and protein expression analysis were performed. Activation of Bcl-2 and Akt are major regulators for

cancer cell survival, growth and proliferation. Signals activating the PI3K pathway and upregulating the Akt is required to trigger cancer cell response such as proliferation or motility. According to the RT-PCR results, ABT-737 (5 μM) treatment for 12h increased AKT but decreased BCL-2 and NF-κB gene levels. After 12h incubation, Western blot analysis showed that 5 μM ABT-737 treatment decreased Bcl-2, Bcl-xL and p-NF-κB but did not change Mcl-1, Bak, c-caspase 9, c-caspase 3, c-PARP, Akt and p-Akt levels. Similarly, 12h treatment of colorectal cancer cells with 5 μM ABT-737 was demonstrated to induce expression of c-caspase 3 and c-caspase 9 [122]. Parrondo et al. used a lower concentration of ABT-737 (1 μM) for 24h and 72h incubation periods. 1 μM ABT-737 treatment for 24h, did not change c-PARP, Mcl-1, Bcl-2 and Bcl-xL levels however slightly increased Bak level. After 72h, 1 μM ABT-737 significantly increased c-PARP, Mcl-1, Bcl-2, Bcl-xL and Bak protein levels [80]. Pandit et al. used 0.35 μM ABT-737 for 48h, did not cause any difference in the expression level of c-caspase 3 [117].

According to the RT-PCR results in PC-3 cells, 6.25 μM ErPC3 treatment for 12h decreased AKT and NF-κB, but increased BCL-2 gene levels. After 12h incubation time, Western blot analysis showed that 6.25 μM ErPC3 decreased Bcl-2, Mcl-1, p-NF-κB, Akt and p-Akt expressions, but did not change Bcl-xL, Bak, c-caspase 9, c-caspase 3 and c-PARP levels. When higher concentrations (12.5 μM and 25 μM) of ErPC3 were used for 48h in PC-3 cells, increased c-PARP and c-caspase-3, decreased p-Akt and unchanged Bak, Bcl-2, Bcl-xL and Mcl-1 levels were observed [114].

According to the RT-PCR results, following 12h incubation period of PC-3 cells with 6.25 μM ErPC3 plus 5 μM ABT-737 combination, decreased AKT, BCL-2 and NF-κB gene levels. At the same incubation period, western blot results showed that combination treatment reduced the expression of Bcl-2, Bcl-xL, Mcl-1, p-NF-κB, c-caspase 3, Akt and p-Akt levels, however did not change Bak, c-caspase 9 and c-PARP expression levels as compared to the NC group. Parrondo et al. published that, ABT-737 (1 μM) plus docetaxel combination for 24h slightly increased c-PARP, Mcl-1, Bak however decreased Bcl-2, Bcl-xL levels. After 72h, ABT-737 (1 μM) plus docetaxel increased c-PARP, Bcl-2 and Bcl-xL and decreased Mcl-1 and Bak levels [80]. In another study, the combination of ABT-737 (0.35 μM) with a transcription inhibitor, ARC, for 48h increased c-caspase 3 level compared to single agent applications in PC-3 cells [117]. Hao JW et al. published that ABT-737 (0.4

μM) plus docetaxel combination for 48h decreased Bcl-2, Bcl-xL and Mcl-1 and increased c-caspase-3 levels [112]. Rudner et al. published, ErPC3 (12.5 μM) with irradiation treatments for 48h, significantly increased c-PARP and c-caspase-3 levels when compared to single agents [114].

ABT-737 does not bind to anti-apoptotic Mcl-1 protein which is highly expressed in DU-145 cells. In addition, DU-145 cells lack pro-apoptotic protein Bax. For these reasons, DU-145 cells are more resistant to ABT-737. According to the RT-PCR results, ABT-737 (5 μM) treatment for 12h increased AKT but decreased BCL-2 and NF-κB gene levels. After 12h incubation, Western blot analysis showed that 5 μM ABT-737-treatment increased the expression of Bcl-xL, Bak, c-PARP and Akt levels and decreased the cleaved caspase 3 level, whereas Bcl-2, Mcl-1, p-NF-κB, cleaved caspase 9 and p-Akt level were similar to the control group. Parrando et al used a lower concentration of ABT-737 (1 μM) which didn't alter c-PARP expression level after 72h incubation period [80]. No change was observed in caspase 3 expression with a lower dose of ABT-737 (0.35 μM) [117]. 15 μM ABT-737 treatment for 48h did not change the expression of c-caspases 3 and 9 and c-PARP but slightly increased p-Akt [115]. 10 μM ABT-737 treatment for 24h did not demonstrate a change in Bak, PARP protein [107].

In DU-145 cells, after 12h incubation time, ErPC3 treatment decreased the AKT, increased BCL-2 and did not change NF-κB gene levels. After 12h incubation, ErPC3 treatment did not change Bcl-2, Bcl-xL, p-NF-κB and caspase 9 levels but increased the Mcl-1 and Bak levels and decreased the PARP, caspase 3, Akt ve p-Akt.

In DU-145 cells, after 12h incubation, ABT-737 and ErPC3 combination decreased AKT but did not change BCL-2 and NF-κB gene levels. The combination treatment reduced the expression of Bcl-2, caspase 3 and Akt protein levels, elevated the Mcl-1, Bak, PARP, caspase 9 levels and did not change Bcl-xL, p-NF-κB and p-Akt levels. In addition, combination therapy increased c-PARP expression compared to ABT-737-treated cells but decreased c-parp level compared to docetaxel-treated cells after 72h [80]. Sub-lethal dose of ABT-737 (0.35 μM) was applied DU-145 cells at 48h. ABT-737 did not change the expression level of cleaved caspase 3. ABT-737 with a transcription inhibitor, ARC, combination induced apoptosis by caspase 3 cleavage compared to single agents [117]. 15 μM ABT-737 in combination with methylseleninic acid increased the expression of c-

caspases 3 and 9 and c-PARP [115]. 10 μM ABT-737 in combination with TRAIL did not demonstrate a change in Bak and PARP protein levels. DU-145 cells were resistant to combination therapy [107].

Proliferation of PNT-1A cells was also inhibited only at high concentrations and after 48 hours of incubation by ABT-737 (10 μM, 20 μM) and ErPC3 (50 μM, 100 μM) alone. With the combination treatment, significant cytotoxicity was evident only at the highest concentrations (20 μM ABT-737 plus 50 μM ErPC3) for all the incubation periods. According to these findings, combination therapy seems to be quite safe with the lower (<10 μM ABT-737; <25 μM ErPC3) concentrations. After 24h, ABT-737 (2.5, 5 and 10 μM) did not significant effect on wound closure, but 20 μM ABT-737 significantly reduced wound closure. ErPC3 at all concentrations and 6.25 μM ErPC3 with 5 μM ABT-737 combination were not significantly different when compared to the NC group and single agents for 24h. In PNT-1A cells, 6.25 μM ErPC3 and 5 μM ABT-737 alone elevated the percentage of total apoptotic cells approximately to 6%-12% for 12h and 1%-5% for 24h, respectively when compared to the control group. Following 12h and 24h, the combination of 5 μM ABT-737 plus 6.25 μM ErPC3 significantly elevated the percentage of total apoptotic cells approximately to 6% and 5%, respectively. 6.25 μM ErPC3 accumulated cells in G2/M phase was 34% versus 29% in the NC group, whereas 5 μM ABT-737 and 5μM ABT-737 plus 6.25 μM ErPC3 did not display significant effect on cell cycle phase distribution.

In PNT-1A cells, according to the RT-PCR results, ABT-737 (5 μM), ErPC3 (6.25 μM) alone and in combination treatment for 12h, AKT, BCL-2 and NF-κB gene levels did not significantly different from control group. After 12h incubation, Western blot analysis showed that 5 μM ABT-737 treatment decreased Bcl-xL, Mcl-1, Bak, c-caspase 3 and c-caspase 9 but did not change Bcl-2, p-NF-κB, c-PARP, Akt and p-Akt levels. 6.25 μM ErPC3 treatment decreased c-caspase 9 and p-Akt levels but did not change Bcl-2, p-NF-κB, c-PARP, Akt and levels. Bcl-xL, Mcl-1, Bak and c-caspase 3. Combination therapy did not affect the expression of Bcl-2 and p-NF-κB, Bcl-xL, Mcl-1, c-PARP, c-caspase 3 and Akt protein levels.

5. CONCLUSION

Healthy cell lines are usually not used in most of the studies involved in the screening of antineoplastic drugs. The design of our study allows comparing chemotherapy induced toxicity by utilizing PNT-1A.

Another alkylphosphocholine, perifosine, has been previously observed display *in vitro* and *in vivo* potential synergism with ABT-737. This is the first *in vitro* study showing the beneficial effect of erufosine and ABT-737 combination in prostate cancer cell lines. The rational for combining erufosine with ABT-737 was to overcome ABT-737 resistance via Akt-inhibition by erufosine. In line with this hypothesis, combining ABT-737 with ErPC3 displays a synergistic cytotoxic effect in PC-3 cells. In addition, a ceiling effect was observed with ABT-737 and ErPC3 combination after 72h, which indicates that there is no need to use higher concentrations for both agents in PC-3 cells.

Bcl-2/Bcl-xL is highly expressed in both PC-3 cells and DU-145 cells. In addition, DU-145 cells display a more resistant phenotype; they do not express the proapoptotic protein Bax (Bax-null) and they overexpress the anti-apoptotic protein Mcl-1. These two specific characteristics render DU-145 cells resistant against ABT-737. ErPC3 alone was more effective than combination therapy in DU-145 cells. These findings emphasize the rational selection of antineoplastic combinations with regard to biomarker expression in prostate cancer cell lines. If the prostate specimen expresses a resistant phenotype with increased Mcl-1, then the efficacy of ErPC3 plus ABT-737 combination seems to be less likely.

Whereas cell viability analysis provided encouraging results for ABT-737 plus ErPC3 combination therapy in PC-3 cells, more *in vitro* studies which address the molecular mechanisms and *in vivo* studies are highly guaranteed to clarify the potential of alkylphosphocholine combinations.

REFERENCES

1. Floor SL, Dumont JE, Maenhaut C, Raspe E. Hallmarks of cancer: of all cancer cells, all the time? Trends in molecular medicine. 2012;18(9):509-15.

2. Hanahan D, Weinberg RA. Hallmarks of cancer: the next generation. cell. 2011;144(5):646-74.

3. Boiteux S, Jinks-Robertson S. DNA repair mechanisms and the bypass of DNA damage in Saccharomyces cerevisiae. Genetics. 2013;193(4):1025-64.

4. Ruddon RW. Cancer biology: Oxford University Press; 2007.

5. Schärer OD. Nucleotide excision repair in eukaryotes. Cold Spring Harbor perspectives in biology. 2013;5(10):a012609.

6. Jonnalagadda VS, Matsuguchi T, Engelward BP. Interstrand crosslink-induced homologous recombination carries an increased risk of deletions and insertions. DNA repair. 2005;4(5):594-605.

7. Dexheimer TS. DNA repair pathways and mechanisms. DNA repair of cancer stem cells: Springer; 2013. p. 19-32.

8. Eggert J, editor The biology of cancer: what do oncology nurses really need to know. Seminars in oncology nursing; 2011: Elsevier.

9. Pecorino L. Molecular biology of cancer: mechanisms, targets, and therapeutics: Oxford university press; 2012.

10. Hanahan D, Weinberg RA. The hallmarks of cancer. cell. 2000;100(1):57-70.

11. Lowe SW, Lin AW. Apoptosis in cancer. Carcinogenesis. 2000;21(3):485-95.

12. Shay JW, Wright WE. Hayflick, his limit, and cellular ageing. Nature reviews Molecular cell biology. 2000;1(1):72-6.

13. Bertram JS. The molecular biology of cancer. Molecular aspects of medicine. 2000;21(6):167-223.

14. Lam DK, Schmidt BL. Molecular Biology of Head and Neck Cancer: Therapeutic Implications. Current Therapy in Oral and Maxillofacial Surgery: Elsevier Inc.; 2012.

15. Thomas S, Balan A. Retinoblastoma Tumor Suppressor Gene: An Overview. Radiol. 2012;24(1):30-5.

16. Rajalingam K, Schreck R, Rapp UR, Albert Š. Ras oncogenes and their downstream targets. Biochimica et Biophysica Acta (BBA)-Molecular Cell Research. 2007;1773(8):1177-95.

17. Lodish H, Berk A, Zipursky SL, Matsudaira P, Baltimore D, Darnell J. Molecular cell biology 4th edition. National Center for Biotechnology InformationÕs Bookshelf. 2000.

18. Goodrich DW. The retinoblastoma tumor suppressor gene, the exception that proves the rule. Oncogene. 2006;25(38):5233.

19. Levine AJ, Momand J, Finlay CA. The p53 tumour supressor gene. Nature. 1991;351(6326):453.

20. van Oijen MG, Slootweg PJ. Gain-of-function mutations in the tumor suppressor gene p53. Clinical Cancer Research. 2000;6(6):2138-45.

21. Rivlin N, Brosh R, Oren M, Rotter V. Mutations in the p53 tumor suppressor gene: important milestones at the various steps of tumorigenesis. Genes & cancer. 2011;2(4):466-74.

22. Vincent TL, Gatenby RA. An evolutionary model for initiation, promotion, and progression in carcinogenesis. International journal of oncology. 2008;32(4):729-37.

23. Helmlinger G, Yuan F, Dellian M, Jain RK. Interstitial pH and pO2 gradients in solid tumors in vivo: high-resolution measurements reveal a lack of correlation. Nature medicine. 1997;3(2):177-82.

24. Salvadori DMF, da Silva GN. Genetic Instability in Normal-Appearing and Tumor Urothelium Cells and the Role of the TP53 Gene in the Toxicogenomic Effects of Antineoplastic Drugs. Advances in the Scientific Evaluation of Bladder Cancer and Molecular Basis for Diagnosis and Treatment: InTech; 2013.

25. Golstein P, Kroemer G. Cell death by necrosis: towards a molecular definition. Trends Biochem Sci 2007;32(1):37-43.

26. Jain MV, Paczulla AM, Klonisch T, Dimgba FN, Rao SB, Roberg K, et al. Interconnections between apoptotic, autophagic and necrotic pathways: implications for cancer therapy development. J Cell Mol Med 2013;17(1):12-29.

27. Levine B, Yuan J. Autophagy in cell death: an innocent convict? J Clin Invest 2005;115(10):2679-88.

28. Nikoletopoulou V, Markaki M, Palikaras K, Tavernarakis N. Crosstalk between apoptosis, necrosis and autophagy. Biochim Biophys Acta. 2013;1833(12):3448-59.

29. Bincoletto C, Bechara A, Pereira G, Santos C, Antunes F, Peixoto da-Silva J, et al. Interplay between apoptosis and autophagy, a challenging puzzle: new perspectives on antitumor chemotherapies. Chem Biol Interact. 2013;206(2):279-88.

30. El-Khattouti A, Selimovic D, Haikel Y, Hassan M. Crosstalk Between Apoptosis and Autophagy: Molecular Mechanisms and Therapeutic Strategies in Cancer. J Cell Death 2013;6:37-55.

31. Maiuri MC, Zalckvar E, Kimchi A, Kroemer G. Self-eating and self-killing: crosstalk between autophagy and apoptosis. Nat Rev Mol Cell Biol. 2007;8(9):741-52.

32. Chen Y, Klionsky DJ. The regulation of autophagy–unanswered questions. J Cell Sci. 2011;124(2):161-70.

33. Wu W, Liu P, Li J. Necroptosis: an emerging form of programmed cell death. Crit Rev Oncol Hematol. 2012;82(3):249-58.

34. Kerr JF, Wyllie AH, Currie AR. Apoptosis: a basic biological phenomenon with wide-ranging implications in tissue kinetics. Br J Cancer. 1972;26(4):239-57.

35. Khan KH, Blanco-Codesido M, Molife LR. Cancer therapeutics: Targeting the apoptotic pathway. Crit Rev Oncol Hematol. 2014;90(3):200-19.

36. Beesoo R, Neergheen-Bhujun V, Bhagooli R, Bahorun T. Apoptosis inducing lead compounds isolated from marine organisms of potential relevance in cancer treatment.

Mutation Research/Fundamental and Molecular Mechanisms of Mutagenesis. 2014;768:84-97.

37. Ghobrial IM, Witzig TE, Adjei A. Targeting apoptosis pathways in cancer therapy. CA Cancer J Clin 2005;55(3):178-94.

38. Hall C, Troutman SM, Price DK, Figg WD, Kang MH. Bcl-2 family of proteins as therapeutic targets in genitourinary neoplasms. Clinical genitourinary cancer. 2013;11(1):10-9.

39. Letai A, Bassik MC, Walensky LD, Sorcinelli MD, Weiler S, Korsmeyer SJ. Distinct BH3 domains either sensitize or activate mitochondrial apoptosis, serving as prototype cancer therapeutics. Cancer cell. 2002;2(3):183-92.

40. Adams J, Cory S. The Bcl-2 apoptotic switch in cancer development and therapy. Oncogene. 2007;26(9):1324-37.

41. Yip K, Reed J. Bcl-2 family proteins and cancer. Oncogene. 2008;27(50):6398.

42. Premkumar DR, Jane EP, DiDomenico JD, Vukmer NA, Agostino NR, Pollack IF. ABT-737 synergizes with bortezomib to induce apoptosis, mediated by Bid cleavage, Bax activation, and mitochondrial dysfunction in an Akt-dependent context in malignant human glioma cell lines. Journal of Pharmacology and Experimental Therapeutics. 2012;341(3):859-72.

43. Courtney KD, Corcoran RB, Engelman JA. The PI3K pathway as drug target in human cancer. J Clin Oncol 2010;28(6):1075-83.

44. Li H, Zeng J, Shen K. PI3K/AKT/mTOR signaling pathway as a therapeutic target for ovarian cancer. Arch Gynecol Obstet. 2014;290(6):1067-78.

45. Yap TA, Garrett MD, Walton MI, Raynaud F, de Bono JS, Workman P. Targeting the PI3K–AKT–mTOR pathway: progress, pitfalls, and promises. Curr Opin Pharmacol. 2008;8(4):393-412.

46. Gaikwad SM, Ray P. Non-invasive imaging of PI3K/Akt/mTOR signalling in cancer. American journal of nuclear medicine and molecular imaging. 2012;2(4):418.

47. Carew JS, Kelly KR, Nawrocki ST. Mechanisms of mTOR inhibitor resistance in cancer therapy. Target Oncol 2011;6(1):17-27.

48. NCI. Targeted Cancer Therapies: National Cancer Institute 2014. Available from: http://www.cancer.gov/cancertopics/factsheet/Therapy/targeted.

49. Fu W, Madan E, Yee M, Zhang H. Progress of molecular targeted therapies for prostate cancers. Biochim Biophys Acta 2012;1825(2):140-52.

50. Chabner BA, Barnes J, Neal J, Olson E, Mujagic H, Sequist L, et al. Targeted Therapies: Tyrosine Kinase Inhibitors, Monoclonal Antibodies, and Cytokines In: Brunton L, Chabner B, Knollman B, editors. Goodman & Gilman's The Pharmacological Basis of Therapeutics. 12 ed. China: The McGraw- Hill Companies, Inc; 2011. p. 1731-69.

51. IARC. World cancer fact sheet 2014. Available from: International Agency for Research on Cancer; World Health Organization http://globocan.iarc.fr/Pages/fact_sheets_cancer.aspx.

52. Rebbeck TR, editor Prostate cancer genetics: Variation by race, ethnicity, and geography. Seminars in radiation oncology; 2017: Elsevier.

53. Grönberg H. Prostate cancer epidemiology. The Lancet. 2003;361(9360):859-64.

54. Nakata S, Ohtake N, Takei T, Yamanaka H. Hereditary prostate cancer. Nihon rinsho Japanese journal of clinical medicine. 2000;58(7):1515-8.

55. Gann PH. Risk factors for prostate cancer. Reviews in urology. 2002;4(Suppl 5):S3.

56. Potter SR, Partin AW. Hereditary and familial prostate cancer: biologic aggressiveness and recurrence. Reviews in urology. 2000;2(1):35.

57. Barve A, Jin W, Cheng K. Prostate Cancer Relevant Antigens and Enzymes for Targeted Drug Delivery. J Control Release. 2014;187:118-32.

58. Moul JW. The evolving definition of advanced prostate cancer. Rev Urol 2004;6(Suppl 8):S10-7.

59. Isbarn H, Boccon-Gibod L, Carroll PR, Montorsi F, Schulman C, Smith MR, et al. Androgen deprivation therapy for the treatment of prostate cancer: consider both benefits and risks. European urology. 2009;55(1):62-75.

60. Sanda MG, Dunn RL, Michalski J, Sandler HM, Northouse L, Hembroff L, et al. Quality of life and satisfaction with outcome among prostate-cancer survivors. N Engl J Med. 2008;358(12):1250-61.

61. NCI. Prostate Cancer Treatment National Cancer Institute [Available from: 2014. Available from: https://www.cancer.gov/types/prostate/patient/prostate-treatment-pdq#section/_142.

62. NCI. Prostate Cancer Treatment National Cancer Institute 2014. Available from: http://www.cancer.gov/cancertopics/pdq/treatment/prostate/HealthProfessional/page4.

63. Schalken J, Fitzpatrick JM. Enzalutamide: targeting the androgen signalling pathway in metastatic castration-resistant prostate cancer. BJU international. 2016;117(2):215-25.

64. Thompson I. Prevalence of prostate cancer among men with a prostate-specific antigen level<= 4.0 ng per milliliter (vol 350, pg 2239, 2004). New England Journal of Medicine. 2004;351(14):1470-.

65. Hotte S, Saad F. Current management of castrate-resistant prostate cancer. Current oncology. 2010;17(Suppl 2):S72.

66. Derleth CL, Yu EY. Targeted therapy in the treatment of castration-resistant prostate cancer. Oncology (Williston Park) 2013;27(7):620-8.

67. Qin Z, Li X, Han P, Zheng Y, Liu H, Tang J, et al. Association between polymorphic CAG repeat lengths in the androgen receptor gene and susceptibility to prostate cancer: A systematic review and meta-analysis. Medicine. 2017;96(25).

68. NCI. Prostate Cancer Treatment National Cancer Institute 2014. Available from: https://www.cancer.gov/types/prostate/prostate-hormone-therapy-fact-sheet.

69. Canil C, Tannock I. Is there a role for chemotherapy in prostate cancer? British journal of cancer. 2004;91(6):1005.

70. Beer T, Raghavan D. Chemotherapy for hormone-refractory prostate cancer: Beauty is in the eye of the beholder. The Prostate. 2000;45(2):184-93.

71. Shore ND. Radium-223 dichloride for metastatic castration-resistant prostate cancer: the urologist's perspective. Urology. 2015;85(4):717-24.

72. Clarke J, Armstrong A. Novel therapies for the treatment of advanced prostate cancer. Current treatment options in oncology. 2013;14(1):109-26.

73. Heath EI, Carducci MA. Targeted therapy trials for prostate cancer. Prostate Cancer. 2008:383-400.

74. Catz S, Johnson J. BCL-2 in prostate cancer: a minireview. Apoptosis. 2003;8(1):29-37.

75. Edlind MP, Hsieh AC. PI3K-AKT-mTOR signaling in prostate cancer progression and androgen deprivation therapy resistance. Asian J Androl. 2014;16(3):378-86.

76. Bitting RL, Armstrong AJ. Targeting the PI3K/Akt/mTOR pathway in castration-resistant prostate cancer. Endocr Relat Cancer 2013;20(3):R83-R99.

77. Morgan TM, Koreckij TD, Corey E. Targeted therapy for advanced prostate cancer: inhibition of the PI3K/Akt/mTOR pathway. Curr Cancer Drug Targets. 2009;9(2):237-49.

78. Zielinski RR, Eigl BJ, Chi KN. Targeting the apoptosis pathway in prostate cancer. The Cancer Journal. 2013;19(1):79-89.

79. Polivka J J, Janku F. Molecular targets for cancer therapy in the PI3K/AKT/mTOR pathway. Pharmacol Ther. 2014;142(2):164-75.

80. Parrondo R, de las Pozas A, Reiner T, Perez-Stable C. ABT-737, a small molecule Bcl-2/Bcl-xL antagonist, increases antimitotic-mediated apoptosis in human prostate cancer cells. PeerJ. 2013;1:e144.

81. Balakrishnan K, Gandhi V. Bcl-2 antagonists: a proof of concept for CLL therapy. Investigational new drugs. 2013;31(5):1384-94.

82. Lieber J, Ellerkamp V, Vogt F, Wenz J, Warmann SW, Fuchs J, et al. BH3-mimetic drugs prevent tumour onset in an orthotopic mouse model of hepatoblastoma. Experimental cell research. 2014;322(1):217-25.

83. Hall C, Troutman SM, Price DK, Figg WD, Kang MH. Bcl-2 family of proteins as therapeutic targets in genitourinary neoplasms. Clin Genitourin Cancer 2013;11(1):10-9.

84. Gao Y, Trivedi S, Ferris RL, Koide K. Regulation of HPV16 E6 and MCL1 by SF3B1 inhibitor in head and neck cancer cells. Scientific reports. 2014;4.

85. Verheij M, Moolenaar WH, Blitterswijk WJ. Combining Anti-tumor Alkyl-Phospholipid Analogs and Radiotherapy: Rationale and Clinical Outlook. Anticancer Agents Med Chem. 2014;14(4):618-28.

86. van Blitterswijk WJ, Verheij M. Anticancer mechanisms and clinical application of alkylphospholipids. Biochim Biophys Acta 2013;1831(3):663-74.

87. Chometon G, Cappuccini F, Raducanu A, Aumailley M, Jendrossek V. The Membrane-targeted Alkylphosphocholine Erufosine Interferes with Survival Signals from the Extracellular Matrix. Anticancer Agents Med Chem 2014;14(4):578-91.

88. Rudner J, Ruiner C, Handrick R, Eibl H, Belka C, Jendrossek V. The Akt-inhibitor Erufosine induces apoptotic cell death in prostate cancer cells and increases the short term effects of ionizing radiation. Radiat Oncol. 2010;5:108.

89. Fiegl M, Lindner LH, Juergens M, Eibl H, Hiddemann W, Braess J. Erufosine, a novel alkylphosphocholine, in acute myeloid leukemia: single activity and combination with other antileukemic drugs. Cancer Chemother Pharmacol 2008;62(2):321-9.

90. Martelli AM, Papa V, Tazzari PL, Ricci F, Evangelisti C, Chiarini F, et al. Erucylphosphohomocholine, the first intravenously applicable alkylphosphocholine, is cytotoxic to acute myelogenous leukemia cells through JNK-and PP2A-dependent mechanisms. Leukemia. 2010;24(4):687-98.

91. Königs SK, Pallasch CP, Lindner LH, Schwamb J, Schulz A, Brinker R, et al. Erufosine, a novel alkylphosphocholine, induces apoptosis in CLL through a caspase-dependent pathway. Leuk Res. 2010;34(8):1064-9.

92. Lemeshko VV, Kugler W. Synergistic inhibition of mitochondrial respiration by anticancer agent erucylphosphohomocholine and cyclosporin A. J Biol Chem. 2007;282(52):37303-7.

93. Kapoor V, Zaharieva MM, Das SN, Berger MR. Erufosine simultaneously induces apoptosis and autophagy by modulating the Akt–mTOR signaling pathway in oral squamous cell carcinoma. Cancer Lett. 2012;319(1):39-48.

94. Lemeshko VV, Kugler W. Synergistic inhibition of mitochondrial respiration by anticancer agent erucylphosphohomocholine and cyclosporin A. Journal of Biological Chemistry. 2007;282(52):37303-7.

95. Veenman L, Alten J, Linnemannstöns K, Shandalov Y, Zeno S, Lakomek M, et al. Potential involvement of F0F1-ATP (synth) ase and reactive oxygen species in apoptosis induction by the antineoplastic agent erucylphosphohomocholine in glioblastoma cell lines. Apoptosis. 2010;15(7):753-68.

96. Nitulescu GM, Margina D, Juzenas P, Peng Q, Olaru OT, Saloustros E, et al. Akt inhibitors in cancer treatment: The long journey from drug discovery to clinical use. International journal of oncology. 2016;48(3):869-85.

97. Yoshino T, Shiina H, Urakami S, Kikuno N, Yoneda T, Shigeno K, et al. Bcl-2 expression as a predictive marker of hormone-refractory prostate cancer treated with taxane-based chemotherapy. Clinical Cancer Research. 2006;12(20):6116-24.

98. Edlind MP, Hsieh AC. PI3K-AKT-mTOR signaling in prostate cancer progression and androgen deprivation therapy resistance. Asian journal of andrology. 2014;16(3):378.

99. Mosmann T. Rapid colorimetric assay for cellular growth and survival: application to proliferation and cytotoxicity assays. J Immunol Methods. 1983;65(1-2):55-63.

100. Kaleağasıoğlu F, Berger MR. Differential effects of erufosine on proliferation, wound healing and apoptosis in colorectal cancer cell lines. Oncol Rep. 2014;31(3):1407-16.

101. Hsieh AC, Liu Y, Edlind MP, Ingolia NT, Janes MR, Sher A, et al. The translational landscape of mTOR signalling steers cancer initiation and metastasis. Nature. 2012;485(7396):55-61.

102. Doğan A, Yalvaç ME, Şahin F, Kabanov AV, Palotás A, Rizvanov AA. Differentiation of human stem cells is promoted by amphiphilic pluronic block copolymers. Int J Nanomedicine 2012;7:4849-60.

103. Scher HI, Fizazi K, Saad F, Taplin M-E, Sternberg CN, Miller K, et al. Increased survival with enzalutamide in prostate cancer after chemotherapy. New England Journal of Medicine. 2012;367(13):1187-97.

104. Wise HM, Hermida MA, Leslie NR. Prostate cancer, PI3K, PTEN and prognosis. Clinical Science. 2017;131(3):197-210.

105. Kim J-H, Lee H, Shin EA, Kim DH, Choi JB, Kim S-H. Implications of Bcl-2 and its interplay with other molecules and signaling pathways in prostate cancer progression. Expert opinion on therapeutic targets. 2017;21(9):911-20.

106. Crawford ED, Petrylak DP, Shore N, Saad F, Slovin SF, Vogelzang NJ, et al. The Role of Therapeutic Layering in Optimizing Treatment for Patients With Castration-resistant Prostate Cancer (Prostate Cancer Radiographic Assessments for Detection of Advanced Recurrence II). Urology. 2017.

107. Song JH, Kandasamy K, Kraft AS. ABT-737 induces expression of the death receptor 5 and sensitizes human cancer cells to TRAIL-induced apoptosis. Journal of Biological Chemistry. 2008;283(36):25003-13.

108. Toren P, Zoubeidi A. Targeting the PI3K/Akt pathway in prostate cancer: challenges and opportunities. International journal of oncology. 2014;45(5):1793-801.

109. Dash R, Azab B, Quinn BA, Shen X, Wang X-Y, Das SK, et al. Apogossypol derivative BI-97C1 (Sabutoclax) targeting Mcl-1 sensitizes prostate cancer cells to mda-7/IL-24–mediated toxicity. Proceedings of the National Academy of Sciences. 2011;108(21):8785-90.

110. Saleem A, Dvorzhinski D, Santanam U, Mathew R, Bray K, Stein M, et al. Effect of dual inhibition of apoptosis and autophagy in prostate cancer. The Prostate. 2012;72(12):1374-81.

111. Tamaki H, Harashima N, Hiraki M, Arichi N, Nishimura N, Shiina H, et al. Bcl-2 family inhibition sensitizes human prostate cancer cells to docetaxel and promotes unexpected apoptosis under caspase-9 inhibition. Oncotarget. 2014;5(22):11399.

112. Hao J, Mao X, Ding D, Du G, Liu Z. The effect of cell killing by ABT-737 synergized with docetaxel in human prostate cancer PC-3 cells. Zhonghua wai ke za zhi [Chinese journal of surgery]. 2012;50(2):161-5.

113. Zhang C, Cai T-y, Zhu H, Yang L-q, Jiang H, Dong X-w, et al. Synergistic antitumor activity of gemcitabine and ABT-737 in vitro and in vivo through disrupting the interaction of USP9X and Mcl-1. Molecular cancer therapeutics. 2011;10(7):1264-75.

114. Rudner J, Ruiner C-E, Handrick R, Eibl H-J, Belka C, Jendrossek V. The Akt-inhibitor Erufosine induces apoptotic cell death in prostate cancer cells and increases the short term effects of ionizing radiation. Radiation Oncology. 2010;5(1):108.

115. Yin S, Dong Y, Li J, Fan L, Wang L, Lu J, et al. Methylseleninic acid potentiates multiple types of cancer cells to ABT-737-induced apoptosis by targeting Mcl-1 and Bad. Apoptosis. 2012;17(4):388-99.

116. Tong J, Yin S, Dong Y, Guo X, Fan L, Ye M, et al. Pseudolaric Acid B Induces Caspase-Dependent Apoptosis and Autophagic Cell Death in Prostate Cancer Cells. Phytotherapy Research. 2013;27(6):885-91.

117. Pandit B, Gartel AL. New potential anti-cancer agents synergize with bortezomib and ABT-737 against prostate cancer. The Prostate. 2010;70(8):825-33.

118. Wnętrzak A, Lipiec E, Łątka K, Kwiatek W, Dynarowicz-Łątka P. Affinity of alkylphosphocholines to biological membrane of prostate cancer: studies in natural and model systems. The Journal of membrane biology. 2014;247(7):581-9.

119. Broecker-Preuss M, Becher-Boveleth N, Müller S, Mann K. The BH3 mimetic drug ABT-737 induces apoptosis and acts synergistically with chemotherapeutic drugs in thyroid carcinoma cells. Cancer cell international. 2016;16(1):27.

120. Kapoor V, Zaharieva MM, Das SN, Berger MR. Erufosine simultaneously induces apoptosis and autophagy by modulating the Akt–mTOR signaling pathway in oral squamous cell carcinoma. Cancer letters. 2012;319(1):39-48.

121. Zaharieva M, Konstantinov S, Pilicheva B, Karaivanova M, Berger M. Erufosine. Annals of the New York Academy of Sciences. 2007;1095(1):182-92.

122. Huang S, Sinicrope F. Celecoxib-induced apoptosis is enhanced by ABT-737 and by inhibition of autophagy in human colorectal cancer cells. Autophagy. 2010;6(2):256-69.